Self-Organized and Chaotic States in Electron-Positron-Ion Magnetoplasma

BY

MUHAMMAD AZEEM

DEPARTMENT OF PHYSICS
QUAID-I-AZAM UNIVERSITY
ISLAMABAD, PAKISTAN

2005

This work is submitted as a thesis in

partial fulfillment of the requirement for the award of the degree

of

DOCTOR OF PHILOSOPHY

IN

PHYSICS

Department of Physics
Quaid-i-Azam University
Islamabad, Pakistan

CERTIFICATE

It is certified that the work contained in this thesis was carried out by **Mr. Muhammad Azeem** under my supervision.

Supervisor:

Dr. Arshad M. Mirza
Associate Professor
Department of Physics
Quaid-i-Azam University
Islamabad 45320
Pakistan.

Submitted through:

Prof. Dr. M. Aslam Baig
Chairman
Department of Physics
Quaid-i-Azam University
Islamabad 45320
Pakistan.

To

My Sweet Parents

Acknowledgements

I would like to first thank my respectable teacher and supervisor **Prof. Dr. Arshad M. Mirza** for providing me invaluable support and guidance during the execution of my research work. This work would not have been possible if it were not for the many long hours he spent teaching me the nonlinear dynamics of e-p-i magnetoplasma. His sympathetic attitude and encouragement enabled me in broadening my knowledge and improving my capability.

Very special thanks to **Prof. Dr. Aslam Baig**, the Chairman Department of Physics. for providing a friendly working environment and facilities in the department of Physics at QAU, Islamabad.

I would like to thank all of faculty members, staff and students with whom I have worked and collaborated during my stay at Quaid-i-Azam University (QAU), Islamabad.

I would like to acknowledge the financial support provided by Higher Education Commission (HEC) in accordance to the "Indigenous Scholarship Scheme 300" of the Ministry of Science and Technology under merit number 17-6(130)/Acad-Sch/2001 and four years leave from Pakistan Atomic Energy Commission (PAEC).

My heartiest thanks to all members of Theoretical Plasma Physics Group at Quaid-i-Azam University, especially, to Adnan Sarwar who helped me out of way. My cordial thanks to my friends specially Mr. Maaz, Assad Abbas, Ijaz Ahmad, Shahzad, Yasir and Mahboob Ahmad with whom it had been a great pleasure to work.

Finally, my deepest sense of acknowledgement goes to my loving parents who always pray for my success in every aspect of life.

(Muhammad Azeem)

ABSTRACT

In this thesis, we have investigated the nonlinear dynamics of low-frequency electrostatic/electromagnetic waves in a nonuniform electron-positron-ion (e-p-i) magnetoplasma with sheared ion flows. The ion dynamics is governed by the ion continuity and momentum balance equations, whereas the electrons and positrons are assumed to follow Boltzmann distributions, for electrostatic case. It is shown that the low-frequency ion-acoustic and electrostatic-drift waves can become unstable due to the ion sheared flow. In a collisional case a drift-dissipative instability can also take place. For the nonlinear case, it is shown that a quasi-stationary solution of the mode coupling equations can be represented in the form of monopolar vortex. We have also generalized the said work by considering nonuniform strongly magnetized electron-positron plasma with finite ion-temperature effect and in the presence of sheared ion flows. In the linear limit, a dispersion relation is obtained that admits new instability of drift-waves. Whereas, the nonlinear interaction between the finite amplitude short-wavelength waves give rise to quadrupolar vortices.

We have extended our earlier studies to the ion-temperature-gradient (ITG) driven electrostatic waves in a collisionless e-p-i magnetoplasma that contain equilibrium density, temperature, magnetic field, velocity and electrostatic potential gradients. We thus use hydrodynamic equations under drift-approximation and derive a set of nonlinear equations composed of ion continuity, the ion equation of motion and ion energy balance equations. In the linear limit, it is shown that non-zero equilibrium ion-temperature-gradient and the presence of positrons modify the basic drift modes. On the other hand, in the nonlinear case, it is shown that under certain conditions possible stationary solutions of the same set of nonlinear equations are reduced in the form of various types of vortex patterns. We have also incorporated the self-gravitational effect of ions in this work and have shown that possible stationary solutions of the nonlinear equations can be represented in the form of dipolar and tripolar vortices of gravitational potential.

Furthermore, we have also extended our study of electrostatic ITG modes to the electromagnetic case and derived a new set of coupled nonlinear equations which governs the dynamics of low-frequency electromagnetic ITG-driven modes in a nonuniform electron-positron-ion magnetoplasma with non-zero ion-temperature-gradients. We re-examined

nonlinear mode coupling equations under various approximations. In the linear limit, a local dispersion relation has been derived and analyzed in several interesting limiting cases. On the other hand, a quasi-stationary solution of the mode coupling equations in the absence of collisions can be represented in the form of dipolar and vortex-chain solutions.

Finally, we have studied the temporal behavior of electrostatic/electromagnetic ITG modes in e-p-i magnetoplasma and showed that the mode coupling equations can be represented in the form of well-known Lorenz and Stenflo type equations that admit chaotic trajectories. The results of our investigations are helpful to understand the wave phenomena in laboratory and astrophysical plasmas.

LIST OF PUBLICATIONS

1. Electrostatic instabilities and nonlinear structures of low-frequency waves in nonuniform electron–positron–ion plasmas with shear flow
   Physics of Plasmas, **10**, 4675 (2003)
   (A. M. Mirza, Asma Hasan, **M. Azeem** and H. Saleem)

2. Sheared-flow-driven ion-acoustic drift-wave instability and the formation of quadrupolar vortices in a nonuniform electron-positron-ion magnetoplasma
   Physics of Plasmas, **11**, 4341 (2004)
   (A. M. Mirza and **M. Azeem**)

3. Electrostatic vortices associated with ion-temperature-gradient driven drift modes in electron-positron-ion plasmas
   Physics of Plasmas, **11**, 4727 (2004)
   (**M. Azeem** and A. M. Mirza)

4. Effect of ion-temperature gradients on the formation of drift-Alfvén vortices in electron-positron-ion magnetoplasma with equilibrium flows
   Physics of Plasmas, **12**, 052306 (2005)
   (**M. Azeem** and A. M. Mirza)

5. Self-gravitation effect on the nonlinear dynamics of electron-positron-ion magnetoplasma
   Physica Scripta (2005) accepted for publication
   (**M. Azeem** and A. M. Mirza)

6. Quadrupolar Vortex Formation due to Nonlinearly Interacting ITG Driven Modes
   Proceedings of the 9th National Symposium on Frontiers in Physics, **6**, 297 (2003) *Pakistan*
   (A. M. Mirza, A. Qamar, **M. Azeem** and G. Murtaza)

Contents

List of Figures

Chapter 1

Introduction

1.1 Existence of Electron-Positron-Ion Plasma

The subject of electron-positron (e-p) plasmas, which are composed of particles with the same mass and opposite charge, is not only important in astrophysical plasmas, but also relevant in laboratory experiments. Electron-positron pairs are thought to be a major constituent of the plasma emanating both from the pulsars and from the inner region of the accretion disks surrounding the central black holes in AGNs (active galactive nuclei) [1-4]. They may be formed in the magnetospheres of pulsars by the pair-production cascade breeding process [5]. Such a plasma is found also in the intergalactic jets, in the early universe, at the centre of our own galaxy, in Van Allen belts, solar flares and fireballs producing γ-ray bursts [6-12]. In laboratory experiments, stellarator device has important advantages for the creation of the first confined electron-positron plasmas, namely the ability to confine electrons and positrons simultaneously, at any degree of neutrality and at relatively high particle kinetic energies, the ability to operate in steady state, and operate at ultra-low densities [13]. Electron-positron pair production is also possible during intense ultra-short laser pulse propagation in plasma [14] and a clean pair-dominated plasma can be achieved by letting the resulting plasma to expand freely after turning off the laser. Electron-positron plasmas are also observed in laboratory experiments in which the positrons can be used to probe the particle transport in tokamak [15-17]. Recently, Helander and Ward [18] have investigated the possibility of pair production in large tokamaks due to collisions between multi-Mev run-away electrons and thermal particles.

For a time t after the Big Bang, plasma of the early universe may be relativistic (for $10^{-2} < t < 1$ sec.) or mildy relativistic or non-relativistic (for $1 < t < 10^{13}$sec.) [8]. Recent experiments have opened up the possibility of creating a non-relativistic e-p plasma in laboratory. In one scheme, a relativistic electron beam impinges on a high-Z target, where positrons are produced copiously. The pair plasma is then trapped in a magnetic mirror and is expected to cool rapidly by emission of radiations [19]. Another scheme for obtaining the pair plasma, by addition of electrons, proposes the accumulation of positrons from a radioactive source [20] in an electrostatic trap and cooling to room temperature. Non-relativistic pair plasmas have also been created in experiments for understanding the dynamics of pairs [17, 21, 22]. The possibility of creating non-relativistic e-p plasma source in the laboratory contributes not only to understanding of various astrophysical phenomena, but also to the development of plasma source in microwave discharges using bulk or surface waves [23]. Therefore the investigation of pair plasma is important in the sense that this is the kind of anti-matter that can be experimentally produced and stored most efficiently.

Although the e-p pairs form the dominant constituent of the several astrophysical situations including active galactic nuclei, the pulsars magnetosphere, in early universe, etc., a minority population of ions is also likely to be present. Various aspects of the presence of ions in pair plasma have been discussed in literature (see e.g., Refs. [24-28]). On the other hand, because of the sufficient life time of the positrons, most of the astrophysical [7, 11, 12] as well as laboratory electron-ion (e-i) plasmas [15-17] become an admixture of electrons, positrons and ions. Such a three-component electron-positron-ion (e-p-i) plasma has in fact been created in laboratory [29] and studied in different models of pulsar magnetospheres [30, 31]. Propagation of intense short laser pulses in a e-i plasma can also lead to pair production resulting in a three-component e-p-i plasma [32]. In fact, three-component plasma has also been seen in laboratory experiments [15-17] carried out with positrons as probe to study transport in tokamaks. In addition to several other applications (like the pulsars magnetosphere modelling), an investigation of e-p-i plasma is also important to understand early universe [7, 33, 34], in particular, the MeV epoch in the evolution of the universe. It may, indeed, be possible that a deeper insight into the behavior of interacting plasma fluid in this era may provide valuable clues to its later evolution. Due to the presence of ions several low-frequency waves can exist in e-p-i plasma which otherwise do not propagate in e-p plasma. Even a small concentration of ions can change the dynamics of e-p plasma and several new linear and nonlinear modes may appear. Therefore, the study of e-p-i or three-component plasma is important to develop an understanding of the behavior of both astrophysical and laboratory plasmas.

The importance of three-component admixture plasma has led to several theoretical investigations. The e-p-i plasma has been studied, for example, in the context of pulsars magnetosphere by Lakhina and Buti [30] and by Lominadze *et al.* [31]. In contrast to the usual plasma with electrons and positive ions, it has been known that the nonlinear waves in plasmas having positrons behave differently [35]. Gallant *et al.* [36] performed particle-in-cell (PIC) simulations of perpendicularly magnetized shocks in electron-positron and e-p-i plasmas. The shocks in pure e-p plasma have been found to produce only thermal distribution downstream, and declared poor candidates as particle acceleration sites. When the upstream plasma flow also contained a smaller population of positive ions, efficient acceleration of positrons, and to a lesser extent of electrons, was observed in the simulations. Nejoh [37] has studied the effect of the ion-temperature on large amplitude ion-acoustic waves in an e-p-i plasma. It has been shown that the region of the existence of the ion-acoustic wave spreads as the ion temperature decreases.

Furthermore, Tsintsadze *et al.* [38] presented a general description for the stability problem of a charged surface of e-p-i plasma in the presence of a negative pressure. Conditions under which the charged surface becomes unstable have been obtained. A potentially important application of the e-p-i plasma may be found in providing an understanding of the nature of the intergalactic jets. It has been proposed [6] that intergalactic jets comprise low-frequency, strong electromagnetic (EM) waves self-focused into a channel, and generated by, for instance, a dense cluster of rapidly spinning pulsars in the galactic nucleus. However, it is now believed that strong monochromatic waves emitted by pulsars are subjected to parametric instabilities even in quite under-dense plasmas. This may tend to rule out pulsars as sources of these well-collimated jets. Honda *et al.* [39] presented a novel model for collimation and transport of e-p-i astrophysical jets. Analytical results show that the filamentary structures can be sustained by self-induced toroidal magnetic fields permeating through the filaments, whose widths significantly expand in the pair-dominant regimes. The magnetic field strength reflects a characteristic of equipartition of excess kinetic energy of the jets. It has been also shown that growth of the hose-like instability is strongly suppressed. Essential features derived from this model have been found consistent with recent results observed by using very long baseline telescopes. Hoshino *et al.* [40] have carried out theoretical investigations of relativistic collisionless shock waves in e-p-i plasmas of relevance to astrophysical sources of synchrotron radiations. Gail *et al.* [41] have performed coupled channel calculations for electron-positron pair production in relativistic collisions of heavy ions. H. Hasegawa *et al.* [42, 43] and S. Hasegawa *et al.* [44] have studied the positron acceleration to ultrarelativistic energies by a shock wave and perpendicular nonlinear waves in an e-p-i plasma. Shukla *et al.* [45] have shown that intense radiation nonlinearly interacts with acoustic-like waves in an e-p-i plasma at non-relativistic temperatures.

1.2 Self-organized Structures in Plasma

Plasma occurs in state of turbulence under a wide range of conditions including space and astrophysical plasmas as well as in stable laboratory confinement devices. The strength of the turbulence increases as the plasma is driven farther away from thermodynamic equilibrium. There are several ways to drive the plasma away from equilibrium with particle beams, laser beams and radio frequency waves, a universally occurring departure from equilibrium is the existence of spatial gradients across an ambient magnetic field. Plasma distributions that are driven away from the thermodynamic equilibrium of a spatially uniform Maxwell-Boltzmann velocity distribution are said to have free energy available to drive plasma turbulence. The nature of the nonlinear saturated state depends on how far into the unstable domain the system parameters reside which typically varies with space and time as the plasma turbulence reacts on the plasma distribution to push the system back toward one of the marginally stable states. The turbulence provides a mechanism for self-organization toward a relaxed dynamical state often containing a mixture of waves, vortices and zonal flows [46]. *Self-organization* refers to a process in which the internal organization of a system, normally an open system, increases automatically without being guided or managed by an outside source. A *vortex* is a spinning turbulent flow (or any spiral whirling motion) with closed streamlines. The shape of media or mass rotating rapidly around a center forms a vortex. The study of self-organizing processes is of interest both for space and laboratory plasma problems. It is also important for recognizing general regularities of the physical world.

The vortex dynamics in fluids in a simplest possible scenario, is governed by the Navier-Stokes (NS) equation which admits a monopolar vortex and dipolar vortices. On the other hand, the nonlinear propagation of two-dimensional Rossby waves in geophysical fluid dynamics, and pseudo-three dimensional electrostatic drift waves in non-uniform magnetized plasmas is governed by the Charney [47] and Hasegawa-Mima [48] equations, respectively. Larichev and Reznik [49] demonstrated that the Charney equation admits a double vortex whose speed is larger than the drift (phase) velocity of the Rossby waves. On the other hand when the speed of the travelling nonlinear structure equals the Rossby wave drift speed, the Charney equation admits a vortex street as a possible stationary state. In the presence of the equilibrium sheared flow, one could have counter rotating, tripolar and quadrupolar vortices within the framework of the Charney equation. In magnetized plasmas, we have the possibility of vortices comprising a monopolar, a dipolar, a tripolar, a quadrupolar or a chain of vortices. Here the vortices are associated with nonlinear dispersive waves that possess, at least, a two-dimensional character. When the velocity of the fluid (or plasma particle) associated with the dispersive waves becomes locally larger than the phase velocity of the wave due to the nonlinear effects, one encounters a curving of the wavefronts which leads to the formation of a two-dimensional travelling vortex structure [50].

The study of nonlinear structures in e-p-i plasma such as solitons, double layers, vortices, etc., has attracted much interest in last two decays. For instance, Rizzato [35] and Berezhiani *et al.* [51] have investigated envelop solitons of electromagnetic waves in an admixture magnetized three-component (e-p-i) plasmas. Later, Berezhiani and Mahajan [52] described the formation of large amplitude electromagnetic solitary structures in cold e-p-i plasma. This work was further extended by Popel *et al.* [25], by considering warm e-p-i plasma and ion-acoustic solitons are found to exist. On the other hand, Pokhotelov *et al.* [28] have investigated the nonlinear dynamics of drift-Alfvén waves in an inhomogeneous e-p plasma with a small fraction of heavy ions. It has been shown that electromagnetic perturbations in the presence of heavy ions in relativistic e-p plasma can saturate into two-dimensional dipolar vortices. Kakati and Goswami [53] have presented a theoretical model to investigate the double layers, associated with the kinetic Alfvén waves, in a magnetized e-p-i plasma and have shown that the existence of small-amplitude double layers requires an appreciably larger density of ions than that of positrons at equilibrium. The properties of the double layers are determined by the ratio between the number densities of positrons and ions at equilibrium, the direction cosines defining the moving frame, as well as the electron to positron temperature ratio.

Vranjes *et al.* [54] have studied the nonlinear propagation of low-frequency sheared Alfvén waves and obtained several types of electromagnetic vortices. Recently the linear and nonlinear electrostatic and electromagnetic drift waves have been studied in e-p-i plasmas in Ref. [55]. The nonlinear vortex structures have been investigated in this work in both electrostatic and electromagnetic limits. In the nonlinear electrostatic case the drift waves can give rise to vortices. It has been shown in this work that the vortex speed in e-p-i plasmas can be equal to the phase speed of the drift-wave, while it is not possible in electron ion (e-i) plasmas. The effects of ion velocity along the external magnetic field has not been taken into account in the investigations [55]. In our opinion the system may become unstable in the linear limit if a free energy source exists in the form of sheared ion flow. *Therefore, we have investigated the nonlinear dynamics of low-frequency electrostatic waves in a magnetized nonuniform e-p-i plasma with sheared ion flows in the cold ion limit. It is found that the low-frequency ion acoustic and electrostatic drift waves can become unstable in uniform electron-positron-ion plasmas due to the ion shear flow. In a collisional e-p-i plasma, a drift-dissipative instability can also take place. On the other hand, a quasi-stationary solution of the mode coupling equations can be represented in the form of monopolar vortex* [56].

Recently, Shukla *et al.* [57] have investigated the linear and nonlinear properties of obliquely propagating coupled low-frequency electrostatic-drift (ED) and ion-acoustic (IA) waves in a strongly magnetized nonuniform e-p-i plasma with sheared ion flows and showed that weakly interacting ED-IA waves admit vortex chain and double vortex type solutions. The effect of finite ion-temperature, which was not considered in the earlier findings [56, 57], can drastically modify the nonlinear dynamics of e-p-i plasma. *Therefore, we considered the effect of finite ion-temperature in a nonuniform strongly magnetized e-p-i plasma in the presence of sheared ion flows. In the linear limit, a dispersion relation is obtained that admits new instabilities of drift-waves. It is found that ion-acoustic and electrostatic drift waves can become unstable due to ion sheared flow. Furthermore, the nonlinear interactions between these finite amplitude short-wavelength waves give rise to quadrupolar vortices* [58].

The search for nonlinear structures in e-p-i magnetoplasma has been continued. Such nonlinear coherent structures could serve as building blocks for the understanding of plasma turbulence, transport and self-organization. Formation of different types of coherent structures, under the effects of ion-temperature-gradient (ITG) and sheared ion flows, have not yet been studied. which could play very important role in understanding the nonlinear dynamics of e-p-i magnetoplasma. *We have therefore extended our earlier investigations* [56, 58] *to electrostatic ITG modes in an electron-positron-ion magnetoplasma in the presence of equilibrium density, temperature, magnetic field, velocity and electrostatic potential gradients. In the linear case, a new linear dispersion relation is derived and a number of interesting limiting cases are discussed. On the other hand, in nonlinear case, it is shown that under certain conditions possible stationary solutions of the nonlinear equations can be reduced to monopolar, dipolar, tripolar, quadrupolar and chain of vortices* [59].

Since in several laboratories and space plasmas, the plasma beta ($\beta = 8\pi nT/B_0^2$, where n is the plasma number density and B_0 is the strength of the ambient magnetic field) could exceed the electron-to-ion mass ratio, necessitating to incorporate electromagnetic effects on ITG-driven modes of e-p-i plasmas. *We have, therefore, studied the linear and nonlinear properties of low-frequency electromagnetic drift-dissipative and drift-Alfvén waves in an electron-positron-ion magnetoplasma containing equilibrium density gradient, ion-temperature gradient and magnetic field gradient with parallel equilibrium flow velocities. In the linear limit, a local dispersion relation has been derived and analyzed in several interesting limiting cases. On the other hand, a quasi-stationary solution of the mode coupling equations in the absence of collisions can be represented in the form of dipolar and vortex-chain solutions* [60].

In the last few years, several investigations have been made on linear as well as nonlinear wave motions in a self-gravitating magnetoplasma. For instance, Pandey *et al.* [61] and Mhanta *et al.* [62] have studied the effect of the gravitational field on dust-acoustic waves by ignoring the ion dynamics. Whereas, Avinash and Shukla [63] and Verheest *et al.* [64] have investigated dust-acoustic waves in a self-gravitating unmagnetized dusty plasma, taking into account the dynamics of dust grains and ions. Furthermore, Vranjes [65] has studied the nonlinear self-organization of perturbations in rotating, nonuniform, gravitating systems and found the stationary solutions in the form of tripolar and vortex chains of gravitational potential. Mamun [66] described the effects of dust temperature and fast ions on gravitational instability in a self-gravitating magnetized dusty plasma and shown that the growth rate of gravitational instability decreases with dust temperature, fast ion, and external magnetic field, but increases with the number of free electrons, with the ratio of ion temperature to electron temperature, and with the ratio of dust mass to dust charge. Later, Mamun and Shukla [67] have shown the existence of new magnetic Jeans type instability due to the combined effects of self-gravitational field and collisions of electrons and ions with the stationary neutral atoms. To the best of our knowledge, so far, the effect of self-gravitation on ion-temperature-gradient in electron-positron-ion magnetoplasma has not been considered in the earlier investigations [61-67]. *Therefore, we incorporated the self-gravitational effect of ions in our previous work* [59]. *In the linear case, new dispersion relation under local approximation is obtained and discussed. On the other hand, we have discussed the possibility of formation of dipolar and tripolar vortices of gravitational potential in nonuniform self-gravitating e-p-i magnetoplasma with non-zero ion-temperature-gradient (ITG) and sheared ion flows* [68].

1.3 Chaotic Behavior

Historically, the study of chaos is strongly rooted in the mathematical study of nonlinear dynamics, going back to the pioneering work of Henri Poincaré at about the turn of the 20th century. Poincaré's motivation was partly provided by the problem of the orbits of three celestial bodies experiencing mutual gravitational attraction (e.g., a star and two planets). By considering the behavior of orbits arising from the sets of initial points (rather than focusing on individual orbits), Poincaré was able to show that very complicated (now called chaotic) orbits were possible. Certain hydrodynamical systems exhibit steady-state flow patterns, while others oscillate in a regular periodic fashion. Still others vary in an irregular, seemingly haphazard manner, and even when observed for long period of time do not appear to repeat their previous history. These modes of behavior may all be observed in the familiar rotating-basin experiments, described by Fultz *et al.* [69] and Hide [70]. In these experiments, a cylindrical vessel containing water is rotated about its axis, and is heated near its rim and cooled near its center in a steady symmetric fashion. Under certain conditions the resulting flow is as symmetric and steady as the heating which gives rise to it. For other conditions a system of regularly spaced waves develops, and progresses at a uniform speed without changing its shape. For different conditions an irregular flow pattern forms, moves and changes its shape in an irregular non-periodic manner.

The first true experimenter in chaos was a meteorologist, named Edward Lorenz. In 1961, Lorentz discovered the *butterfly effect* while trying to forecast the weather. The butterfly effect reflects how changes on the small scale affect things on the large scale. It is the classic example of chaos, as small changes lead to large changes at a later time. An example of this is how a butterfly flapping its wings in Hong Kong could change tornado patterns in Texas. He was running a long series of computations on a computer when he decided he needed another run. Rather than doing the entire run again, he decided to save some time by typing in some numbers from a previous run. Later, when he looked over the printout, he found an entirely new set of results. The results should have been the same as before. After thinking about this unexpected result, he discovered that the numbers he typed in had been slightly rounded off. In principle, this tiny difference in initial conditions should not have made any difference in the result, but it did. From this, Lorentz concluded that long-distant weather forecasts are impossible to predict. Tiny differences in weather conditions, on any one day, will show dramatic differences, after a few weeks, and these differences are entirely unpredictable. Although Lorentz's discovery was an accident, it planted the seed for the new field called *Nonlinear Dynamics*.

Well known Lorenz equations were first presented in 1963 [71]. They define a three-dimensional system of ordinary differential equations (ODEs) that depends on three real positive parameters. As we vary the parameters, we change the behavior of the flow determined by the equation. For some parameter values, numerically computed solutions of the equations oscillate, apparently, forever in the pseudo-random way, we now call it *chaotic*. This is the main reason for the immense amount of interest generated by the Lorenz equations. Recently, Stenflo [72] has shown that short-wavelength acoustic gravity waves in a rotational system can be described by a set of four nonlinear ordinary differential equations with four constant non-dimensional parameters. These equations contains as a subset of Lorentz equations. A detailed investigation of Lorenz-Stenflo nonlinear equations contributes not only to the understanding of certain atmospheric phenomena, but also to the possible quantitative verification of modern nonlinear theories and their predictions. Yu *et al.* [73] have presented the bifurcation characteristics of these nonlinear equations. Mirza *et al.* [74, 75] have shown that temporal behavior of the nonlinear dissipative plasma systems can be expressed in the form of well known Lorentz and Stenflo type equations that admit chaotic trajectories. It is therefore of interest to investigate the temporal behavior of nonlinearly interacting finite amplitude electrostatic/electromagnetic ITG-driven modes in e-p-i magnetoplasma.

In this work, we have also derived the set of nonlinear equations to study the temporal behavior of low frequency electrostatic and electromagnetic ITG modes in e-p-i magnetoplasma and have reduced, under certain conditions, the nonlinear equations in the form of a matrix which is a generalization of the Lorenz matrix admitting chaotic behavior.

1.4 Layout of the Thesis

The thesis is arranged in the following fashion: In chapter one, justification for studying self-organized and chaotic states of e-p-i magnetoplasma and layout of the thesis is given. In chapter two, the nonlinear set of equations is derived to study the nonlinear dynamics of low-frequency electrostatic and electromagnetic ITG-driven waves in the presence of equilibrium density, temperature, magnetic field and velocity gradients for a collisional e-p-i magnetoplasma. Chapter 3 deals with nonlinear dynamics of low-frequency electrostatic waves in a magnetized nonuniform e-p-i plasma with sheared ion flows in the cold and hot ions limits. Chapter 4 and 5 deals with nonlinear dynamics of low-frequency electrostatic/electromagnetic ITG-driven waves in a magnetized nonuniform e-p-i plasma with sheared ion flows. In chapter 6, a temporal behavior of the electrostatic/electromagnetic ITG mode is discussed. A brief summary and conclusion of our findings is presented in chapter 7.

Chapter 2

Derivation of Nonlinear Equations

2.1 Introduction

Collective plasma dynamics is most conveniently modelled within the fluid description. Fluid models play a central role in plasma research because their reduced dimensionality makes it more feasible to analyze realistic configurations, with broad ranges of plasma parameters, in three-dimensional space geometry. The more standard fluid models are derived for regimes of high collisionality but a majority of plasmas of interest in space and in magnetic fusion experiments are collisionless or weakly collisional. For these, a fluid description can still make sense under strong magnetization conditions, as long as the dynamics perpendicular to the magnetic field is concerned. In plasma fluid theory, a plasma is characterized by a few local parameters, such as the particle density, the kinetic temperature, and the flow velocity, the time evolution of which are determined by means of fluid equations. These equations are analogous to, but generally more complicated than, the equations of hydrodynamics due to the presence of electric and magnetic fields and currents.

There are three fundamental orderings in plasma fluid theory. In the first ordering, the fluid velocities are much greater than the thermal velocities. This ordering is called the *cold-plasma approximation*. The cold-plasma approximation applies not only to cold plasmas, but also to very fast disturbances which propagate through conventional plasmas. In particular, the cold-plasma equations provide a good description of the propagation of electromagnetic waves through plasmas. Note that the electron, positron and ion kinetic pressures can be neglected in the cold-plasma limit, since the thermal velocities are much smaller than the fluid velocities. It follows that there is no need for energy evolution equation for any species. Furthermore, the motion of the plasma is so fast, in this limit, that relatively slow transport effects, such as viscosity and thermal conductivity, play no role in the cold-plasma fluid equations.

In second ordering, the fluid velocities are of the order of thermal velocities. This ordering is called the *MHD approximation*. The MHD equations are conventionally used to study macroscopic plasma instabilities, possessing relatively fast growth-rates. Note that the electron, positron and ion pressures cannot be neglected in the MHD limit, since the fluid velocities are of the order the thermal velocities. Thus, electron and ion energy evolution equations are needed in this limit. However, MHD motion is sufficiently fast that transport effects, such as viscosity and thermal conductivity, are too slow to play a role in the MHD equations. In fact, the only collisional effects which appear in these equations are resistivity, the thermal force, and collisional energy exchange between the particles.

The final ordering corresponds to the fluid velocities which are of the order of drift velocities. Likewise, the ordering is called the *drift approximation* and we may use the term drift velocity in place of fluid velocity and vice versa. The drift equations are conventionally used to study equilibrium evolution, and the slow growing microinstabilities which are responsible for turbulent transport in tokamaks. In general, all terms in the Braginskii equations must be retained in this limit. We shall work in the limit of drift approximation.

Electromagnetic waves don't propagate in a conductor beyond the skin depth. However, in a fluid of high electrical conductivity and in the presence of magnetic field, waves of low frequency do propagate. The velocity of propagation of these waves can be many orders of magnitude less than speed of light. The frequency of these waves must be less than the ion cyclotron frequency (ω_{ci}) and are referred as low frequency waves. In inhomogeneous magnetized plasmas, low frequency modes with frequency much less than the ion cyclotron frequency are considered to be the most dangerous one which give the largest transport. This chapter presents the derivation of the nonlinear equations to study the nonlinear dynamics of low frequency electrostatic and electromagnetic ITG-driven waves in a collisional e-p-i magnetoplasma. For this purpose, we use Braginskii's transport equations for the ions and the continuity and momentum equations for the electrons and positrons using drift-approximation. The system of equations is closed by specifying some explicit relations of quasineutrality condition and/or Maxwell's equations.

2.2 Drift-Motion Across the Ambient Magnetic Field

In a magnetized plasma, the particle dynamics is usually very different in the direction parallel or perpendicular to the magnetic field. In the perpendicular direction, the particles are highly localized due to strong magnetic field and fluid description is usually valid. For fluid approximation in the direction along the magnetic field, the conditions are more restrictive and will basically be fulfilled when the phase velocity of the perturbation is zero (holds for electrons/positrons) or much larger than the thermal velocity (corresponds to the cold plasma approximation) or mean-free-path is much shorter than the perturbation wavelength, the particles are not free to maintain communication between different parts of perturbation and are thus localized.

The low-frequency region for which $\omega \ll \omega_{cj}$ is particularly simple to treat from the fluid motion point of view, since here the equation of motion may be solved by an algebraic iterative method. We write the equation of motion for the jth species as follows:

$$\left(\frac{\partial}{\partial t} + \nu_j + \mathbf{v}_j \cdot \nabla\right) \mathbf{v}_j = \frac{q_j}{m_j}\left(\mathbf{E} + \frac{\mathbf{v}_j}{c} \times \mathbf{B}_0\right) - \frac{1}{m_j n_j}\nabla p_j - \nabla \Psi_g, \tag{2.1}$$

where $p_j = n_j T_j$ is the kinetic pressure, $\mathbf{E} = -\nabla\phi$ is the electrostatic field, n_j is the number density. T_j is the temperature. $\mathbf{v}_j$ is the fluid velocity. ν_j is the collision frequency. m_j is the mass, $\mathbf{B}_0$ is the ambient magnetic field. Ψ_g (ϕ) is the gravitational (electrostatic) potential and c is the speed of light. The ion temperature perturbation can be obtained by using ion energy balance equation. Assuming $\mathbf{B}_0 = B_0\hat{\mathbf{z}}$, where $\hat{\mathbf{z}}$ is a unit vector along the z-axis. we obtain by taking the vector product of Eq. (2.1) with $\hat{\mathbf{z}}$:

$$\left(\frac{\partial}{\partial t} + \nu_j + \mathbf{v}_j \cdot \nabla\right) \hat{\mathbf{z}} \times \mathbf{v}_j = \frac{q_j}{m_j}\left\{\nabla\phi\times\hat{\mathbf{z}} + \frac{B_0}{c}\left[\mathbf{v}_j(\hat{\mathbf{z}}\cdot\hat{\mathbf{z}}) - \hat{\mathbf{z}}(\hat{\mathbf{z}}\cdot\mathbf{v}_j)\right]\right\} - \frac{1}{m_j n_j}\hat{\mathbf{z}} \times \nabla\left(n_j T_j\right) - \hat{\mathbf{z}} \times \nabla\Psi_g. \tag{2.2}$$

By writing $d/dt = \partial/\partial t + \nu_j + \mathbf{v}_j \cdot \nabla$, we find from Eq. (2.2)

$$\mathbf{v}_{j\perp} = \frac{c}{B_0}\hat{\mathbf{z}} \times \nabla\phi + \frac{c}{q_j n_j B_0}\hat{\mathbf{z}} \times \nabla\left(n_j T_j\right) + \frac{m_j c}{q_j B_0}\hat{\mathbf{z}} \times \nabla\Psi_g + \frac{m_j c}{q_j B_0}\frac{d}{dt}\left(\hat{\mathbf{z}} \times \mathbf{v}_j\right) \tag{2.3}$$

Here the terms on the right-hand-side are, respectively, the $\mathbf{E} \times \mathbf{B}_0$, the diamagnetic, the gravitational and polarization drift velocities. For low-frequency variations, we assume that $\mathbf{E} \times \mathbf{B}_0$ drift to be the dominating part of the perturbed velocity and we may substitute it into the polarization drift. We then write the perpendicular velocity as

$$\mathbf{v}_{j\perp} = \mathbf{v}_E + \mathbf{v}_{Dj} + \mathbf{v}_{gj} + \mathbf{v}_{pj}, \tag{2.4}$$

where

$$\mathbf{v}_E = \frac{c}{B_0}\hat{\mathbf{z}} \times \nabla\phi. \tag{2.5}$$

$$\mathbf{v}_{Dj} = \frac{c}{q_j n_j B_0}\hat{\mathbf{z}} \times \nabla\left(n_j T_j\right), \tag{2.6}$$

$$\mathbf{v}_{gj} = \frac{m_j c}{q_j B_0}\hat{\mathbf{z}} \times \nabla\Psi_g \tag{2.7}$$

and

$$\mathbf{v}_{pj} = -\frac{m_j c^2}{q_j B_0^2}\frac{d}{dt}\nabla_{\perp}\phi. \tag{2.8}$$

Here $\nabla_{\perp} = \hat{\mathbf{x}}\partial/\partial x + \hat{\mathbf{y}}\partial/\partial y$. This is the procedure for obtaining explicit expressions for the fluid drifts known as the drift approximation, and the resulting closed equations are referred to as reduced fluid model.

Let us interpret briefly the above-mentioned drifts i.e., Eqs. (2.5)-(2.8). The fluid drifts may differ from actual particle or guiding centre drifts. The reason for the difference is that the fluid picture averages particle velocities at a point, regardless of where the guiding centres are located, while the particle drifts are obtained by first averaging over the gyro-motion, thus identifying a particle with its guiding centre.

When we take the temporal average over one gyration period of particle motion in static and uniform fields it would yield perpendicular component equal to the same $\mathbf{E}\times\mathbf{B}_0$ drift velocity i.e., $\mathbf{v}_E$, showing that $\mathbf{v}_E$ is the average cross-field drift of the particle. It may be noted here that this drift is independent of the particle charge and mass and hence corresponds to a collective bulk motion of plasma. This drift is caused by the change in the gyro-radius due to the particle acceleration by the electric field during the gyrating motion.

The polarization drift $\mathbf{v}_{pj}$, on the other hand, may be regarded as a correction to the $\mathbf{E}\times\mathbf{B}_0$ drift when the E field is time dependent. Due to the large difference in mass of electrons/positrons and ions, the polarization drift of electrons and positrons can be ignored. There is strong similarity between the polarization drift caused by a time variation of E and the finite larmor radius drift, which is due to the space variation of E. This is because a gyrating particle has no way of deciding if the variation in E originates due to the time or space. Contrary to $\mathbf{v}_E$, $\mathbf{v}_{gj}$ (the gravitational drift velocity) leads to (slow) charge separation because the drift direction is of opposite sign for electrons and ions/positrons. This charge separation causes electric field and subsequent $\mathbf{E}\times\mathbf{B}_0$ drift.

On the other hand, the diamagnetic drift velocity $\mathbf{v}_{Dj}$ is purely a fluid velocity. The diamagnetic drift is due to a pressure gradient. This drift is in opposite direction for the oppositely charged particles and produces the diamagnetic current j. This $\mathbf{j}\times\mathbf{B}_0$ current flows in such a way as to cancel the imposed field. It is also the source of magnetic field variation across a plasma boundary as indicated by its name. The diamagnetic drift does not cause charge separation because $\nabla \cdot (n_j \mathbf{v}_{Dj}) = 0$. This case is in contrast to the ∇B_0 and curvature drifts which are particle drifts but not fluid drifts. It has been shown in Ref. [76] that by taking into account the magnetization drift, that the guiding centre and reduced fluid descriptions yield identical results for the cross-field motion of non-uniformly magnetized plasmas. Therefore, the above-mentioned particle drifts may be treated for fluid description as well.

Consider the case when the magnetic field is perturbed, i.e.,

$$\mathbf{B} = \mathbf{B}_0 + \mathbf{B}_1, \tag{2.9}$$

where $\mathbf{B}_0$ and $\mathbf{B}_1$ are the equilibrium and perturbed parts of magnetic field. If we consider low-β plasma case, we may neglect the compressional magnetic field. Then we may write

$$\hat{\mathbf{z}} \times (\mathbf{v}_j \times \mathbf{B}) = B_0 \mathbf{v}_{j\perp} - (v_{j0} + \mathbf{v}_{jz}) \mathbf{B}_1 \tag{2.10}$$

for a plasma with equilibrium flow velocity v_{j0}. We now solve for $\mathbf{v}_\perp$, the Eq. (2.1) in the same way but for the electromagnetic case to get

$$\begin{aligned} \mathbf{v}_{j\perp} &= \frac{c}{B_0} \hat{\mathbf{z}} \times \nabla \phi + \frac{c}{q_j n_j B_0} \hat{\mathbf{z}} \times \nabla (n_j T_j) + \frac{m_j c}{q_j B_0} \hat{\mathbf{z}} \times \nabla \Psi_g \\ &\quad - \frac{m_j c^2}{q_j B_0^2} \frac{d}{dt} \nabla_\perp \phi + (v_{j0} + \mathbf{v}_{jz}) \frac{\mathbf{B}_1}{B_0}. \end{aligned} \tag{2.11}$$

2.3 Derivation of Electromagnetic Nonlinear Equations

Let us consider the nonlinear propagation of low-frequency electromagnetic waves in a nonuniform collisional e-p-i magnetoplasma containing equilibrium density gradient $\partial_x n_{j0}$, equilibrium ion-temperature gradient $\partial_x T_{i0}$, equilibrium magnetic field gradient $\partial_x B_0$ and equilibrium velocity gradient $\partial_x \mathbf{v}_{j0}$, where $\mathbf{v}_{j0}$ is the equilibrium plasma flow velocity of the particle species j (j equals e for the electrons, p for positrons and i for the ions) in the direction along the equilibrium magnetic field $B_0\hat{\mathbf{z}}$. In equilibrium, the charge neutrality condition reads

$$\sum_j q_j n_{j0} = e\left(n_{i0} + n_{p0} - n_{e0}\right) = 0, \tag{2.12}$$

where q_j stands for the charge of the jth-species. The ion dynamics is governed by the ion continuity equation

$$\frac{\partial n_i}{\partial t} + \nabla \cdot (n_i \mathbf{v}_i) = D_i \nabla_\perp^2 n_i, \tag{2.13}$$

the momentum transfer equation (ignoring the self-gravitational effect of ions)

$$m_i n_i \left(\frac{\partial}{\partial t} + \nu_i + \mathbf{v}_i \cdot \nabla\right) \mathbf{v}_i = e n_i \left(\mathbf{E} + \frac{1}{c}\mathbf{v}_i \times \mathbf{B}\right) - \nabla\left(n_i T_i\right), \tag{2.14}$$

and ion temperature perturbation using the ion energy balance equation,

$$\frac{3}{2}\left(\frac{\partial}{\partial t} + \mathbf{v}_i \cdot \nabla\right) T_i + T_i \nabla \cdot \mathbf{v}_i \approx -\frac{1}{n_i} \nabla \cdot \mathbf{q}_i. \tag{2.15}$$

where D_i represents ion diffusion coefficient, n_i is the ion number density, $\mathbf{v}_i$ is the ion fluid velocity, m_i is the ion mass, ν_i is the ion collision frequency, $\mathbf{E}$ is the electric field, T_i is the ion temperature, c is the speed of light, $\mathbf{q}_i = -\chi_i \nabla_\perp T_i + (5cn_i T_i/2eB_0)$ $\hat{\mathbf{z}} \times \nabla T_i$ is the ion-heat flux, χ_i is the ion thermal conductivity and the second term is the collisionless cross-field (or Righi-Leduce) ion heat flux [113].

For low-frequency waves (in comparison with the ion gyrofrequency), the light particles (electrons and positrons) would thermalize very quickly to achieve the same temperature such that we may assume $T_{e0} = T_{p0} = T_0$. Under this approximation, the continuity and momentum equations for species j ($j = e$, p) can be written as

$$\frac{\partial n_j}{\partial t} + \nabla \cdot (n_j \mathbf{v}_j) = D_j \nabla_\perp^2 n_j. \tag{2.16}$$

$$m_j n_j \left(\frac{\partial}{\partial t} + \nu_j + \mathbf{v}_j \cdot \nabla \right) \mathbf{v}_j = q_j n_j \left(\mathbf{E} + \frac{1}{c} \mathbf{v}_j \times \mathbf{B} \right) - T_0 \nabla n_j. \qquad (2.17)$$

Using Eq. (2.11), we may write the following expressions (including the effect of ion-gyroviscosity) for the fluid velocity perturbations for ions and electrons/positrons corresponding to the Eq. (2.14) and (2.17), respectively:

$$\begin{aligned} \mathbf{v}_i \approx & \frac{c}{B_0} \hat{\mathbf{z}} \times \nabla \phi + \frac{c}{eB_0 n_i} \hat{\mathbf{z}} \times \nabla (n_i T_i) - \frac{c}{B_0 \omega_{ci}} \left[\partial_t + \nu_i + \frac{c}{B_0} \hat{\mathbf{z}} \times \nabla \phi \cdot \nabla \right. \\ & \left. + \frac{c}{eB_0 n_i} \hat{\mathbf{z}} \times \nabla (n_i T_i) \cdot \nabla + \mu_i \nabla_\perp^2 \right] \nabla_\perp \phi + (v_{i0} + v_{iz}) \frac{\mathbf{B}_1}{B_0} + \hat{\mathbf{z}} v_{iz}, \qquad (2.18) \end{aligned}$$

$$\mathbf{v}_j \approx \frac{c}{B_0} \hat{\mathbf{z}} \times \nabla \phi + \frac{cT_0}{eB_0 n_j} \hat{\mathbf{z}} \times \nabla n_j + (v_{j0} + v_{jz}) \frac{\mathbf{B}_\perp}{B_0} + \hat{\mathbf{z}} v_{jz}, \qquad (2.19)$$

where v_{iz} is the z-component of the ion velocity, ω_{ci} is the ion gyrofrequency, $\mu_i = 3\nu_i \rho_i^2/10$ is the coefficient of ion-gyroviscosity, ρ_i is the ion Larmor radius, ν_j is the collision frequency of jth species [113] and v_{jz} is the parallel component of the fluid velocity of the particle species $j(= e, p)$. For low-β plasma case, we may neglect the compressional magnetic field. Then magnetic and electric field perturbations can be expressed via corresponding potentials:

$$\mathbf{B}_1 = \mathbf{B}_\perp = \hat{\mathbf{z}} \times \nabla_\perp A_z, \mathbf{E} = -\nabla \phi - \hat{\mathbf{z}}\, \partial_t A_z, \qquad (2.20)$$

where A_z is the component of the vector potential along the z axis. Inserting (2.18) into the ion continuity equation (2.13) and letting $n_{i1} = n_i - n_{i0}$ and $T_{i1} = T_i - T_{i0}$, where $n_{i1} \ll n_{i0}$ and $T_{i1} \ll T_{i0}$, where $n_{i1}$and T_{i1} are respectively, perturbations in the equilibrium ion number density and temperature, we obtain

$$\begin{aligned} & \left(\mathcal{L}_t^i - \mathbf{v}_{Bi} \cdot \nabla - D_i \nabla_\perp^2 \right) N_i - \tau (\mathbf{v}_{Bi} - \mathbf{v}_{ni}) \cdot \nabla \Phi - \rho_i^2 \left[\mathcal{L}_t^i + \nu_i - \mathbf{v}_{Di0} \cdot \nabla + \mu_i \nabla_\perp^2 \right] \nabla_\perp^2 \Phi \\ & + \mathbf{v}_{Bi} \cdot \nabla T - \rho_i^2 \nabla \cdot \left[(\mathbf{v}_{Di1} \cdot \nabla) \nabla_\perp \Phi \right] + c_i\, \mathcal{L}_z V_i + \frac{T_0}{n_{i0} e} \nabla_\perp A_z \times \hat{\mathbf{z}} \cdot \nabla \left(\frac{J_{i0}}{eB_0} \right) = 0 \qquad (2.21) \end{aligned}$$

where $\mathcal{L}_t^i \equiv \partial_t + \mathbf{v}_{EB} \cdot \nabla + (v_{i0} + v_{iz}) \partial_z$, $\mathcal{L}_z = \partial_z + (T_0/eB_0) \nabla_\perp A_z \times \hat{\mathbf{z}} \cdot \nabla$ and $J_{i0} = e n_{i0} v_{iz}$.

The parallel component of the ion momentum equation can be written as

$$\left(\mathcal{L}_t^i + \nu_i + \mathrm{v}_{Di0} \cdot \nabla\right) V_i = -c_i \left[\left(\partial_z - \mathbf{S}_{vo}^i \cdot \nabla\right) \Phi + \frac{1}{c}\left(\mathcal{L}_t^i + \mathrm{v}_{Di0} \cdot \nabla\right) A_z + \tau^{-1} \mathcal{L}_z \left(T + N_i\right)\right]. \tag{2.22}$$

where $V_j = v_{jz}/\sqrt{(T_0/m_j)}$. Using Eq. (2.18) into the ion energy equation and using the ion continuity equation, we get

$$\left(\mathcal{L}_t^i + \frac{5}{3}\mathrm{v}_{Bi} \cdot \nabla - \frac{2\chi_i}{3n_{i0}}\nabla_-^2\right) T - \frac{2}{3}\mathcal{L}_t^i N_i - \tau\left(\eta_i - \frac{2}{3}\right) \mathrm{v}_{ni} \cdot \nabla\Phi = 0, \tag{2.23}$$

Substituting Eq. (2.19) into electron and positron continuity equation (2.16), we get

$$\left(\mathcal{L}_t^e - \mathrm{v}_{Be} \cdot \nabla - D_e\nabla_\perp^2\right) N_e - \left(\mathrm{v}_{Be} - \mathrm{v}_{ne}\right) \cdot \nabla\Phi + v_{te}\mathcal{L}_z V_e - \frac{T_0}{n_{e0}e}\nabla_\perp A_z \times \hat{\mathbf{z}} \cdot \nabla\left(\frac{J_{e0}}{eB_0}\right) = 0 \tag{2.24}$$

and

$$\left(\mathcal{L}_t^p + \mathrm{v}_{Bp} \cdot \nabla - D_p\nabla_\perp^2\right) N_p + \left(\mathrm{v}_{Bp} - \mathrm{v}_{np}\right) \cdot \nabla\Phi + v_{te}\mathcal{L}_z V_p + \frac{T_0}{n_{p0}e}\nabla_\perp A_z \times \hat{\mathbf{z}} \cdot \nabla\left(\frac{J_{p0}}{eB_0}\right) = 0. \tag{2.25}$$

Substituting the z-component of electric field into the parallel component of the resistive electron and positron momentum equation (2.17) and using Eq. (2.19), we obtain

$$\left(\mathcal{L}_t^e + \nu_e - \mathrm{v}_{ne} \cdot \nabla\right) V_e = v_{te}\left[\left(\partial_z + \mathbf{S}_{vo}^e \cdot \nabla\right) \Phi + \frac{1}{c}\left(\mathcal{L}_t^e + \mathrm{v}_{ne} \cdot \nabla\right) A_z - \mathcal{L}_z N_e\right] \tag{2.26}$$

and

$$\left(\mathcal{L}_t^p + \nu_p - \mathrm{v}_{np} \cdot \nabla\right) V_p = -v_{te}\left[\left(\partial_z - \mathbf{S}_{vo}^p \cdot \nabla\right) \Phi + \frac{1}{c}\left(\mathcal{L}_t^p + \mathrm{v}_{np} \cdot \nabla\right) A_z + \mathcal{L}_z N_p\right] \tag{2.27}$$

where $\mathcal{L}_t^j \equiv \partial_t + \mathrm{v}_{EB} \cdot \nabla + (v_{j0} + v_{jz})\partial_z$, $\mathbf{S}_{vo}^j(x) = (\hat{\mathbf{z}} \times \nabla v_{j0})/\omega_{cj}$, $J_{j0} = q_j n_{j0} v_{jz}$, $N_j = n_{j1}/n_{j0}$, $\mathbf{v}_{Bj} = (cT_{j0}/q_j B_0)\hat{\mathbf{z}} \times \nabla \ln B_0$ is the ∇B_0 drift, $\mathrm{v}_{nj} = (cT_{j0}/q_j B_0)\hat{\mathbf{z}} \times \nabla \ln n_{j0}$ is the ∇n_{j0} drift, D_j is the diffusion coefficient. Also, we have denoted $c_i = \sqrt{T_0/m_i}$, $\rho_i = c_i/\omega_{ci}$, $\Phi = e\phi/T_0$, $A_z = eA_z/T_0$, $T = T_{i1}/T_0$, $\tau = T_0/T_{i0}$, $v_{te} = \sqrt{T_0/m_e}$, $\mathrm{v}_{Ti} =$

$(cT_{i0}/eB_0)\hat{\mathbf{z}} \times \nabla \ln T_{i0}$ is the ∇T_{i0} drift and $\mathbf{v}_{Di1} = (cT_{i0}/eB_0)\hat{\mathbf{z}} \times \nabla (T_{i1}/T_{i0} + n_{i1}/n_{i0})$, $\mathbf{v}_{Di0} = (1+\eta_i)\mathbf{v}_{ni}$ is the zeroth order ion diamagnetic drift with $\eta_i \equiv d_x(\ln T_{i0})/d_x(\ln n_{i0})$.

To close our nonlinear system of equations, we may use the quasineutrality condition $N_{i1} = \alpha_e N_{e1} - \alpha_p N_{p1}$, $\alpha_p = n_{p0}/n_{i0}$, $\alpha_e = n_{e0}/n_{i0}$ and Ampere's law $j_z = e(n_i v_{iz} + n_p v_{pz} - n_e v_{ez}) = -(cT_0/4\pi e)\nabla_\perp^2 A_z$. Equations (2.21)-(2.27) are the desired nonlinear mode coupling equations to study the electromagnetic ITG-driven drift-dissipative and drift-Alfvén waves in an inhomogeneous e-p-i magnetoplasma with sheared plasma flows.

2.4 Derivation of Electrostatic Nonlinear Equations

Consider the nonlinear propagation of low-frequency electrostatic waves in a nonuniform collisional e-p-i magnetoplasma. In equilibrium, the e-p-i plasma satisfies the charge neutrality condition (2.12), which is justified as long as the ion plasma frequency (ω_{pi}) is much larger than the ion gyrofrequency (ω_{ci}). The ion dynamics, in electrostatic case, is governed by the same set of equations, i.e., Eqs. (2.13)-(2.15). For low-frequency modes (much less than the ion-gyrofrequency), the electrons and positrons are assumed to follow the Boltzmann distribution, such that

$$n_e = n_{e0}(x)\exp\left(\frac{e\phi}{T_{e0}}\right) \tag{2.28}$$

and

$$n_p = n_{p0}(x)\exp\left(-\frac{e\phi}{T_{p0}}\right), \tag{2.29}$$

where $T_{e0}(T_{p0})$ are the electron (positron) temperatures. For very low-frequency processes, the light particles (electrons and positrons) would thermalize very quickly to achieve the same temperature such that $T_{e0} = T_{p0} = T_0$.

Using Eq. (2.4), the ion-fluid velocity perturbation, including the effect of ion-gyroviscosity and neglecting the self-gravitational term, can be written as:

$$\begin{aligned}
\mathbf{v}_i \approx & \frac{c}{B_0}\hat{\mathbf{z}}\times\nabla\phi + \frac{c}{eB_0 n_i}\hat{\mathbf{z}}\times\nabla\left(n_i T_i\right) - \frac{c}{B_0\omega_{ci}}\left[\partial_t + \nu_j + \frac{c}{B_0}\hat{\mathbf{z}}\times\nabla\phi\cdot\nabla\right. \\
& \left. + \frac{c}{eB_0 n_i}\hat{\mathbf{z}}\times\nabla\left(n_i T_i\right)\cdot\nabla + \mu_i\nabla_\perp^2\right]\nabla_\perp\phi + \hat{\mathbf{z}}v_{iz}. \qquad (2.30)
\end{aligned}$$

Inserting Eq. (2.30) into Eqs. (2.13)-(2.15) and letting $n_{i1} = n_i - n_{i0}$ and $T_{i1} = T_i - T_{i0}$, where $n_{i1} \ll n_{i0}$ and $T_{i1} \ll T_{i0}$. Here, $n_{i1}$and T_{i1} are respectively, perturbations in the equilibrium ion number density and temperature. We obtain the following nonlinear set of equations for electrostatic case:

$$\begin{aligned}
& \left(\mathcal{L}_t^i + \mathbf{v}_{Bi}\cdot\nabla - D_i\nabla_\perp^2\right)N_i + \mathbf{v}_{Bi}\cdot\nabla T - \rho_i^2\left[\mathcal{L}_t^i + \nu_i + \mathbf{v}_{Di0}\cdot\nabla + \mu_i\nabla_\perp^2\right]\nabla_\perp^2\Phi \\
& + \tau(\mathbf{v}_{Bi} - \mathbf{v}_{ni})\cdot\nabla\Phi - \rho_i^2\nabla\cdot\left[\left(\mathbf{v}_{Di1}\cdot\nabla\right)\nabla_\perp\Phi\right] + c_i\partial_z V_i = 0, \qquad (2.31)
\end{aligned}$$

$$\left(\mathcal{L}_t^i + \nu_i + \mathbf{v}_{Di0}\cdot\nabla\right)V_i = -c_i\left[\left(\partial_z - \mathbf{S}_{vo}^i\cdot\nabla\right)\Phi + \tau^{-1}\partial_z\left(T + N_i\right)\right] \qquad (2.32)$$

and

$$\left(\mathcal{L}_t^i + \frac{5}{3}\mathbf{v}_{Bi}\cdot\nabla - \frac{2\chi_i}{3n_{i0}}\nabla_\perp^2\right)T - \frac{2}{3}\mathcal{L}_t^i N_i - \tau\left(\eta_i - \frac{2}{3}\right)\mathbf{v}_{ni}\cdot\nabla\Phi = 0. \qquad (2.33)$$

Eqs. (2.31)-(2.33) can also be obtained by setting $A_z = 0$ in Eqs. (2.21)-(2.23) respectively. To close our nonlinear system of equations, we may use the following quasineutrality condition,

$$N_i = \frac{1}{n_{i0}}\left(n_{e1} - n_{p1}\right) \approx \alpha_e e\phi/T_{e0} + \alpha_p e\phi/T_{p0} \approx \alpha\Phi, \qquad (2.34)$$

where $\alpha = N_0/n_{i0}$ and $N_0 = n_{e0} + n_{p0}$. Equations (2.31)-(2.34) are the desired nonlinear mode coupling equations to study the ITG-driven electrostatic waves in a collisional e-p-i magnetoplasma with sheared ion flows.

Chapter 3

Nonlinear Dynamics in Cold and Hot Ions Limits

3.1 Introduction

There have been a lot of studies of wave propagation in relativistic and non-relativistic pair plasmas, with [25, 35] or without [77, 78] the presence of ions, in cold [79] and hot [80] limits. Recently, it has been suggested in Ref. [55] that low-frequency drift waves can play an important role in the dynamics of pair plasmas comprising some concentration of ions. The nonlinear vortex structures have been investigated in this work in both electrostatic and electromagnetic limits. In the nonlinear electrostatic case, the drift waves can give rise to dipolar vortices. The equilibrium parallel ion flow effect has not been taken into account in some previous investigations [55, 79, 80]. In our opinion the system may become unstable in the linear limit, if a free energy source exists in the form of sheared ion flows. Therefore, in the first half of this chapter, we have presented an investigation of the nonlinear dynamics of low-frequency electrostatic waves in a magnetized nonuniform e-p-i plasma with sheared ion flows in the cold ion limit [56]. In our model the ion dynamics is governed by the ion continuity and momentum balance equations, whereas the electron and positron fluids are assumed to follow the Boltzmann distribution. We derive a new set of mode coupling equations. In the linear case, we found that the coupled ion acoustic and drift waves can become unstable due to nonuniform ion-flow in a collisionless plasma case. It is interesting to note that the ion acoustic wave becomes unstable in both homogeneous e-i and e-p-i plasmas. Physically, the instability arises because of the free energy available in equilibrium ion velocity gradient. In a collisional plasma a drift-dissipative instability may also arise under certain conditions. On the other hand, a quasi-stationary solution of the mode coupling equations can be represented in the form of monopolar vortex [56].

Quite recently, Shukla *et al.* [57], investigated the linear and nonlinear properties of obliquely propagating coupled low-frequency electrostatic-drift (ED) and ion-acoustic (IA) waves in a strongly magnetized nonuniform e-p-i plasma with sheared ion flows and it has been shown that weakly interacting ED-IA waves admit vortex chain and double vortex solutions. The effect of finite ion-temperature, which was not considered in the earlier investigations [56, 57], drastically modify the nonlinear dynamics and give rise to vortex structures in the form of quadrupolar vortices. Therefore, in the second half of this chapter, we have generalized the said work by considering a nonuniform strongly magnetized e-p plasma with ions at nonrelativistic hot temperature in the presence of sheared ion flows [58].

3.2 Cold Ions

3.2.1 Nonlinear Equations

Let us consider the nonlinear propagation of low-frequency (in comparison with the ion gyrofrequency) electrostatic waves in an e-p-i plasma in a uniform magnetic field $B_0 = B_0\ \hat{\mathbf{z}}$, where B_0 is the strength of external magnetic field which is directed along the z-axis. Furthermore, the electrons and positrons are assumed to be hot and ions are assumed to be cold. The ions have equilibrium velocity gradients which are maintained by some external sources. Equilibrium ion velocity $(\partial v_{i0}/\partial x)$, and density $(\partial n_{j0}/\partial x)$

gradients are assumed to be along the x-axis and, in equilibrium, e-p-i plasma satisfies the charge neutrality condition (2.12). We further assume that $D_i = \mu_i = 0$. Under these conditions, Eqs. (2.31), (2.32) and (2.34) can be combined to yield [56]

$$(d_t + \nu_i + v_{iz}\partial_z)v_{iz} - \frac{c}{B_0} J\left[\phi, v_{iz}\right] = -\frac{e}{m_i}\left[\partial_z - S_i\partial_y\right]\phi \tag{3.1}$$

and

$$\begin{aligned}(d_t + v_{iz}\partial_z)\phi - u_n\partial_y\phi - \alpha_1'\phi\partial_y\phi + \frac{T_0 n_{i0}}{e n_{e0}}(1+\delta)^{-1}\partial_z v_{iz} \\ -\rho_s^2\left[(d_t + \nu_i)\nabla_\perp^2\phi + \frac{c}{B_0}J[\phi, \nabla_\perp^2\phi]\right] - \rho_s^2\nabla\cdot\left[(v_{iz}\partial_z)\nabla_\perp\Phi\right] = 0,\end{aligned} \tag{3.2}$$

where $d_t \equiv \partial_t + v_{i0}\partial_z$, $u_n \equiv cT_0 d_x(n_{i0})/\left(eB_0 n_{e0}(1+\delta)\right)$, $\alpha_1' \equiv cT_0 d_x\left(F(x)\right)/\left(B_0 n_{e0}(1+\delta)\right)$, $\rho_s^2 \equiv cT_0 n_{i0}/\left(eB_0\omega_{ci} n_{e0}(1+\delta)\right)$, $\delta \equiv n_{p0}/n_{e0}$, $F(x) \equiv (n_{e0} + n_{p0})/T_0$, $S_i = (d_x v_{i0})/\omega_{ci}$ is the ion shear parameter and the Jacobian is defined as $J[a, b] \equiv (\partial_x a\partial_y b - \partial_y a\partial_x b)$. The pair of coupled equations (3.1) and (3.2) are the desired nonlinear mode coupling equations for the study of vortical motion in nonuniform collisional e-p-i magnetoplasma with sheared ion flows in the cold ion limit.

3.2.2 Linear Analysis

In the linear limit, we assume that ϕ and v_{iz} are proportional to $\exp\left[i\left(\mathbf{k}\cdot\mathbf{r} - \omega t\right)\right]$, where $\mathbf{k}$ and ω are the wavevector and the frequency, respectively. Equations (3.1) and (3.2) are transformed and combined to obtain a local dispersion relation

$$k_\perp^2\rho_s^2(\omega' + i\nu_i)^2 + (\omega' + k_y u_n)(\omega' + i\nu_i) - \frac{T_0 n_{i0} k_z^2}{m_i n_{e0}(1+\delta)}\left(1 - \frac{k_y S_i}{k_z}\right) = 0, \tag{3.3}$$

where $\omega' = \omega - k_z v_{i0}$ is the Doppler shifted frequency and $k_\perp^2 = k_x^2 + k_y^2$. For non-dissipative plasma, Eq. (3.3) reduces to

$$(1 - \rho_s^2 k_\perp^2)\omega'^2 + k_y u_n \omega' - \frac{T_0 n_{i0} k_z^2}{m_i n_{e0}(1+\delta)} \left(1 - \frac{k_y S_i}{k_z}\right) = 0, \tag{3.4}$$

which is the coupled equation for drift and ion-acoustic waves in the presence of sheared ion-flow (S_i-term). If we define modified ion acoustic velocity $c_s = \sqrt{n_{i0}T_0/(m_i n_{e0}(1+\delta))}$ and $\omega^* = -u_n k_y$, then the above equation can be re-written as

$$(1 + \rho_s^2 k_\perp^2)\omega'^2 - \omega^* \omega' - c_s^2 k_z^2 \left(1 - \frac{k_y S_i}{k_z}\right) = 0 \tag{3.5}$$

For a uniform density profile ($\omega^* = 0$), and assuming $k_y S_i / k_z \gg 1$, Eq. (3.5) becomes

$$(\omega - k_z v_{i0})^2 = -\frac{k_y k_z c_s^2 d_x(v_{i0})}{(1 + \rho_s^2 k_\perp^2)\,\omega_{ci}}. \tag{3.6}$$

It is evident from Eq. (3.6) that depending upon the magnitude and direction of the velocity gradient, the mode can become unstable. Thus the equilibrium shear flow is found to be responsible for the instability [56].

On the other hand, in the absence of ion background velocity, the dispersion relation (3.5) reduces to,

$$\omega^2 - \frac{\omega^*}{(1 + \rho_s^2 k_\perp^2)}\,\omega - \frac{c_s^2 k_z^2}{(1 + \rho_s^2 k_\perp^2)} = 0, \tag{3.7}$$

which is a dispersion relation [56] for the coupled ion acoustic and electrostatic drift-waves in electron-ion (e-i) plasmas in the limit $n_{z0} = 0$. Equation (3.5) admits two roots ($\omega_{1,2}$):

$$\omega_{1,2} = \frac{1}{2}\left[-b \pm \sqrt{b^2 - 4d}\right], \tag{3.8}$$

where

$$b = -\frac{\omega^*}{(1 + \rho_s^2 k_\perp^2)} \text{ and } d = \frac{c_s^2 k_z^2}{(1 + \rho_s^2 k_z^2)} \left|\frac{k_y S_i}{k_z} - 1\right|.$$

One of the modes become unstable if the linear and nonlinear propagation of ion acoustic and electrostatic drift-waves in an e-p-i plasma has $4d > b^2$.

Notice that the ion-acoustic wave can become unstable even if the plasma is homogeneous. The ion-acoustic instability can take place in both e-i and e-p-i plasmas due to $v_{i0}(x) \neq 0$. If $\nu_i \neq 0$ in Eq. (3.3), then a drift-dissipative instability may also occur under certain conditions. If we let $\omega = \omega_r + i\gamma$ and $\gamma^2 \ll \omega_r^2$, then the imaginary part of the mode can be written as

$$\gamma = -\frac{\nu_i \left(\omega^* + (1 + 2\rho_s^2 k_\perp^2)\omega_r\right)}{(2\omega_r - b)\left(1 + \rho_s^2 k_\perp^2\right)}. \tag{3.9}$$

Note that $\gamma > 0$ if $\omega_r < b/2$. Therefore, a drift-dissipative instability may exist in the presence of collisions and ion sheared flow.

3.2.3 Nonlinear Solutions

In the proceeding section, we have shown that how velocity gradient and collisions can cause instability of electrostatic drift waves and ion acoustic waves. However, the nonlinear interaction between finite amplitude modes can be responsible for the formation of ordered structures. Although, it is very difficult to find an analytical general stationary or non-stationary solution of Eqs. (3.1)-(3.2), we discuss here some approximate solutions. First, we present the nonlinear coherent vortex solutions of Eqs. (3.1) and (3.2). Accordingly, the stationary solution of equations (3.1) and (3.2) in the moving frame $\xi = y + \eta_0 z - u_0 t$, where η_0 is a constant and u_0 is the translational speed of the vortex, by ignoring dissipative term, can be re-written as:

$$\mathcal{L}_\phi \left[v_{iz} - \frac{e}{m_i U}\left(\eta_0 - S_i\right)\phi\right] = 0, \tag{3.10}$$

$$\left(U + u_n - \eta_0 v_{iz}\right)\partial_\xi \phi + \alpha_1' \phi \partial_\xi \phi - \rho_s^2 \left[U \partial_\xi \nabla_\perp^2 \phi - \frac{c}{B_0}\mathcal{J}[\phi, \nabla_\perp^2 \phi]\right] - \frac{T_0 n_{i0} \eta_0}{e n_{e0}(1+\delta)}\partial_\xi v_{iz} = 0, \tag{3.11}$$

where $U = u_0 - \eta_0 v_{i0}$, $\mathcal{L}_\phi = \partial_\xi - (c/UB_0)\left(\partial_x\phi\partial_\xi - \partial_\xi\phi\partial_x\right)$, $\nabla_\perp^2 = \partial^2/\partial x^2 + \partial^2/\partial\xi^2$ and the Jacobian is now defined as $\mathcal{J}[a, b] \equiv (\partial_x a\partial_\xi b - \partial_\xi a\partial_x b)$.

A typical solution of Eq. (3.10) is

$$v_{iz} = \frac{e}{m_i U}\left(\eta_0 - S_i\right)\phi.$$

Substituting the above value of v_{iz} in Eq. (3.11), we readily obtain

$$\left(U + u_n - \frac{U_*^2}{U}\right)\partial_\xi\phi + \left(\alpha_1' - \frac{\eta_0 e}{m_i U}(\eta_0 - S_i)\right)\phi\partial_\xi\phi - \rho_s^2 U\left[\partial_\xi\nabla_\perp^2\phi - \frac{c}{UB_0}\mathcal{J}[\phi, \nabla_\perp^2\phi]\right] = 0. \tag{3.12}$$

where $U_*^2 = T_0 n_{i0}\eta_0(\eta_0 - S_i)/\left(m_i n_{e0}(1+\delta)\right)$. It is somewhat difficult to find the general solution of Eq. (3.12) for a localized vortex solution. However, if we consider the case when the scalar nonlinearity is dominant compared with the Jacobian nonlinearity $\mathcal{J}[\phi, \nabla_\perp^2\phi]$, then we get

$$\rho_s^2\partial_\xi\nabla_\perp^2\phi - \left[1 + \frac{u_n}{U} - \left(\frac{U_*}{U}\right)^2\right]\partial_\xi\phi + \frac{\alpha_2'}{U}\phi\partial_\xi\phi = 0, \tag{3.13}$$

where $\alpha_2' = (\eta_0 e(S_i - \eta_0)/m_i U) - \alpha_1'$. If we normalize the space variables with ρ_s, we may integrate Eq. (3.13) and obtain the following result:

$$\nabla_\perp^2\phi - \left[1 + \frac{u_n}{U} - \left(\frac{U_*}{U}\right)^2\right]\phi + \frac{\alpha_2'}{2U}\phi^2 = 0. \tag{3.14}$$

Equation (3.14) admits spatially bounded monopolar vortex type solution [81] for $(1 + u_n/U - U_*^2/U^2) = 1$ and $\alpha_2'/2U = 1$.

3.3 Hot Ions

3.3.1 Nonlinear Equations

Let us consider the nonlinear propagation of low-frequency (in comparison with the ion gyrofrequency $\omega_{ci} = eB_0/m_i c$, where e is the magnitude of the electron charge, m_i is the mass of ion, c is the speed of light, and $B_0(x)$ is the strength of external nonuniform magnetic field which is pointing along the z-axis) electrostatic waves in a nonuniform e-p-i magnetoplasma. In equilibrium, there exists ion-drift velocity $\hat{\mathbf{z}}\ v_{i0}(x)$ which has a gradient along the x-axis and e-p-i plasma satisfies the charge neutrality condition (2.12). For low-frequency waves and for inertialess electrons and positrons, the pressure gradient of electrons/positrons is balanced by electrostatic force which leads to Boltzmann distribution of electrons and positrons. Assuming $D_i = \nu_i = \mu_i = 0$, Eqs. (2.31), (2.32) and (2.34) can be combined in the limit of hot ions at non-relativistic temperature T_{i0} (with $T_{i0} \neq 0$) to give [58]

$$
\begin{aligned}
&D_t\phi + u_n^*\partial_y\phi - \alpha_3'\phi\partial_y\phi + \mathbf{v}_{Bi}\cdot\nabla\phi - \rho_s^2\left(D_t + \mathbf{v}_{ni}\cdot\nabla\right)\nabla_\perp^2\phi \\
&-\rho_s^2\left(\mathbf{v}_{ni1}\cdot\nabla\right)\nabla_\perp^2\phi + (\frac{T_0}{e\alpha})\partial_z v_{iz} = 0
\end{aligned}
\tag{3.15}
$$

and

$$
(D_t + v_{iz}\partial_z)v_{iz} = -\frac{e}{m_i}\left[\left(1+\alpha\tau^{-1}\right)\partial_z - S_i\partial_y\right]\phi, \tag{3.16}
$$

where $D_t = \partial_t + \mathbf{v}_{EB}\cdot\nabla + v_{iz}\partial_z$, $\tau = T_0/T_{i0}$, $u_n^* = -\rho_s c_s\partial_x\left(n_{i0}/B_0\right)$, $\alpha = N_0/n_{i0}$, $\alpha_3' = c/B_0\partial_x\ln\left(N_0/B_0\right)$, $\mathbf{v}_{ni1} = \left(cT_{i0}/eB_0 n_{i0}\right)\hat{\mathbf{z}}\times\nabla n_{i1}$ is the diamagnetic drift velocity, $S_i = (d_x v_{i0})/\omega_{ci}$ is the ion shear parameter and $\rho_s = c_s/\omega_{ci}$ is the ion gyro-radius with $c_s = \sqrt{(n_{i0}T_0)/(N_0 m_i)}$.

Let us introduce the normalized parameters $t' = c_s t/L_{ni}$, $x' = x/\rho_s$, $y' = y/\rho_s$, $z' = z/L_{ni}$, $L_{ni} = \left[d_x(\ln n_{i0})\right]^{-1}$, $v_{iz}' = L_{ni}v_{iz}/(\rho_s c_s)$, $\phi' = \left(e\phi L_{ni}N_0\right)/\left(\rho_s n_{i0}T_0\right)$. Hereafter, we shall drop the superscript prime for simplicity of the notation. Thus equations (3.15) and (3.16) take the following form

$$\partial_t(1-\nabla_\perp^2)\phi - \alpha_4'\phi\partial_y\phi - \left(1+\alpha\tau^{-1}\right) J\left[\phi, \nabla_\perp^2\phi\right]$$
$$-\left[1-(\alpha+\tau)K_{Bi} + \alpha\tau^{-1}\nabla_\perp^2\right]\partial_y\phi + \partial_z v_{iz} = 0, \tag{3.17}$$

and

$$\mathcal{L}_t v_{iz} = \left[(d_x v_{i0})\,\partial_y - \left(1+\alpha\tau^{-1}\right)\partial_z\right]\phi, \tag{3.18}$$

where $\mathcal{L}_t \equiv \partial_t + (\partial_x\phi\partial_y - \partial_y\phi\partial_x)$, $\alpha_4' = (\partial_x \ln N_0 - \tau\delta_i K_{Bi})$, $\delta_i = \rho_s/L_{ni}$, $K_{Bi} = L_{ni}/(\tau L_{Bi})$ and $L_{ni}(L_{Bi})$ represents the magnitude of equilibrium density (magnetic field) inhomogeneity scale length. Equations (3.17)–(3.18) are the governing equations for non-linearly coupled electrostatic waves in a nonuniform warm e-p-i magnetoplasma with sheared ion flows which is produced by a radial electric field.

3.3.2 Linear Analysis

In this section, we present a derivation of linear dispersion relation by neglecting the nonlinear terms in Eqs. (3.15)-(3.16) and by assuming that the perturbation wavelength is much smaller than the scale lengths of the equilibrium velocity, density and magnetic field gradients. The governing equations (3.15) and (3.16) are then Fourier transformed by assuming that the perturbed quantities ϕ and v_{iz} vary as $\exp\left[i\left(\mathbf{k}\cdot\mathbf{r}-\omega t\right)\right]$, where $\mathbf{k}$ and ω are the wavevector and the frequency, respectively. Thus, from Eqs. (3.15) and (3.16), we obtain the following dispersion relation [58]

$$(1+k_\perp^2\rho_s^2)\Omega^2 - \left[\left(1+\alpha^{-1}\tau\right)\omega_{Bi} - \left(\alpha^{-1}\tau - k_\perp^2\rho_s^2\right)\omega_{ni}\right]\Omega$$
$$-c_s^2k_z^2\left[(1+\alpha^{-1}\tau) - \frac{k_y S_i}{k_z}\right] = 0, \tag{3.19}$$

where $\Omega = \omega - \mathbf{k}\cdot\mathrm{v}_{i0}$ is the Doppler shifted frequency, $k_\perp^2 = k_x^2 + k_y^2$, $\omega_{ni} = \mathbf{k}\cdot\mathrm{v}_{ni}$ and $\omega_{Bi} = \mathbf{k}\cdot\mathrm{v}_{Bi}$ are the ion diamagnetic and magnetic-drift frequencies, respectively. Equation (3.19) shows that drift and ion acoustic waves are coupled in the presence of ion sheared flow and finite Larmor radius effects.

For uniform density plasma case and in the limit of vanishing perpendicular ion inertia ($k_\perp \rho_s = 0$) and for homogeneous magnetic field case, the above dispersion relation reduces to

$$(\omega - \mathbf{k}\cdot\mathbf{v}_{i0})^2 = c_s^2 k_z^2 \left[(1+\alpha^{-1}\tau) - \frac{k_y S_i}{k_z}\right]. \tag{3.20}$$

This shows that ion acoustic mode would become unstable due to equilibrium sheared ion flows.

On the other hand, for homogeneous magnetic field case and in the absence of ion streaming flow and $k_\perp \rho_s = 0$, the local dispersion relation becomes

$$\omega^2 + \omega_{*n}\omega - c_s^2 k_z^2 (1+\alpha^{-1}\tau) = 0, \tag{3.21}$$

which is the dispersion relation of coupled ion acoustic waves and drift waves in electron-ion plasma with $n_{p0} = 0$. Here $\omega_{*n} = \alpha^{-1}\tau\omega_{ni}$.

Further, equation (3.19) predicts instability of the ion drift waves for a finite value of sheared flow parameter (S_i) with $\omega_{Bi} = 0 = k_\perp \rho_s$, $k_y S_i / k_z > (1+\alpha^{-1}\tau)$ and $k_y k_z c_s^2 |S_i| \gg \omega_{*n}^2$. The growth rate of the instability is given by

$$\gamma = \sqrt{k_y k_z c_s^2 |S_i| - \omega_{*n}^2/4}. \tag{3.22}$$

3.3.3 Nonlinear Solution

In the following section, we present a possible solution of Eqs. (3.17) and (3.18) by involving vortex scenario, i.e., we search for travelling solutions that are stationary in a reference frame which is moving with some velocity u_0. We introduce a new frame $\xi = y + \eta_0 z - u_0 t$, where η_0 and u_0 are constants, and assume that ϕ and v_{iz} are functions of x and ξ only. The effect of equilibrium perpendicular ion flow velocity which is caused by the radial electric field $-\nabla\phi_0$, is incorporated in the $\mathbf{E}\times\mathbf{B}$ drift by writing down the total electrostatic potential as a sum of equilibrium (ϕ_0) and perturbed (ϕ)

potentials. We choose the equilibrium potential $\phi_0 \approx V_{\perp 0}(x-x_0) + \frac{1}{2}V'_{\perp 0}(x-x_0)^2$, such that it describes only the linearly varying perpendicular flows[24]. Since the flow is sheared, we may assume Gaussian type density and magnetic field profiles, so that we may approximate $K_{Bi} \approx K_{Bi0} + K_{Bi1}x$. With this choice of K_{B}, and ϕ_0, equations (3.17) and (3.18) can be re-written as

$$\partial_\xi v_{iz} = \partial_\xi \phi. \tag{3.23}$$

Ignoring the scalar nonlinearity[22, 25] in Eq. (3.17) and using Eq. (3.23), we get

$$\mathcal{J}\left[\phi - \nabla_\perp^2\phi - \frac{(\tau K_{Bi1} - V'_{\perp 0})(x-x_1)^2}{2}, \phi + \frac{V'_{\perp 0}(x-x_2)^2}{2}\right] = 0. \tag{3.24}$$

where

$$x_1 = \left((V_{\perp 0} - V'_{\perp 0}x_0) + \left(1 - \eta_0 - \alpha\tau^{-1} - (\alpha+\tau)K_{Bi0}\right)\left(1+\alpha\tau^{-1}\right)^{-1}\right) / \left(\tau K_{Bi1} - V'_{\perp 0}\right).$$

and

$$x_2 = \left(\left(u_0 + \alpha\tau^{-1}\right)\left(1+\alpha\tau^{-1}\right)^{-1} - \left(V_{\perp 0} + V'_{\perp 0}x_0\right)\right) / V'_{\perp 0}.$$

Setting $x_1 = x_2$, we may write the general solution of Eq. (3.24) as

$$\left(\nabla_\perp^2 - 1\right)\varphi + bX^2 = F\left(\varphi + X^2\right), \tag{3.25}$$

where $\varphi = 2\phi/V'_{\perp 0}$, $b = \left(\tau K_{Bi1} - V'_{\perp 0}\right)/V'_{\perp 0}$, $X = (x - x_1)$ and F is an arbitrary function of the given argument and we choose it as a linear one, i.e., $F \approx F_0 + (\varphi + X^2)F_1$. With this choice of F, we can re-write Eq. (3.25) as

$$\left(\nabla_\perp^2 - 1\right)\varphi + bX^2 = F_0 + \left(\varphi + X^2\right)F_1 \tag{3.26}$$

A localized quadrupolar vortex solution can be obtained, if we divide the space by a circle of radius r_0 and solve Eq. (3.26) by using cylindrical coordinates in which

$r = (X^2 + Y^2)^{1/2}$ and $\theta = \arctan(Y/X)$ independently outside and inside a circle, such that the constants F_0 and F_1 can have different values in these regions.

For outer solution, we may write

$$\left[\nabla_\perp^2 - (1+F_1^{out})\right]\varphi^{out} + bX^2 - F_0^{out} - F_1^{out}X^2 = 0.$$

By letting $F_0^{out} = 0$ and $\lambda_1^2 = (1 + F_1^{out})$ and $F_1^{out} = b$, the above equation takes the following form:

$$\left[\nabla_\perp^2 - \lambda_1^2\right]\varphi^{out} = 0.$$

The general solution of the above equation can be written as a combination of Bessel functions, such that

$$\varphi^{out}(r,\theta) = \beta_0 K_0(\lambda_1 r) + \beta_2 K_2(\lambda_1 r)\cos 2\theta, \quad r > r_0 \tag{3.27}$$

where $K_{0,2}$ are the modified Bessel functions of the given order.

For the inner solution, Eq. (3.26) can be re-written as

$$\left[\nabla_\perp^2 - \left(1 + F_1^{in}\right)\right]\varphi^{in} + bX^2 - F_0^{in} - F_1^{in}X^2 = 0.$$

If we let $\lambda_2^2 = -\left(1 + F_1^{in}\right)$, then we have

$$\left[\nabla_\perp^2 + \lambda_2^2\right]\varphi^{in} - F_0^{in} + (b - F_1^{in})X^2 = 0.$$

The solution of above differential equation takes the following form:

$$\varphi^{in}(r,\theta) = \alpha_0 J_0(\lambda_2 r) - A\frac{r^2}{2} - B + \left[\alpha_2 J_2(\lambda_2 r) - A\frac{r^2}{2}\right]\cos 2\theta, r < r_0, \tag{3.28}$$

where $A = (b - F_1^{in})/\lambda_2^2$ and $B = -(F_0^{in}/\lambda_2^2 + 2(b - F_1^{in})/\lambda_2^4)$. Here, $J_{0,2}$ are the zero and second order Bessel functions of the first kind, and the unknown constants β_0, β_2, α_0,

α_2, A, B, and λ_2 can be found from the appropriate continuity conditions at the given circle, i.e., from the continuity of the function Γ, the continuity of the potential φ and the continuity of $\partial\varphi/\partial r$ at $r = r_0$ [82].

The above continuity conditions yield the following set of equations:

$$F_1^{out}\left(\beta_0 K_0(\lambda_1 r_0) + r_0^2\right) = F_0^{in} + F_1^{in}\left[\alpha_0 J_0\left(\lambda_2 r_0\right) + \left(1 - \frac{A}{2}\right) r_0^2 - B\right], \tag{3.29}$$

$$\beta_0 K_0(\lambda_1 r_0) = \alpha_0 J_0\left(\lambda_2 r_0\right) - \frac{A}{2} r_0^2 - B. \tag{3.30}$$

$$\beta_0 K_0'(\lambda_1 r_0) = \alpha_0 J_0'\left(\lambda_2 r_0\right) - A r_0. \tag{3.31}$$

$$\beta_2 K_2(\lambda_1 r_0) + r_0^2 = 0, \tag{3.32}$$

$$\alpha_2 J_2\left(\lambda_2 r_0\right) + \left(1 - \frac{A}{2}\right) r_0^2 = 0, \tag{3.33}$$

and

$$\beta_2 K_2'(\lambda_1 r_0) = \alpha_2 J_2'\left(\lambda_2 r_0\right) - A r_0. \tag{3.34}$$

From Eqs. (3.32) and (3.33), we get

$$\beta_2 = -\frac{r_0^2}{K_2\left(\lambda_1 r_0\right)}, \tag{3.35}$$

$$\alpha_2 = -\frac{(1 - A/2)}{J_2\left(\lambda_2 r_0\right)} r_0^2, \tag{3.36}$$

Substituting the values of α_2 and β_2 using Eqs. (3.35) and (3.36) into Eq. (3.34), we obtain the following nonlinear dispersion relation

$$r_0 \frac{K_2'\left(\lambda_1 r_0\right)}{K_2\left(\lambda_1 r_0\right)} = \left(1 - \frac{A}{2}\right) r_0 \frac{J_2'\left(\lambda_2 r_0\right)}{J_2\left(\lambda_2 r_0\right)} + A, \tag{3.37}$$

where the prime denotes the derivative with respect to r at $r = r_0$. Choosing $b = 1$ and $\lambda_1 = 1.41$, and $r_0 = 2$, from equations (3.29)-(3.37), we may find the other unknown constants.

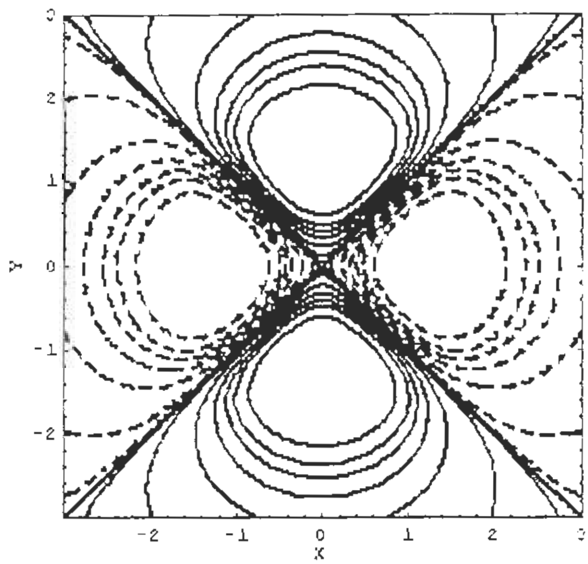

Figure 3-1: Contour plot of quadrupolar vortex given by Eqs. (3.27) and (3.28). The dashed lines represent negative values of the potential.

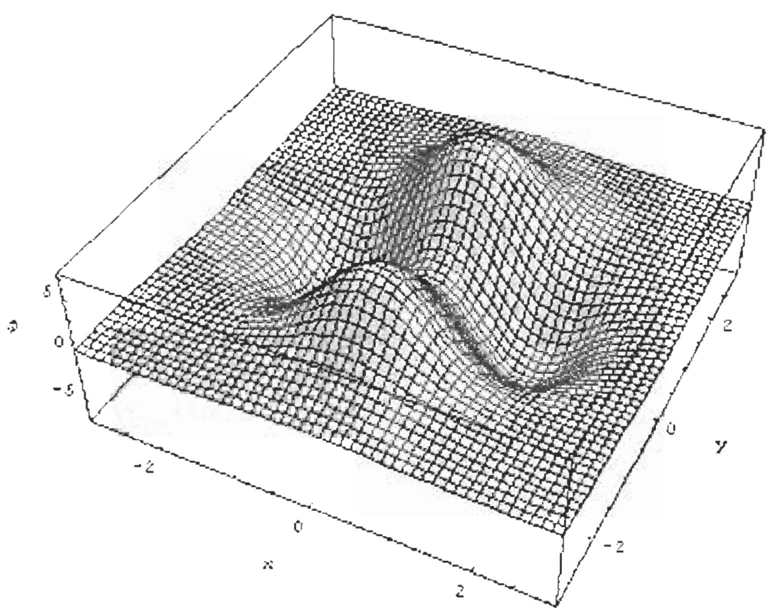

Figure 3-2: Three-dimensional view of the potential for the quadrupolar vortex from Fig 3-1.

The contour plot of the quadrupole vortex solution is given in Fig. 3-1. The contours show a dipole vortex between the lobes of an other dipole-like structure. The dashed lines represents negative values of the potential ϕ. The 3D-view of the vortex is presented in Fig. 3-2

3.4 Summary

In the first half of this chapter, linear and nonlinear propagation of ion acoustic and electrostatic drift waves in an e-p-i plasma have been investigated in the presence of ion sheared flow along the external magnetic field. It has been found that the free energy available in the form of shear flow can give rise to electrostatic instabilities of ion acoustic and drift waves in the linear limit. It is important to note that the ion acoustic wave can become unstable in both e-i and e-p-i plasmas due to ion shear flow even in the absence of density gradient. In the presence of ion collisions a drift-dissipative instability may also take place under suitable conditions. On the other hand, when the finite amplitude disturbances weakly interact among themselves, the nonlinear coupling of various modes may lead to the formation of coherent nonlinear structures (monopolar vortex) in a collisionless plasma.

In the second half of this chapter, we have studied the linear and nonlinear dynamics of low-frequency ion-acoustic and drift-waves in a nonuniform e-p-i plasma with sheared ion flow. In the linear case, we have shown that ion-acoustic and electrostatic drift-waves become unstable due to equilibrium sheared ion flow. In the nonlinear case, we have shown that for some specific profiles of the equilibrium density and sheared plasma flows, the nonlinear equations admit quadrupolar vortices.

Chapter 4

Nonlinear Dynamics of ITG-driven Electrostatic Waves

4.1 Introduction

A plasma is said to be in a state of stable thermodynamic equilibrium, if it has a Maxwellian velocity distribution and is homogeneous in space. If the plasma is inhomogeneous or different kinds of free energy sources are available to drive instabilities, then the state of plasma will always be a non-equilibrium state. Coulomb collisions would drive transport in an inhomogeneous plasma by scattering particles from one gyro-orbit to another. In a turbulent plasma the collective turbulent field has a similar influence to the microscopic field in Coulomb collisions. There is, however, a phase difference required between density or temperature perturbation and electric field perturbation to obtain a net transport. For turbulence driven by linear instabilities, this phase difference is caused by the linear growth. The linear growth thus acts as a source of turbulence, at the same time giving a correlation between density or temperature perturbation and driving electric field necessary for transport. Among other instabilities, several experimental results are in favor of ITG mode (also known as η_i-mode, where $\eta_i = d\ln T_i/d\ln n_i$) as a major candidate for explaining anomalous transport. The η_i instability was first discovered by

Rudakov and Sagdeev [83], within the context of a local fluid analysis in a slab geometry, where it was shown that the growth of the ionic-electrostatic-wave was caused by a continuous inflow of heat from a region with a high unperturbed temperature into the region where the temperature was rising on account of the compression due to the plasma wave under the conditions of zero density gradient and finite temperature gradient. Later, Kadomtsev and Pogutse [84] presented a detailed analysis which was based on the fluid and kinetic models, and derived local dispersion relation, the critical value of η_i for the marginal stability and localization of mode based on local approximation. Hahm and Tang [85] have presented some new properties of ITG mode in the presence of magnetic shear.

Recently, a great deal of interest has aroused in the study of ITG modes. Several authors [86-89] have investigated the ITG mode by employing Braginskii's transport equations for the ions and Boltzmann distribution for the electrons. Shukla *et al.* [90] extended the work of Jarmen *et al.* [91] by including the parallel ion dynamics for the electrostatic ITG mode for a nonuniform magnetized plasma. Therefore, due to the importance of ITG mode, we have extended our earlier work [56, 58] and this chapter presents same extension [59] dealing with the nonlinear dynamics of low-frequency ITG-driven electrostatic waves in a collisionless e-p-i magnetoplasma in the presence of equilibrium density, temperature, magnetic field, velocity and electrostatic potential gradients. In our model the ion dynamics is governed by the ion continuity, momentum and energy balance equations, whereas the electron and positron fluids are assumed to follow the Boltzmann distributions. We have also incorporated the self-gravitational effect of ions and showed that possible stationary solutions of the nonlinear equations can be represented in the form of dipolar and tripolar vortices of gravitational potential.

4.2 Electrostatic ITG Modes

4.2.1 Nonlinear Equations

We consider e-p-i plasma embedded in an inhomogeneous external magnetic field $B_0(x)$ $\hat{\mathbf{z}}$, where B_0 is the strength of external magnetic field and $\hat{\mathbf{z}}$ is the unit vector along the z-axis. The plasma also contains equilibrium ion velocity $(\partial_x v_{i0})$, equilibrium ion-temperature $(\partial_x T_{i0})$ and density $(\partial_x n_{j0})$ gradients, which are maintained by external sources. In equilibrium, the e-p-i plasma satisfies the charge neutrality condition (2.12). Eqs. (2.31)-(2.34) for electrostatic ITG mode, and for collisionless case (i.e. $D_i = \nu_i = \mu_i = 0$), can be rewritten as [59]

$$(d_t + v_{iz}\partial_z)v_{iz} + \frac{c}{B_0}J\left[\phi, v_{iz}\right] = -\frac{e}{m_i}\left[\left\{\left(1+\alpha\tau^{-1}\right)\partial_z - S_i(x)\partial_y\right\}\phi + \partial_z\left(\frac{T_{i1}}{e}\right)\right], \quad (4.1)$$

$$\left(d_t + \frac{5}{3}\mathbf{v}_{Bi}\cdot\nabla\right)T_{i1} + \frac{c}{B_0}J\left[\phi, T_{i1}\right] - \frac{2e\alpha\tau^{-1}c}{3B_0}\partial_x\left(\ln N_0\right)\phi\partial_y\phi$$
$$-\frac{2}{3}e\alpha\tau^{-1}d_t\phi - e\left(\eta_i - \frac{2}{3}\right)\mathbf{v}_{ni}\cdot\nabla\phi = 0 \quad (4.2)$$

and

$$(d_t + v_{iz}\partial_z)\left(1-\rho_s^2\nabla_\perp^2\right)\phi + u_n^*\partial_y\phi - \alpha_3'\phi\partial_y\phi + \mathbf{v}_{Bi}\cdot\nabla\phi + \tau\left(\alpha e\right)^{-1}\mathbf{v}_{Bi}\cdot\nabla T_{i1}$$
$$-\rho_s^2\left[\left(\mathbf{v}_{Di0}\cdot\nabla\right)\nabla_\perp^2\phi - \frac{c}{B_0}J\left[\phi, \nabla_\perp^2\phi\right]\right] - \rho_s^2\nabla\cdot\left[\left(\mathbf{v}_{Di1}\cdot\nabla\right)\nabla_\perp\phi\right] + \frac{m_i c_s^2}{e}\partial_z v_{iz} = 0 \quad (4.3)$$

where $d_t \equiv \partial_t + v_{i0}\partial_z$, $S_i(x) = (d_x v_{i0})/\omega_{ci}$ is the ion shear flow parameter, $N_0 = n_{e0} + n_{p0}$, $\alpha_3' = c/B_0\partial_x \ln\left(N_0/B_0\right)$, $u_n^* = -\rho_s c_s \partial_x \ln\left(n_{i0}/B_0\right)$, $c_s = \sqrt{(n_{i0}T_0/N_0 m_i)}$ is the ion acoustic speed, $\rho_s = c_s/\omega_{ci}$, $\tau = T_0/T_{i0}$, $\alpha = N_0/n_{i0}$, $\mathbf{v}_{Bi} = (cT_{i0}/eB_0)\hat{\mathbf{z}}\times\nabla\ln B_0$ is the ion ∇B_0 drift, $\mathbf{v}_{ni} = (cT_{i0}/eB_0)\hat{\mathbf{z}}\times\nabla\ln n_{i0}$ is the ∇n_{i0} drift, $\mathbf{v}_{Ti} = (cT_{i0}/eB_0)\hat{\mathbf{z}}\times\nabla\ln T_{i0}$ is the ∇T_{i0} drift, $\mathbf{v}_{Di1} = (cT_{i0}/eB_0)\hat{\mathbf{z}}\times\nabla\left(T_{i1}/T_{i0} + n_{i1}/n_{i0}\right)$ and the zeroth order ion diamagnetic drift velocity $\mathbf{v}_{Di0} = (1-\eta_i)\mathbf{v}_{ni}$ with $\eta_i \equiv d_x(\ln T_{i0})/d_x(\ln n_0)$. Equations

(4.1)-(4.3) are the desired nonlinear mode coupling equations to study the ITG-driven electrostatic waves in an inhomogeneous e-p-i magnetoplasma with sheared ion flows.

4.2.2 Linear Analysis

In this section, we present a derivation of linear dispersion relation. In the linear limit, we neglect the nonlinear terms in Eqs. (4.1)-(4.3) and assume that ϕ, T_{i1} and v_{iz} are proportional to $\exp\left[-i\left(\omega t - \mathbf{k}\cdot\mathbf{r}\right)\right]$, where $\mathbf{k}$ and ω are the wavevector and the frequency of the perturbed quantities, respectively. Equations (4.1)-(4.3) become

$$\Omega v_{iz} = \frac{e}{m_i}k_z\left[\left(1-\alpha\tau^{-1}-\frac{S_i k_y}{k_z}\right)\phi + \frac{T_{i1}}{e}\right], \tag{4.4}$$

$$\left(\Omega - \frac{5}{3}\omega_{Bi}\right)T_{i1} = \left[\frac{2}{3}e\alpha\tau^{-1}\Omega - e\left(\omega_{Ti} - \frac{2}{3}\omega_{ni}\right)\right]\phi \tag{4.5}$$

and

$$\begin{aligned}&\left[\Omega\left(1+k_\perp^2\rho_s^2\right) - \omega_{Bi}\left(1+\alpha\tau^{-1}\right) + \omega_{ni}\left(\alpha\tau^{-1} - k_\perp^2\rho_s^2\right) - \omega_{Ti}\left(k_\perp^2\rho_s^2\right)\right]\phi\\ &-\frac{\alpha^{-1}\tau}{e}\omega_{Bi}T_{i1} - \frac{m_i c_s^2}{e}k_z v_{iz} = 0,\end{aligned} \tag{4.6}$$

where $\Omega = \omega - \mathbf{k}\cdot\mathbf{v}_{i0}$ is the Doppler shifted frequency, $\omega_{ni} = \mathbf{k}\cdot\mathbf{v}_{ni}$ ion-density drift frequency, $\omega_{Bi} = \mathbf{k}\cdot\mathbf{v}_{Bi}$, and $\omega_{Ti} = \mathbf{k}\cdot\mathbf{v}_{Ti}$. Combining Eqs. (4.4), (4.5) and (4.6), we obtain a local dispersion relation

$$\begin{aligned}&\Omega(\Omega - \frac{5}{3}\omega_{Bi})[\Omega(1+k_\perp^2\rho_s^2) - \omega_{Bi}(1+\alpha\tau^{-1}) + \omega_{ni}(\alpha\tau^{-1} - k_\perp^2\rho_s^2) - \omega_{Ti}(k_\perp^2\rho_s^2)]\\ &-(\Omega\omega_{Bi} + \alpha\tau^{-1}c_s^2k_z^2)[\frac{2}{3}\Omega - \alpha^{-1}\tau(\omega_{Ti} - \frac{2}{3}\omega_{ni})] - (\Omega - \frac{5}{3}\omega_{Bi})[(1+\alpha\tau^{-1})c_s^2k_z^2\\ &-k_y k_z c_s^2 S_i(x)] = 0\end{aligned} \tag{4.7}$$

In the absence of ion sheared flow and uniform equilibrium temperature and magnetic field case, the above dispersion relation takes the following form for $\omega \gg \tau\omega_{ni}/(\tau + 5\alpha/3)$

and $k^2 v_{ti}^2/\omega_{ci} \ll 1$:

$$\omega^2\left(1+k_\perp^2\rho_s^2\right)+\alpha\tau^{-1}\omega_{ni}\omega-\left(1+\frac{5\alpha}{3\tau}\right)k_z^2c_s^2=0. \tag{4.8}$$

The above dispersion relation is the usual coupled drift and modified ion-acoustic waves in e-p-i plasma. Here the modified ion acoustic velocity $c_s \equiv \sqrt{n_{i0}T_0/m_i(n_{e0}+n_{p0})}$. For a uniform density plasma ($\omega_{ni}=0$) case, we have the following modified ion-acoustic mode

$$\omega=\frac{(1+5\alpha/3\tau)^{1/2}}{\sqrt{(1+k_\perp^2\rho_a^2)}}k_zc_s. \tag{4.9}$$

However, for $\omega \gg k_zc_s$, we have the usual drift waves defined by

$$\omega=\frac{\alpha\tau^{-1}\omega_{ni}}{(1+k_\perp^2\rho_s^2)}. \tag{4.10}$$

Similarly, if we consider a uniform density plasma case in which $\omega_{ni}=0$, with $k_\perp\rho_s=0$ and neglecting the parallel ion dynamics with $k_z=0$, Eq. (4.7) takes the following form

$$\omega^2-(\frac{10}{3}+\alpha^{-1}\tau)\omega_{Bi}\omega+\omega_{Bi}^2[\frac{5}{3}(1+\alpha^{-1}\tau)+\alpha^{-1}\tau\frac{\omega_{Ti}}{\omega_{Bi}}]=0. \tag{4.11}$$

The roots of above equation are

$$\omega=\omega_{Bi}\left[\frac{5}{3}+\frac{\tau}{2\alpha}\pm(\frac{\tau}{\alpha})^{1/2}\sqrt{\eta_\tau-L_{Bi}/L_{Ti}}\right], \tag{4.12}$$

where $\eta_\tau=(10\alpha/9\tau+\tau/4\alpha)$. Notice that the modified ion-temperature-gradient mode becomes unstable, if $\eta_\tau < L_{Bi}/L_{Ti}$, with a growth rate [59]

$$\gamma=\omega_{Bi}\left(\frac{\tau}{\alpha}\right)^{1/2}|L_{Bi}/L_{Ti}-\eta_\tau|^{1/2}, \tag{4.13}$$

where L_{Bi} and L_{Ti} are the scale lengths of magnetic field and equilibrium temperature gradients, respectively.

Furthermore, if we consider homogeneous magnetic field case, Eq. (4.7) yields the following result

$$\Omega(1 + k_\perp^2\rho_s^2) + \left(\alpha^{-1}\tau - k_\perp^2\rho_s^2\right)\omega_{ni} - k_\perp^2\rho_s^2\omega_{Ti}$$
$$-\frac{k_z^2c_s^2}{\Omega}\left[\left(1+\frac{5\alpha}{3\tau}\right) - \frac{k_yS_i}{k_z} + \frac{(2/3)\omega_{ni} - \omega_{Ti}}{\Omega}\right] = 0. \tag{4.14}$$

For uniform density plasma, Eq. (4.14) for $\omega_{Ti} \gg \Omega(1+5\alpha/3\tau)$ and $k_\perp^2\rho_s^2 = 0$, reduces to

$$\Omega^3 + (k_yk_zc_a^2S_i)\Omega + k_z^2c_a^2\omega_{Ti} = 0. \tag{4.15}$$

This equation represents a dispersion relation for the coupled ion-acoustic and electrostatic ion-temperature-gradient mode in the presence of sheared ion flow. One of the roots of the above cubic dispersion relation would always be unstable irrespective the direction of the shear and ion-temperature gradient. Furthermore, the earlier results of Mirza *et al.* [56], can be recovered from Eq. (4.14) by considering the cold ion case.

On the other hand, Eq. (4.14) with $v_{i0} = 0$ reduces to

$$\omega^3 = -k_z^2c_s^2\omega_{Ti}. \tag{4.16}$$

This cubic equation predicts the Rudakov-Sagdeev [83] instability which has been modified in this case for e-p-i plasma. The growth rate of the instability can be expressed as [59],

$$\gamma = \frac{\sqrt{3}}{2}\left|k_z^2c_s^2\omega_{Ti}\right|^{1/3}. \tag{4.17}$$

4.2.3 Nonlinear Solutions

In the proceeding section, we have shown that how velocity, temperature, density and magnetic field gradients causes instability of electrostatic drift waves and modified ion acoustic waves. At a certain stage in the development of the instability, for some values of the perturbed quantities, nonlinear effects seems to become important. Although it is very difficult and almost impossible to find an exact analytical solution of equations (4.1)-(4.3), we discuss here some approximate solutions.

Let us introduce the normalized parameters $t' = c_s t/L_{ni}$, $x' = x/\rho_s$, $y' = y/\rho_s$, $z' = z/L_{ni}$, $\phi' = (e\phi L_{ni}N_0)/(\rho_s n_{i0}T_0)$, $T = (T_{i1}L_{ni})/(\rho_s T_{i0})$, $v = L_{ni}v_{iz}/(\rho_s c_s)$, $L_{ni} = [d_x(\ln n_{i0})]^{-1}$, $c_s = \sqrt{(n_{i0}T_0)/(N_0 m_i)}$, and $\rho_s = c_s/\omega_{ci}$. Hereafter, we shall drop the superscript prime for simplicity of the notation. Equations (4.1)-(4.3) can be written as

$$D_t v = [d_x v_{i0}\partial_y - \left(1+\alpha\tau^{-1}\right)\partial_z]\phi - \alpha\tau^{-1}\partial_z T, \tag{4.18}$$

$$(D_t + \frac{5}{3}\alpha K_{Bi}\partial_y)T - \frac{2}{3}D_t\phi - \frac{2}{3}\partial_x\left(\ln N_0\right)\phi\partial_y\phi + (\frac{5}{3} - \tau K_{Ti})\partial_y\phi = 0 \tag{4.19}$$

and

$$\begin{aligned}&\partial_t(1-\nabla_\perp^2)\phi - \alpha_4'\phi\partial_y\phi + \alpha K_{Bi}\partial_y T - [1-(\alpha+\tau)K_{Bi} + \alpha K_{Ti}\nabla_\perp^2]\partial_y\phi \\ &-\left(1+\alpha\tau^{-1}\right)\mathcal{J}\left[\phi, \nabla_\perp^2\phi\right] - \alpha\tau^{-1}\nabla\cdot J\left[T, \nabla_\perp\phi\right] + \partial_z v = 0,\end{aligned} \tag{4.20}$$

where $D_t \equiv \partial_t + (\partial_x\phi\partial_y - \partial_y\phi\partial_x)$, $\alpha_4' = (\partial_x \ln N_0 - \tau\delta_i K_{Bi})$, $\delta_i = \rho_s/L_{ni}$, $K_{Bi} = L_{ni}/(\tau L_{Bi})$, $K_{Ti} = (1+\eta_i)/\tau$, $L_{ni}(L_{Bi})$ represents equilibrium density (magnetic field) inhomogeneity scale length. Here, we have assumed $|(c/B_0)\,\hat{\mathbf{z}}\times\nabla\phi\cdot\nabla| \gg v_{iz}\partial_z$.

To obtain stationary solution of Eqs. (4.18)-(4.20), we assume that v, T and ϕ are functions of x and $\xi = y + \eta_0 z - u_0 t$, where η_0 is a constant and u_0 is the translational speed of the vortex. In stationary frame Eqs. (4.18) to (4.20) can be re-written as

$$D_\xi v = \frac{1}{u_0}\partial_\xi\left[\left(\left(1+\alpha\tau^{-1}\right)\eta_0 - d_x v_{i0}\right)\phi + \alpha\tau^{-1}\eta_0 T\right], \tag{4.21}$$

$$(D_\xi - \frac{5}{3}\frac{\alpha K_{Bi}}{u_0}\partial_\xi)T - \frac{2}{3}D_\xi\phi + \frac{2}{3u_0}\partial_x\left(\ln N_0\right)\phi\partial_\xi\phi - \frac{1}{u_0}(\frac{5}{3} - \tau K_{Ti})\partial_\xi\phi = 0 \tag{4.22}$$

and

$$\partial_\xi(1-\nabla_\perp^2)\phi+\frac{\alpha_4'}{u_0}\phi\partial_\xi\phi-\frac{\alpha K_{Bi}}{u_0}\partial_\xi T+\frac{1}{u_0}[1-(\alpha+\tau)K_{Bi}+\alpha K_{Ti}\nabla_\perp^2]\partial_\xi\phi$$
$$+\frac{(1+\alpha\tau^{-1})}{u_0}\mathcal{J}\left[\phi,\nabla_\perp^2\phi\right]+\frac{\alpha\tau^{-1}}{u_0}\nabla\cdot\mathcal{J}\left[T,\nabla_\perp\phi\right]-\frac{\eta_0}{u_0}\partial_\xi v=0. \tag{4.23}$$

where $D_\xi \equiv \partial/\partial\xi-(1/u_0)[(\partial_x\phi)\,\partial_\xi-(\partial_\xi\phi)\partial_x]$ and $\nabla_\perp^2=\partial^2/\partial x^2+\partial^2/\partial\xi^2$.

Monopolar vortex

When the scalar nonlinearity is stronger than the vector nonlinearity (or Jacobian nonlinearity) in the Eqs. (4.21)-(4.23), Eq. (4.22) can be rewritten as

$$(1-\frac{5}{3}\frac{\alpha K_{Bi}}{u_0})\partial_\xi T-\frac{2}{3}\partial_\xi\phi+\frac{1}{3u_0}\partial_x(\ln N_0)\,\partial_\xi\phi^2-\frac{1}{u_0}(\frac{5}{3}-\tau K_{Ti})\partial_\xi\phi=0.$$

The above equation can be integrated, yielding

$$T=a_0\phi-b_0\phi^2, \tag{4.24}$$

where $a_0=(2u_0+5-3\tau K_{Ti})\,/\,(3u_0-5\alpha K_{Bi})$ and $b_0=(\partial_x\ln N_0)\,/\,(3u_0-5\alpha K_{Bi})$.

Using the above relation for T in Eq. (4.21), we readily integrate to obtain the following result

$$v=a_1\phi-b_1\phi^2, \tag{4.25}$$

where $a_1=(\eta_0\alpha\tau^{-1}(1+a_0+\alpha^{-1}\tau)-d_xv_{i0})/u_0$ and $b_1=\alpha\tau^{-1}\eta_0 b_0/u_0$.

Finally, eliminating T and v from Eqs. (4.23) by using Eqs. (4.24) and (4.25), we obtain

$$\nabla_\perp^2\phi-\chi_1\phi+\chi_2\phi^2=0. \tag{4.26}$$

with $\chi_1=(u_0+1-(1+a_0+\alpha^{-1}\tau)\,\alpha K_{Bi}-\eta_0 a_1)/\,(u_0-\alpha K_{Ti})$ and $\chi_2=(\delta_i\tau K_{Bi}-\partial_x\ln N_0-2\alpha b_0 K_{Bi}-2\eta_0 b_1)/\,(2u_0-2\alpha K_{Ti})$. Eq. (4.26) admits a cylindrically symmetric monopolar vortex [81] when $\chi_1>0$.

Chain of vortex

On the other hand, if the Jacobian nonlinearity is stronger than the scalar nonlinearity in Eqs. (4.21)-(4.23), then we may integrate Eq. (4.22) to obtain a trivial solution of the form

$$T = \frac{(2u_0 + 5 - 3\tau K_{Ti})}{(3u_0 - 5\alpha K_{Bi})}\phi = a_2\phi. \tag{4.27}$$

Eliminating T from Eqs. (4.21) and (4.27), we get

$$v = \frac{1}{u_0}\left(\eta_0\alpha\tau^{-1}\left(1 + a_2 + \alpha^{-1}\tau\right) - d_x v_{i0}\right)\phi = a_3\phi. \tag{4.28}$$

Inserting T and v from Eqs. (4.27) and (4.28) into Eq. (4.23), we obtain

$$\begin{aligned}&\left[\left(\alpha\left(1 + a_2\right) + \tau\right)K_{Bi} - u_0 - 1 + \eta_0 a_3\right]\partial_\xi\phi + \left(u_0 - \alpha K_{Ti}\right)\partial_\xi\nabla_\perp^2\phi \\ &- \left(1 + \alpha\tau^{-1}\left(1 + a_2\right)\right)\mathcal{J}\left[\phi, \nabla_\perp^2\phi\right] = 0.\end{aligned} \tag{4.29}$$

If we set $u_0 = (\alpha\left(1 + a_2\right) + \tau)K_{Bi} - 1 + \eta_0 a_3$ in Eq. (4.29), then we obtain a well known stationary Navier-Stokes equation

$$\partial_\xi\nabla_\perp^2\phi = \frac{\mu_1}{u}\mathcal{J}\left[\phi, \nabla_\perp^2\phi\right], \tag{4.30}$$

where $\mu_1 = \left(1 - \alpha\tau^{-1}\left(1 + a_2\right)\right)$ and $u = \left(u_0 - \alpha K_{Ti}\right)$. For $\mu_1 > 0$ and $u_0 \neq \alpha K_{Ti}$, Eq. (4.30) is satisfied by

$$\nabla_\perp^2\phi = \frac{4\phi_0 K^2}{a_4^2}\exp\left[-\frac{2}{\phi_0}\left(\phi - \frac{u}{\mu_1}x\right)\right]. \tag{4.31}$$

where ϕ_0, K, and a_4 are some arbitrary constants. The analytical solution of Eq. (4.31) is

$$\phi = \frac{u}{\mu_1}x + \phi_0\ln\left[2\cosh(Kx) + 2\left(1 - \frac{1}{a_4^2}\right)\cos(K\xi)\right] \tag{4.32}$$

which represents the Kelvin-Stuart "cat's eyes" that are chains of vortices [92] for $a_4 > 1$.

Here a_4 represents the size of the vortex.

Dipolar vortex

Let us now present another stationary solution of Eq. (4.29) by letting

$$\mu_2 = [u_0 - (\alpha(1+a_2)+\tau)K_{Bi} + 1 - \eta_0 a_3] / (u_0 - \alpha K_{Ti}) > 0.$$

In this case, Eq. (4.29) is satisfied by the ansatz

$$\nabla_\perp^2 \phi = a_5\phi + a_6 x. \tag{4.33}$$

where a_5 and a_6 satisfy the following condition

$$1 - \frac{a_5}{\mu_2} - \left[\frac{1+\alpha\tau^{-1}(1+a_2)}{\mu_2(u_0 - \alpha K_{Ti})}\right] a_6 = 0 \tag{4.34}$$

Equation (4.33) is a second order inhomogeneous differential equation which admits a dipolar vortex solution [93,94]. The constants a_5 and a_6 can be determined by matching the inner and outer solutions of ϕ at the vortex interface. This exercise has been done in Ref. [93,94] in some detail where explicit expressions of various constants are obtained.

Tripolar vortex

Now we look for another type of stationary solution of Eqs. (4.21)-(4.23) called tripolar vortex solution. In order to find the stationary vortex type solution in the presence of ion sheared flow in e-p-i plasma, we may assume Gaussian type [98] density, temperature and magnetic field profiles, so that we may approximate $K_{Bi} = K_{Bi0} + K_{Bi1}x$ and $K_{Ti} = K_{Ti0} + K_{Ti1}x$. The effect of the equilibrium perpendicular ion flow velocity, which is caused by a radial electric field $-\nabla\phi_0$, is incorporated in the $E \times B$ drift, by writing down the total electrostatic potential as a sum of the equilibrium (ϕ_0) and perturbed (ϕ) potentials, where $\phi_0 \propto V_{\perp 0}(x - x_0) + V'_{\perp 0}(x - x_0)^2/2$. It may be noted here that the equilibrium potential profile only describes the linearly varying perpendicular flows [95]. With this choice of K_{Bi} and K_{Ti}, and in the absence of scalar nonlinearity, Eq. (4.22) can be re-written as follows

$$\mathcal{J}\left[\phi + (V'_{\perp 0} + \frac{5}{3}\alpha K_{Bi1})\frac{(x-x_1)^2}{2}, T + K_{Ti1}\tau\frac{(x-x_2)^2}{2}\right] = 0, \tag{4.35}$$

where

$$x_1 = \left(u_0 - V_{\perp 0} + V'_{\perp 0}x_0 - (5/3)\alpha K_{Bi0}\right) / \left(V'_{\perp 0} + (5/3)\alpha K_{Bi1}\right)$$

and

$$x_2 = \left(2u_0 + 5 - 3\tau K_{Ti0}\right) / 3\tau K_{T1}$$

Although it is very difficult to analytically solve Eq. (4.35) for a localized vortex solution. However, If we set $x_1 = x_2$, then one may integrate Eq. (4.35) to obtain

$$T + K_{T1}\tau\frac{(x-x_1)^2}{2} = f_1\left(\phi + \left(V'_{\perp 0} + \frac{5}{3}\alpha K_{Bi1}\right)\frac{(x-x_1)^2}{2}\right), \tag{4.36}$$

where the condition $x_1 = x_2$, basically determines the phase velocity of the vortex. Here f_1 is an arbitrary function of its argument. On the condition of vanishing perturbations at infinity, we have

$$T = \frac{K_{Ti1}\tau}{(V'_{\perp 0} + (5/3)\alpha K_{Bi1})}\phi = a_7\phi \tag{4.37}$$

Inserting T in equation (4.21), which, in turn, is satisfied by

$$v = f_2\left(\phi + V'_{\perp 0}\frac{(x-x_3)^2}{2}\right) + \eta_0\alpha\tau^{-1}\left(1 + a_7 + \alpha^{-1}\tau\right)(x - x_4), \tag{4.38}$$

where $x_3 = \left(u_0 - V_{\perp 0} + V'_{\perp 0}x_0\right)/V'_{\perp 0}$ and $x_4 = v_{i0}/\left(\eta_0\alpha\tau^{-1}\left(1 + a_7 + \alpha^{-1}\tau\right)\right)$ and f_2 is an arbitrary function and we take it as a linear form such that $f_2(\chi) = F_2.\chi$, we get

$$\partial_\xi v = F_2\partial_\xi\phi \tag{4.39}$$

Equations (4.37), (4.38) and (4.23) can be combined to give the Jacobian

$$\mathcal{J}\left[\phi+\frac{\left(\alpha K_{Ti1}\left(1+\alpha\tau^{-1}\left(1+a_7\right)\right)^{-1}+V'_{\perp 0}\right)\left(x-x_5\right)^2}{2},\nabla_\perp^2\phi+\frac{\tau K_{Bi1}\left(x-x_6\right)^2}{2}\right]=0, \tag{4.40}$$

where

$$x_5=\frac{\left(u_0+\left(1+\alpha\tau^{-1}\left(1+a_7\right)\right)\left(V'_{\perp 0}x_0-V_{\perp 0}\right)-\alpha K_{Ti0}\right)}{\left(\left(1+\alpha\tau^{-1}\left(1+a_7\right)\right)V'_{\perp 0}+\alpha K_{Ti1}\right)}$$

and

$$x_6=\frac{\left(u_0+1-(\alpha+\tau)K_{Bi0}+\alpha a_7 K_{Bi0}+\eta_0 F_2\right)}{\alpha K_{B1}\left(1+a_7+\alpha^{-1}\tau\right)}$$

Again setting $x_5=x_6$, Eq. (4.40) can be integrated to obtain a general solution of following form:

$$\nabla_\perp^2\phi+\frac{\tau K_{Bi1}\left(x-x_5\right)^2}{2}=f_3\left(\phi+\frac{\left(\alpha K_{Ti1}\left(1+\alpha\tau^{-1}\left(1+a_7\right)\right)^{-1}+V'_{\perp 0}\right)\left(x-x_5\right)^2}{2}\right), \tag{4.41}$$

where f_3 is an arbitrary function. Using the appropriate boundary conditions for a localized vortex solution, we obtain

$$\nabla_\perp^2\phi=\frac{\beta^2}{\gamma^2}\phi, \tag{4.42}$$

where $\beta^2/\gamma^2=\left(\tau K_{Bi1}\right)/\left(\alpha K_{Ti1}\left(1+\alpha\tau^{-1}\left(1+a_7\right)\right)^{-1}+V'_{\perp 0}\right)$. Using the standard procedure [96], Eq. (4.42) can be solved in cylindrical coordinates, independently inside and outside a circle with the radius $r=a$. The solution of Eq. (4.42) is obtained in the form of tripolar vortex [97, 98].

Quadrupolar vortex

Equation (4.41) can also be expressed as

$$\nabla_\perp^2\phi+a_8X^2=f_4\left(\phi+a_9X^2\right). \tag{4.43}$$

where $a_8 = \tau K_{B11}/2$, $a_9 = \left(\alpha K_{T11}\left(1 + \alpha\tau^{-1}\left(1 + a_7\right)\right)^{-1} + V'_{\perp 0}\right)/2$, $X = (x - x_5)$ and f_4 is an arbitrary function of the given argument and we choose it as a linear one, i.e., $f_4 \approx f_{40} + \left(\phi + X^2\right) f_{41}$. With this choice of f_4, we can re-arrange Eq. (4.43) defining new constants

$$\left(\nabla_\perp^2 - 1\right)\phi - a_{10}X^2 = f_{40} + \left(\phi + X^2\right) f'_{41}, \tag{4.44}$$

where $a_{10} = 1 + a_8 + f_{41} - a_9 f_{41}$, $f'_{41} = 1 + f_{41}$. A localized quadrupolar vortex of the above equation has been obtained in Ref. [99].

4.3 Self-Gravitation Effect of Ions

4.3.1 Nonlinear Equations

Consider the three-component plasma in the self-gravitational field of ions, consisting of thermally distributed ions and Boltzmann distributed electrons and positrons embedded in an inhomogeneous external magnetic field $B_0(x)\,\hat{\mathbf{z}}$, where B_0 is the strength of external magnetic field and $\hat{\mathbf{z}}$ is the unit vector along the z-axis. The plasma also contains equilibrium ion velocity $(\partial_x v_{i0})$, equilibrium ion-temperature $(\partial_x T_{i0})$ and density $(\partial_x n_{j0})$ gradients, which are maintained by external sources. In equilibrium, the e-p-i magnetoplasma satisfies the charge neutrality condition (2.12). The ion dynamics is governed by ion continuity equation (2.13) with $D_i = 0$, and the momentum transfer equation (2.1) with $\nu_j = 0$. The ion temperature perturbation can be obtained by using ion energy balance equation (2.14). The gravitational potential Ψ_g is given by Eq. (2.1) such that

$$\nabla^2\Psi_g = 4\pi G m_i n_i, \tag{4.45}$$

where G is the universal gravitational constant. Taking the cross product of Eq. (2.1) with $\hat{\mathbf{z}}$, we obtain the ion-fluid velocity perturbation under drift-approximation. We express dependent variables n_i, T_i, φ, Ψ_g and v_{iz} in terms of their equilibrium and perturbed parts as

$$\begin{aligned}
n_i &= n_{i0} + n_{i1} \\
T_i &= T_{i0} + T_{i1} \\
v_{iz} &= v_{i0} + v \\
\varphi &= 0 + \phi \\
\Psi_g &= \Psi_{G0} + \Psi_G.
\end{aligned} \tag{4.46}$$

For low-frequency processes (much less than the ion-gyrofrequency) and Boltzmann distributed electrons and positrons, the quasi-neutrality condition leads to Eq. (2.34). Considering collisionless plasma ($\nu_i = 0$) and keeping the leading order nonlinear terms, we obtain

$$\begin{aligned}
&d_t\left(1-\rho_s^2\nabla_\perp^2\right)(e\phi) + u_n^*\partial_y\left(e\phi + m_i\Psi_G\right) + \mathbf{v}_{Bi}\cdot\nabla(e\phi) \\
&+\alpha^{-1}\tau\mathbf{v}_{Bi}\cdot\nabla T_{i1} - \rho_s^2\left[\left(\mathbf{v}_{Di0}\cdot\nabla\right)\nabla_\perp^2(e\phi)\right] + m_i c_s^2\partial_z v = 0,
\end{aligned} \tag{4.47}$$

$$m_i d_t v = -\left[\left\{\left(1+\alpha\tau^{-1}\right)\partial_z - S_i(x)\partial_y\right\}(e\phi) + \partial_z\left(T_{i1} + m_i\Psi_G\right)\right], \tag{4.48}$$

$$\left(d_t + \frac{5}{3}\mathbf{v}_{Bi}\cdot\nabla\right)T_{i1} - \frac{2}{3}\alpha\tau^{-1}d_t(e\phi) - \left(\eta_i - \frac{2}{3}\right)\mathbf{v}_{ni}\cdot\nabla\left(e\phi + m_i\Psi_G\right) = 0 \tag{4.49}$$

and

$$T_0\nabla^2\Psi_G = \alpha\omega_J^2(e\phi), \tag{4.50}$$

where $\omega_J^2 = 4\pi G m_i n_{i0}$ is the Jeans frequency of ions [100]. Equations (4.47)-(4.50) is the desired nonlinear set of mode coupling equations to study the dynamics of low-frequency ITG-driven waves in a self-gravitating e-p-i magnetoplasma with sheared ion flows.

4.3.2 Linear Analysis

In the linear limit, we neglect the nonlinear terms in Eqs. (4.47)-(4.50) and assume that ϕ, Ψ_G, T_{i1} and v are proportional to $\exp\left[-i\left(\omega t - \mathbf{k}\cdot\mathbf{r}\right)\right]$, where $\mathbf{k}$ and ω are the wavevector and the frequency of the perturbed quantities, respectively. Equations (4.47)-(4.50) in the transformed space, can be written as,

$$\Omega m_i v = k_z \left[\left(1 + \alpha\tau^{-1} - \frac{S_i k_y}{k_z} \right) (e\phi) + (T_{i1} + m_i \Psi_G) \right], \tag{4.51}$$

$$\left(\Omega - \frac{5}{3}\omega_{Bi} \right) T_{i1} = \left(\frac{2}{3}\alpha\tau^{-1}\Omega \right) (e\phi) - \left(\omega_{Ti} - \frac{2}{3}\omega_{ni} \right) (e\phi + m_i \Psi_G), \tag{4.52}$$

$$\begin{aligned} &\left[\Omega (1 + b_i) - \omega_{Bi} \left(1 + \alpha^{-1}\tau\right) + \omega_{ni} \left(\alpha^{-1}\tau - b_i\right) - b_i\omega_{Ti}\right] (e\phi) \\ &-\alpha^{-1}\tau\omega_{Bi} T_{i1} + \alpha^{-1}\tau \left(\omega_{ni} - \omega_{Bi}\right) m_i \Psi_G - k_z c_s^2 m_i v = 0, \end{aligned} \tag{4.53}$$

$$m_i \Psi_G = -\delta_J (e\phi). \tag{4.54}$$

Here, $\Omega = \omega - \mathbf{k} \cdot \mathbf{v}_{i0}$ is the Doppler shifted frequency, $\omega_{ni} = \mathbf{k} \cdot \mathbf{v}_{ni}$ is ion-density drift frequency, $\omega_{Bi} = \mathbf{k} \cdot \mathbf{v}_{Bi}$, $\omega_{Ti} = \mathbf{k} \cdot \mathbf{v}_{Ti}$, $b_i = k_\perp^2 \rho_s^2$ and $\delta_J = \omega_J^2 / k^2 c_s^2$. Combining Eqs. (4.51)-(4.54), we obtain a local dispersion relation

$$\begin{aligned} &\Omega(\Omega - \frac{5}{3}\omega_{Bi}) \left[\Omega(1 + b_i) - \omega_{Bi}(1 + \alpha^{-1}\tau) + \omega_{ni}(\alpha^{-1}\tau - b_i) - b_i\omega_{Ti}\right] \\ &- (\omega_{Bi}\Omega + \alpha\tau^{-1} k_z^2 c_s^2) \left[\frac{2}{3}\Omega - \alpha^{-1}\tau(\omega_{Ti} - \frac{2}{3}\omega_{ni})\right] \\ &- (\Omega - \frac{5}{3}\omega_{Bi})[(1 + \alpha\tau^{-1})\, k_z^2 c_s^2 - k_y k_z\, c_s^2 S_i(x)] \\ &- \left[(\Omega - \frac{5}{3}\omega_{Bi})(\, \alpha^{-1}\tau\, (\omega_{ni} - \omega_{Bi})\, \Omega - k_z^2 c_s^2)\right] \delta_J \\ &- \left[(\omega_{Ti} - \frac{2}{3}\omega_{ni})(\alpha^{-1}\tau\omega_{Bi}\Omega \, + k_z^2 c_s^2)\right] \delta_J = 0. \end{aligned} \tag{4.55}$$

Equation (4.55) is a new dispersion relation modified by the combined effects of ion-temperature-gradient, self-gravitational force, ion shear flow, inhomogeneity in the background plasma density and external magnetic field. Assuming $v_{i0} \approx 0$, $\omega_{Bi} \approx \omega_{Ti} \approx 0$

and $\omega \gg \alpha\tau^{-1}\omega_{ni}, \omega_{ni}$, Eq. (4.55) simplifies to

$$\omega^2(1+b_i) + \omega\left[1 - \delta_J + b_i\alpha\tau^{-1}\right]\omega_{ni} - \left(1 + \alpha^{-1}\tau - \delta_J\right)k_z^2c_s^2 = 0 \tag{4.56}$$

Which is a dispersion relation of coupled drift and modified ion-acoustic mode in a self-gravitating e-p-i magnetoplasma. For a uniform density plasma ($\omega_{ni} = 0$) case, we have the following modified ion-acoustic mode

$$\omega = \frac{\left(1 + \alpha^{-1}\tau - \delta_J\right)^{1/2}}{\sqrt{(1+b_i)}}\, k_z c_s \tag{4.57}$$

However, for $\omega \gg k_z c_s$, we have a modified dispersion relation for drift waves defined by

$$\omega = \frac{\left[\delta_J - (1 + b_i\alpha\tau^{-1})\right]}{(1+b_i)}\omega_{ni} \tag{4.58}$$

Further, if we assume $b_i \approx 0$, $(1 + 5\alpha\tau^{-1}/3)\,\Omega \ll \omega_{Ti}$, and $\omega_{Bi} \approx \omega_{ni} \approx 0$, then Eq. (4.55) takes the following form:

$$\Omega^3 + k_z^2c_s^2\left[\frac{k_y S_i}{k_z}\Omega + \omega_{Ti}\left(1 - \delta_J\right)\right] = 0. \tag{4.59}$$

Equation (4.59) represents a dispersion relation for the coupled ion-acoustic and ITG-driven mode in the presence of ion sheared flow and self-gravitational field. If we take $\omega_{Ti} = 0$. The dispersion relation reduces to

$$\bar{\Omega}^2 = \frac{k_y S_i}{k_z}, \tag{4.60}$$

where $\bar{\Omega} = \Omega/k_z c_s$. The above equation predicts an instability, if $S_i < 0$. Thus the mode described by Eq. (4.60) may become unstable depending upon the direction of ion sheared flow. The growth rate for the instability is

$$\gamma = \left|\frac{k_y S_i}{k_z}\right|^{1/2} k_z c_s$$

If $S_i = 0$, in Eq. (4.59), we get

$$\Omega^3 + \omega_{Ti} (1 - \delta_J) k_z^2 c_s^2 = 0. \tag{4.61}$$

Equation (4.61) represents a dispersion relation for the ion-temperature-gradient mode in the presence of self-gravitational field. This cubic dispersion relation reduces to the Rudakov-Sagdeev [83] equation in the absence of positrons and self-gravitational field. The growth rate of the instability can be expressed as

$$\gamma = \frac{\sqrt{3}}{2} \left| [\omega_{Ti} (1 - \delta_J)] k_z^2 c_s^2 \right|^{1/3}. \tag{4.62}$$

This is an interesting result which shows that the effect of self-gravitation, although very weak, tends to suppress the well known Rudakov-Sagdeev [83] instability.

4.3.3 Nonlinear Solutions

In the proceeding section, we have shown that how velocity, temperature, density and magnetic field gradients causes instability of electrostatic drift-waves and modified ion acoustic waves in the presence of self-gravitational field. At a certain stage in the development of the instability, for some values of the perturbed quantities, nonlinear effects seems to become important. Although it is very difficult and almost impossible to find an exact analytical solution of equations (4.47) to (4.50), we shall discuss here some approximate solutions.

Let us first introduce the normalized parameters $t' = c_s t / L_{ni}$, $x' = x/\rho_s$, $y' = y/\rho_s$, $z' = z/L_{ni}$, $\Psi = (\Psi_G L_{ni} m_i N_0) / (\rho_s n_{i0} T_0)$, $\phi' = (e\phi L_{ni} N_0) / (\rho_s n_{i0} T_0)$, $T = (T_{i1} L_{ni}) / (\rho_s T_{i0})$, $v' = L_{ni} v / (\rho_s c_s)$, $L_{ni} = [d_x (\ln n_{i0})]^{-1}$, $c_s = \sqrt{(n_{i0} T_0) / (N_0 m_i)}$ and $\rho_s = c_s / \omega_{ci}$. Hereafter, we shall drop the superscript prime for simplicity of the notation. Thus equations

(4.47)-(4.50) takes the following form

$$\partial_t v = [d_x v_{i0}\partial_y - \left(1+\alpha\tau^{-1}\right)\partial_z]\phi - \partial_z\left(\Psi + \alpha\tau^{-1}T\right), \tag{4.63}$$

$$(\partial_t + \frac{5}{3}\alpha K_{Bi}\partial_y)T - \frac{2}{3}\partial_t\phi + (\frac{5}{3} - \tau K_{Ti})\partial_y\left(\phi + \Psi\right) = 0, \tag{4.64}$$

$$\begin{aligned}&\partial_t(1-\nabla_\perp^2)\phi + \alpha K_{Bi}\partial_y T - (1-\tau K_{Bi})\partial_y\Psi\\ &-[1-(\alpha+\tau)K_{Bi} + \alpha K_{Ti}\nabla_\perp^2]\partial_y\phi + \partial_z v = 0\end{aligned} \tag{4.65}$$

and

$$\nabla_\perp^2\Psi = \alpha_J\phi, \tag{4.66}$$

where $\alpha_J = \omega_J^2/\omega_{ci}^2$, $\delta_i = \rho_s/L_{ni}$, $K_{Bi} = L_{ni}/(\tau L_{Bi})$, $K_{Ti} = (1+\eta_i)/\tau$, $L_{ni}(L_{Bi})$ represents equilibrium density (magnetic field) inhomogeneity scale length. Here, we have assumed $\delta_i^2 \ll 1$ and $|(c/B_0)\,\hat{\mathbf{z}}\times\nabla\phi\cdot\nabla| \gg v_{iz}\partial_z$.

To obtain stationary solution of Eqs. (4.63)–(4.66), we assume that v, T and ϕ are functions of x and $\xi = y + \eta_0 z - u_0 t$, where η_0 is a constant and u_0 is the translational speed of the vortex. Transforming Eqs. (4.63) to (4.66) in stationary frame and using Eq. (4.66), we get

$$\partial_\xi v = \frac{1}{u_0}\partial_\xi\left[\left(\left(1+\alpha\tau^{-1}\right)\eta_0 - d_x v_{i0}\right)\frac{1}{\alpha_J}\nabla_\perp^2\Psi + \eta_0\Psi + \alpha\tau^{-1}\eta_0 T\right], \tag{4.67}$$

$$(\partial_\xi - \frac{5}{3}\frac{\alpha K_{Bi}}{u_0}\partial_\xi)T - \frac{2}{3\alpha_J}\partial_\xi\nabla_\perp^2\Psi - \frac{1}{\alpha_J u_0}(\frac{5}{3} - \tau K_{Ti})\partial_\xi\left(\nabla_\perp^2\Psi + \alpha_J\Psi\right) = 0 \tag{4.68}$$

and

$$\begin{aligned}&u_0\partial_\xi(1-\nabla_\perp^2)\nabla_\perp^2\Psi - \alpha\alpha_J K_{Bi}\partial_\xi T + \alpha_J(1-\tau K_{Bi})\partial_\xi\Psi +\\ &[1-(\alpha+\tau)K_{Bi} + \alpha K_{Ti}\nabla_\perp^2]\partial_\xi\nabla_\perp^2\Psi - \alpha_J\eta_0\partial_\xi v = 0,\end{aligned} \tag{4.69}$$

where $\nabla_\perp^2 = \partial^2/\partial x^2 + \partial^2/\partial\xi^2$.

We may integrate Eq. (4.68) to obtain a trivial solution of the form

$$\partial_\xi T = \frac{(2u_0 + 5 - 3\tau K_{Ti})}{\alpha_J (3u_0 - 5\alpha K_{Bi})} \partial_\xi \nabla_\perp^2 \Psi + \frac{(5 - 3\tau K_{Ti})}{\alpha_J (3u_0 - 5\alpha K_{Bi})} \partial_\xi \Psi = b_1 \partial_\xi \nabla_\perp^2 \Psi + b_2 \partial_\xi \Psi. \quad (4.70)$$

Eliminating T from Eq. (4.67), we get

$$\begin{aligned} \partial_\xi v &= \left[\left(\left(1 + \alpha\tau^{-1}\right) \eta_0 + \alpha_J b_1 \alpha \tau^{-1} \eta_0 - d_x v_{i0} \right) \frac{1}{\alpha_J u_0} \right] \partial_\xi \nabla_\perp^2 \Psi + \frac{1}{u_0} \left(\eta_0 + b_2 \alpha \tau^{-1} \eta_0 \right) \partial_\xi \Psi \\ &= b_3 \partial_\xi \nabla_\perp^2 \Psi + b_4 \partial_\xi \Psi. \end{aligned} \quad (4.71)$$

Inserting $\partial_\xi T$ and $\partial_\xi v$ from Eqs. (4.70) and (4.71) into Eq. (4.69) and integrating, we get

$$\nabla_\perp^4 \Psi + b_5 \nabla_\perp^2 \Psi + b_6 \Psi - b_7 x = 0, \quad (4.72)$$

where

$$b_5 = \left[u_0 + (1 - (\alpha + \tau) \ K_{Bi}) - \alpha_J \left(b_1 \alpha K_{Bi} + b_3 \eta_0 \right) \right] / \left(\alpha K_{Ti} - u_0 \right),$$

$$b_6 = \alpha_J \left[(1 - \tau \ K_{Bi}) - \alpha b_2 K_{Bi} - b_4 \eta_0 \right] / \left(\alpha K_{Ti} - u_0 \right), b_7 = f / \left(\alpha K_{Ti} - u_0 \right)$$

and f is an arbitrary constant. Eq. (4.72) is a well known fourth order differential equation which admits a spatially-bounded dipolar vortex solution [101] of the gravitational potential. If we set $f = 0$ then the solution of Eq. (4.72) in the outer region ($r > R$) can be expressed as

$$\Psi^o = \left[b_8 K_1 (s_1 r) + b_9 K_1 (s_2 r) \right] \cos\theta, \quad (4.73)$$

where b_8 and b_9 are constants. K_1 is the modified Bessel function of first order, and $s_{1,2}^2 = \left[-b_5 \pm \left(b_5^2 - 4b_6 \right)^{1/2} \right] / 2$ for $b_5 < 0$ and $b_5^2 > 4b_6 > 0$. On the other hand, for the inner region ($r < R$), we write the solution as

$$\Psi^i = \left[b_{10} J_1 (s_3 r) + b_{11} I_1 (s_4 r) - \frac{f \omega_{ci}^2}{\omega_J^2 \left[(1 - \tau K_{Bi}) - \alpha b_2 K_{Bi} - b_4 \eta_0 \right]} r \right] \cos\theta, \quad (4.74)$$

where J_1 (I_1) is the Bessel function of the first order having real (imaginary) argument.

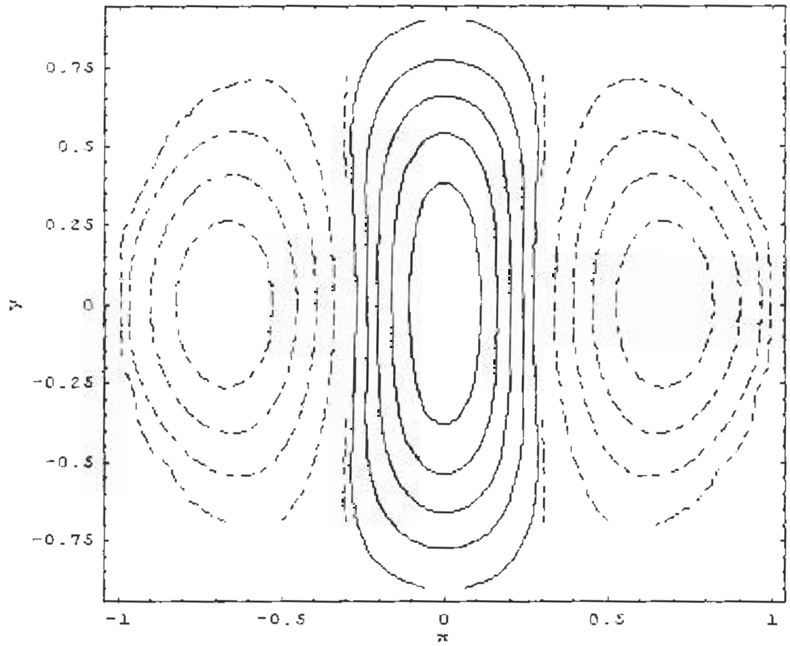

Figure 4-1: A typical tripolar vortex for the equipotential contour for the electrostatic potential Ψ for $\beta = 1.225$.

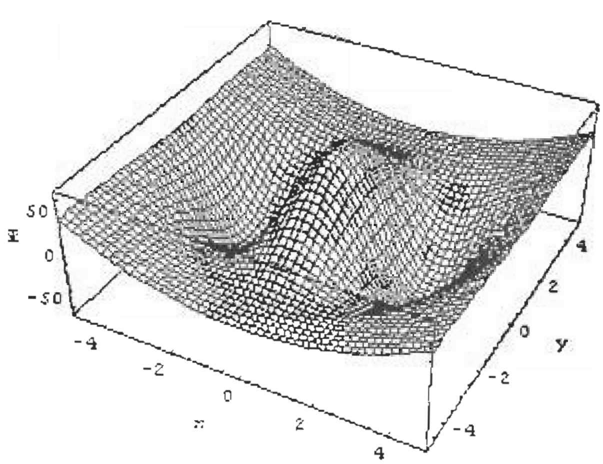

Figure 4-2: A three-dimensional view of the potential for the tripolar vortex from Fig. 4-1.

and b_{10} and b_{11} are constants. Here, $s_{3,4}^2 = \left[(b_5^2 - 4b_6)^{1/2} \pm b_5\right]/2$ for $b_6 < 0$. It is worthwhile to mention here that even in the absence of all inhomogeneities, the dipolar vortex structure is completely localized in the outer region. If we set $u_0 = \alpha K_{Ti}$ and $f = 0$, then equation (4.72) takes the following form

$$\nabla_\perp^2 \Psi = \left(\beta^2/\gamma^2\right) \Psi, \tag{4.75}$$

where $\beta^2/\gamma^2 = \alpha_J \left[1 - (\tau\ + \alpha b_2) K_{Bi} - b_4 \eta_0\right] / \left[1 + u_0 - (\alpha + \tau + \alpha_J b_1 \alpha) K_{Bi} - \alpha_J b_3 \eta_0\right]$. Using the standard procedure [96], Eq. (4.75) can be solved in cylindrical coordinates, independently inside (Ψ^i) and outside (Ψ^o) a circle with radius $r = a$.

$$\Psi^i (r, \theta) = b_{12} J_0 (\xi_1) + \left(1 + \frac{\beta^2}{\epsilon^2}\right) - b_{13} \left(\frac{r^2}{2}\right) + \left[b_{14} J_2 (\xi_1) - \left(1 + \frac{\beta^2}{\epsilon^2}\right) r^2\right] \cos 2\theta \tag{4.76}$$

and

$$\Psi^o (r, \theta) = b_{15} K_0 (\xi_2) + b_{16} K_2 (\xi_2) \cos 2\theta, \tag{4.77}$$

where $\xi_1 = \epsilon r/a$, $\xi_2 = \beta r/a$, $K_{0,2}$ and $J_{0,2}$ are the modified Bessel functions of the given order, respectively. Here, $r = x^2 + y^2$, $\cos\theta = x/r$, and b_{12}, b_{13}, b_{14}, b_{15} and b_{16} are arbitrary constants which can be determined by matching the outer and inner solutions at the boundary $r = a$.For a vortex of unit radius, the contour plot of the tripolar vortex is presented in Fig. 4-1. The contours show a tripolar vortex, i.e., a vortex core between the lobs of a dipole-like structure having positive values of the potential. Fig. 4-2 shows a three-dimensional view of the potential for the tripolar vortex.

4.4 Summary

In summary, we have described the ion-temperature-gradient driven electrostatic waves with sheared ion flows in an inhomogeneous e-p-i magnetoplasma. By employing the ion continuity, momentum and energy balance equations to describe the ion dynamics and Boltzmann distributed electrons and positrons, we have derived a new set of nonlinear mode coupling equations that contain scalar as well as vector nonlinearities. Neglecting the nonlinear terms, we have carried out the normal mode analysis to derive a general dispersion relation. It has been shown that non-zero equilibrium ion temperature (i.e. $\tau^{-1} \neq 0$) and the presence of positrons (i.e. $\alpha \neq 1$) modify the previously known results in the appropriate limits. For flat density profile, ITG drift wave destabilize on account of free energy stored in the inhomogeneous ion temperature and magnetic field gradients. We also have derived a cubic dispersion relation for the coupled ion-acoustic and electrostatic ion-temperature-gradient mode in the presence of sheared ion flow. One of the roots of this cubic dispersion relation predicts an instability irrespective the direction of velocity and ion-temperature gradients. On the other hand, in the nonlinear case, it is shown that under certain conditions possible stationary solutions of the same set of nonlinear equations are reduced in the form of monopolar, chain of vortices, dipolar, tripolar and quadrupolar vortices. We have also shown that if we incorporate the self-gravitational effect of ions then in the linear limit, the self-gravitation effect tends to suppress the well known Rudakov-Sagdeev instability. On the other hand, in the nonlinear limit, the possible stationary solutions of the nonlinear equations can be represented in the form of dipolar and tripolar vortices of gravitational potential.

Chapter 5

Nonlinear Dynamics of ITG-driven Electromagnetic Waves

5.1 Introduction

In the previous chapter, we have discussed in some detail the nonlinear dynamics of low-frequency ITG-driven electrostatic waves in the presence of equilibrium density, temperature, magnetic field, velocity and electrostatic potential gradients. Since in several laboratories and space plasmas, the plasma beta ($\beta = 8\pi nT/B_0^2$, where n (T) is the plasma number density (temperature) and B_0 is the strength of the ambient magnetic field) could exceed the electron-to-ion mass ratio, necessitating to incorporate electromagnetic effects on ITG-driven modes of e-p-i plasmas. Basically there are two different branches of the ITG modes. One is called "slab type", which is the drift wave coupled with the ion acoustic wave that is destabilized by the local ion-temperature-gradient. The other one is called "interchange type" or "toroidal branch", which is destabilized by bad curvature of the magnetic field lines in the presence of the finite ion-temperature-gradients [102]. It has been suggested that the turbulence associated with these two branches of ITG mode is likely to be the cause of the anomalous thermal transport observed in tokamaks and stellarator device. When the effect of magnetic shear is stronger than the effect of magnetic field curvature, the slab type ITG-driven instability is excited and become a dominant source of the experimentally observed anomalous heat transport [103, 104]. It may be added here that the electromagnetic effects also become relevant when the pressure gradient associated with shear Alfvén wave couples to the ion sound branch via (magnetic) curvature effects [105-107]. Here, in this chapter, we are using the slab model, leaving out the consideration of the magnetic curvature effects and dealing with the study of linear and nonlinear properties of low-frequency electromagnetic drift-dissipative and drift-Alfvén type waves in an e-p-i plasma containing equilibrium density gradient, ion-temperature and magnetic-field gradients with parallel equilibrium ion flow velocity.

5.2 Electromagnetic ITG Modes

5.2.1 Nonlinear Equations

Consider the nonlinear propagation of low-frequency electromagnetic waves in a nonuniform magnetized e-p-i plasma containing equilibrium density gradient $\partial_x n_{j0}$, equilibrium ion-temperature gradient $\partial_x T_{i0}$, equilibrium magnetic field gradient $\partial_x B_0$ and equilibrium velocity gradient $\partial_x \mathbf{v}_{j0}$, where $\mathbf{v}_{j0}$ is the equilibrium plasma flow velocity of the particle species j(j equals e for the electrons, p for positrons and i for the ions) in the direction along the equilibrium magnetic field $B_0\hat{\mathbf{z}}$. In equilibrium, the e-p-i plasma satisfies the charge neutrality condition (2.12), which is justified as long as the ion plasma frequency (ω_{pi}) is much larger than the ion gyrofrequency (ω_{ci}). Eqs. (2.21)-(2.27) would be the desired equations along with the quasineutrality condition and Ampere's law to study the electromagnetic ITG-driven drift-dissipative and drift-Alfvén waves in an inhomogeneous e-p-i magnetoplasma with sheared plasma flows [60].

5.2.2 Linear Analysis

In the linear limit, we neglect the nonlinear terms in Eqs. (2.21)-(2.27) and assume that the perturbation wavelength is much smaller than the velocity, density, temperature, and magnetic-field gradient scale-lengths. Furthermore, assuming that Φ, A_z, N_j, V_j and T are proportional to $\exp\left[-i\left(\omega t - \mathbf{k}\cdot\mathbf{r}\right)\right]$, where $\mathbf{k}$ and ω are the wavevector and the frequency, respectively, Eqs. (2.21)-(2.27) become

$$\left(\Omega_i - \omega_{Bi} + ik_\perp^2 D_i\right) N_i + \left[\tau\left(\omega_{ni} - \omega_{Bi}\right) + b_i\left(\Omega_i - \omega_{Di0} + i\nu_i - i\mu_i k_\perp^2\right)\right]\Phi$$
$$-\omega_{Bi} T - c_i k_z V_i - \left[\frac{T_0 k_y}{n_{i0} e}\partial_x\left(\frac{J_{i0}}{eB_0}\right)\right] A_z = 0, \tag{5.1}$$

$$\left(\Omega_i + i\nu_i - \omega_{Di0}\right) V_i = c_i k_z\left[\left(1 - \frac{\mathbf{S}^i_{vo}\cdot\mathbf{k}}{k_z}\right)\Phi - \frac{c}{k_z}\left(\Omega_i - \omega_{Di0}\right) A_z + \tau^{-1}\left(N_i + T\right)\right], \tag{5.2}$$

$$\left(\Omega_i - \frac{5}{3}\omega_{Bi} + i\frac{2\chi_i}{3n_{i0}}k_\perp^2\right) T - \frac{2}{3}\Omega_i N_i + \tau\left(\eta_i - \frac{2}{3}\right)\omega_{ni}\Phi = 0, \tag{5.3}$$

$$\left(\Omega_e - \omega_{Be} + ik_\perp^2 D_e\right) N_e - \left(\omega_{ne} - \omega_{Be}\right)\Phi + \left[\frac{T_0 k_y}{n_{e0} e}\partial_x\left(\frac{J_{eo}}{eB_0}\right)\right] A_z - v_{te} k_z V_e = 0, \tag{5.4}$$

$$\left(\Omega_p + \omega_{Bp} + ik_\perp^2 D_p\right) N_p + \left(\omega_{np} - \omega_{Bp}\right)\Phi - \left[\frac{T_0 k_y}{n_{p0} e}\partial_x\left(\frac{J_{po}}{eB_0}\right)\right] A_z - v_{te} k_z V_p = 0, \tag{5.5}$$

$$\left(\Omega_e + i\nu_e - \omega_{ne0}\right) V_e = -v_{te} k_z\left[\left(1 + \frac{\mathbf{S}^e_{vo}\cdot\mathbf{k}}{k_z}\right)\Phi - \frac{c}{k_z}\left(\Omega_e - \omega_{ne}\right) A_z - N_e\right], \tag{5.6}$$

$$\left(\Omega_p + i\nu_p - \omega_{np0}\right) V_p = v_{te} k_z\left[\left(1 - \frac{\mathbf{S}^p_{vo}\cdot\mathbf{k}}{k_z}\right)\Phi - \frac{c}{k_z}\left(\Omega_p - \omega_{np}\right) A_z + N_p\right], \tag{5.7}$$

where $\Omega_j = \omega - k_z v_{j0}$ is the Doppler shifted frequency of the jth species, $\omega_{ni} = \mathbf{k}\cdot\mathbf{v}_{ni}$, $\omega_{Bi} = \mathbf{k}\cdot\mathbf{v}_{Bi}$, $\omega_{Ti} = \mathbf{k}\cdot\mathbf{v}_{Ti}$, $\omega_{nj0} = \mathbf{k}\cdot\mathbf{v}_{nj}$, $\omega_{Bj} = \mathbf{k}\cdot\mathbf{v}_{Bj}$, $\omega_{Ti} = \mathbf{k}\cdot\mathbf{v}_{Ti}$, $b_i = \rho_i^2 k_\perp^2$ and $k_\perp^2 = k_y^2 + k_x^2$.

Electrostatic Cases

For the electrostatic case in which $A_z = 0$ and assuming electrons and positrons to be inertialess, Eqs. (5.6) and (5.7) can be combined to yield

$$N_i = \frac{1}{n_{i0}}(n_{e1} - n_{p1}) \approx \frac{1}{n_{i0}}(n_{e0}\Phi + n_{p0}\Phi) \approx \frac{N_0}{n_{i0}}\Phi \approx \alpha\Phi, \tag{5.8}$$

where $N_0 = n_{e0} + n_{p0}$ and $\alpha = N_0/n_{i0}$. Using the above result in the equations (5.1)-(5.3), we get

$$\left[\Omega_i - \omega_{Bi} + ik_\perp^2 D_i + \alpha^{-1}\tau\left\{(\omega_{ni} - \omega_{Bi}) + \rho_a^2 k_\perp^2\left(\Omega_i - \omega_{Di0} + i\nu_i - i\mu_i k_\perp^2\right)\right\}\right]\Phi$$
$$-\alpha^{-1}\omega_{Bi}T - \alpha^{-1}c_i k_z V_i = 0, \tag{5.9}$$

$$(\Omega_i + i\nu_i - \omega_{Di0})V_i = c_i k_z\left[\left(1 + \alpha\tau^{-1} - \frac{\mathbf{S}^i_{vo}\cdot\mathbf{k}}{k_z}\right)\Phi + \tau^{-1}T\right]. \tag{5.10}$$

$$\left(\Omega_i - \frac{5}{3}\omega_{Bi} + i\frac{2\chi_i}{3n_{i0}}k_\perp^2\right)T = \left(\frac{2\alpha}{3}\Omega_i - \tau(\eta_i - \frac{2}{3})\omega_{ni}\right)\Phi. \tag{5.11}$$

Substituting the values of V_i and T in Eq. (5.9), we obtain the following local dispersion relation for the electrostatic case

$$\left[(\Omega_i + i\nu_i - \omega_{Di0})\left(\Omega_i - \frac{5}{3}\omega_{Bi} + i\frac{2\chi_i}{3n_{i0}}k_\perp^2\right)\right]$$
$$\times\left[\Omega_i - \omega_{Bi} + ik_\perp^2 D_i + \alpha^{-1}\tau(\omega_{ni} - \omega_{Bi}) + \rho_s^2 k_\perp^2\left(\Omega_i - \omega_{Di0} + i\nu_i - i\mu_i k_\perp^2\right)\right]$$
$$-\left[\left\{\omega_{Bi}\left(\Omega_i - \frac{5}{3}\omega_{Bi} + i\frac{2\chi_i}{3n_{i0}}k_\perp^2\right) + \alpha^{-1}v_{ti}^2 k_z^2\right\}\left(\frac{2}{3}\Omega_i - \alpha^{-1}\tau(\eta_i - \frac{2}{3})\omega_{ni}\right)\right]$$
$$-\left[c_s^2 k_z^2\left(\Omega_i - \frac{5}{3}\omega_{Bi} + i\frac{2\chi_i}{3n_{i0}}k_\perp^2\right)\left(1 + \alpha\tau^{-1} - \frac{\mathbf{S}^i_{vo}\cdot\mathbf{k}}{k_z}\right)\right] = 0, \tag{5.12}$$

where $c_s^2 = \alpha^{-1}c_i^2$ is the sound velocity in e-p-i plasma and $\rho_s = c_s/\omega_{ci}$. Note that for nondissipative plasma for which $\nu_i = \chi_i = \mu_i = D_j = 0$, Eq. (5.12) reduce to our earlier result (see e.g., Eq. (4.7)) [59]. Since we have already discussed possible electrostatic modes for collisionless plasma in Ref. [59] in some detail, therefore we shall discuss here some other interesting modes.

Parallel propagation (i. e., $k_\perp = 0$): Equation (5.12) for parallel propagation (i.e. $k_\perp = 0$) case, reduces to

$$(\Omega_i + i\nu_i)\,\Omega_i = \left(1 + \left(\alpha + \frac{2}{3}\right)\tau^{-1}\right) c_s^2 k_z^2. \tag{5.13}$$

which clearly shows a dissipative ion-acoustic mode. For highly collisional plasma case, for which $\omega \ll \nu_i$, the above dispersion relation shows a damping of the ion-acoustic mode.

Perpendicular propagation (i.e., $k_z = 0$): For the waves propagating perpendicular to the external magnetic field, equation (5.12) yields the following result

$$\omega = \frac{5}{3}\omega_{Bi} - i\frac{2\chi_i}{3n_{i0}}k_\perp^2. \tag{5.14}$$

and

$$\begin{aligned}(\omega + i\nu_i - \omega_{Di0})\left[\omega - \omega_{Bi} + \alpha^{-1}\tau\left(\omega_{ni} - \omega_{Bi}\right) + \rho_s^2 k_\perp^2\left(\omega - \omega_{Di0} + i\nu_i + iD_i/\rho_s^2 - i\mu_i k_\perp^2\right)\right] \\ -\omega_{Bi}\left(\frac{2}{3}\omega - \alpha^{-1}\tau(\eta_i - \frac{2}{3})\omega_{ni}\right) = 0.\end{aligned} \tag{5.15}$$

Assuming $\omega - \omega_{Di0} \ll \nu_i \ll 2\omega_{Bi}/3$, equation (5.15) predicts an instability with a growth rate

$$\gamma = \frac{3\nu_i}{2}\left[\frac{\alpha^{-1}\tau L_{Bi}}{L_{ni}} - \left(1 + \alpha^{-1}\tau\right)\right]. \tag{5.16}$$

It is evident from Eq. (5.16) that the above mode would be unstable if $\alpha^{-1}\tau L_{Bi}/L_{ni} > (1 + \alpha\tau^{-1})$, where L_{Bi} and L_{ni} are the scale lengths of magnetic field and equilibrium ion density gradients, respectively.

Oblique propagation: If we assume that the wave phase speed is much higher than the ion-thermal speed so that $\Omega_i \gg \alpha^{-1}v_{ti}^2 k_z^2/\omega_{Bi}$ and ignore the finite Larmor radius effect, then Eq. (5.12) yields the following mode along-with the mode given by Eq. (5.14):

$$\left(\Omega_i + i\nu_i - \omega_{Di0}\right)\left[\Omega_i - \left(\left(1+\alpha^{-1}\tau\right)\omega_{Bi} + \alpha^{-1}\tau\omega_{ni}\right)\right] - \frac{2}{3}\omega_{Bi}\left(\Omega_i - \omega_{d*}\right)$$
$$-c_s^2 k_z^2\left(1+\alpha\tau^{-1} - \frac{\mathbf{S}_{vo}^i \cdot \mathbf{k}}{k_z}\right) = 0. \tag{5.17}$$

where $\omega_{d*} = \alpha^{-1}\tau(\frac{3}{2}\eta_i - 1)\omega_{ni}$. Equation (5.17) predicts an oscillatory instability of the ion drift waves for $\Omega_i - \omega_{Di0} < \nu_i$. Letting $\Omega_i = \omega_{d*} + i\gamma$ in the Eq. (5.17), we obtain the growth rate of the instability

$$\gamma = \frac{c_s^2 k_z^2}{\nu_i}\left(\frac{k_y \partial_x v_{i0}}{k_z \omega_{ci}} - \left(1+\alpha\tau^{-1}\right)\right). \tag{5.18}$$

which for $\left(1+\alpha\tau^{-1}\right)k_z\omega_{ci} < k_y\partial_x v_{i0}$ predicts a dissipative instability and a coupling of ion-acoustic and sheared flow-driven instability.

Electromagnetic Cases

Dissipative case: For flute type electromagnetic perturbations ($k_z = 0$) and for uniform magnetic field case ($\omega_{Bj} = 0$), Eqs. (5.1)-(5.7) yields the following liner dispersion relation

$$\left[\frac{\alpha_e\omega_{ne}}{(\omega + ik_\perp^2 D_e)} + \frac{\alpha_p\omega_{np}}{(\omega + ik_\perp^2 D_p)} + \frac{\left[\tau\omega_{ni} + b_i(\omega - \omega_{Di0} + i\nu_i - i\mu_i k_\perp^2)\right]}{(\omega + ik_\perp^2 D_i)}\right]$$
$$\times\left[\frac{\alpha_e(\omega - \omega_{ne})}{(\omega + i\nu_e - \omega_{ne})} + \frac{\alpha_p(\omega - \omega_{np})}{(\omega + i\nu_p - \omega_{np})} + \frac{m_e}{m_i}\frac{(\omega - \omega_{Di0})}{(\omega + i\nu_i - \omega_{Di0})} + b_{ep}\right]$$
$$= \frac{c_i^2 k_y^2}{\omega_{ci}\omega_{ce}}\left[\frac{n_{e0}\partial_x v_{e0}}{(\omega + i\nu_e - \omega_{ne})} - \frac{n_{p0}\partial_x v_{p0}}{(\omega + i\nu_p - \omega_{np})} - \frac{n_{i0}\partial_x v_{i0}}{(\omega + i\nu_i - \omega_{Di0})}\right]$$
$$\times\left[\frac{\partial_x J_{e0}}{(\omega + ik_\perp^2 D_e)} + \frac{\partial_x J_{p0}}{(\omega + ik_\perp^2 D_p)} + \frac{\partial_x J_{i0}}{(\omega + ik_\perp^2 D_i)}\right], \tag{5.19}$$

where $\alpha_p = n_{p0}/n_{i0}$, $\alpha_e = n_{e0}/n_{i0}$ and $b_{ep} = k_\perp^2 \lambda_{ep}^2 = c^2 k_\perp^2/(\omega_{pe}^2 + \omega_{pp}^2)$. In the limit $b_i \approx 0$ and $D_e = D_i = D_p$, Eq.(5.19) reduces to

$$\frac{n_{i0}\partial_x v_{i0}}{(\omega + i\nu_i - \omega_{Di0})} + \frac{n_{p0}\partial_x v_{p0}}{(\omega + i\nu_p - \omega_{np})} - \frac{n_{e0}\partial_x v_{e0}}{(\omega + i\nu_e - \omega_{ne})} = 0. \tag{5.20}$$

In the absence of the equilibrium density gradients and taking $\nu_e = \nu_p$, Eq. (5.20) demonstrates a mode having real frequency ω_r and the growth rate γ as

$$\omega_r = \frac{(n_{e0}\partial_x v_{e0} + n_{p0}\partial_x v_{p0})\,\omega_{Ti}}{(n_{i0}\partial_x v_{i0} + n_{e0}\partial_x v_{e0} + n_{p0}\partial_x v_{p0})}. \tag{5.21}$$

and

$$\gamma = -\frac{(n_{i0}\partial_x v_{i0})\,\nu_e + (n_{e0}\partial_x v_{e0} + n_{p0}\partial_x v_{p0})\,\nu_i}{(n_{i0}\partial_x v_{i0} + n_{e0}\partial_x v_{e0} + n_{p0}\partial_x v_{p0})}. \tag{5.22}$$

It follows from Eq. (5.22), the mode is damped. On the other hand, if we consider density gradients, then equation (5.20) can be written as

$$A\omega^2 + (B - iC)\,\omega + (D + iE) = 0, \tag{5.23}$$

where

$$A = n_{i0}\partial_x v_{i0} + n_{p0}\partial_x v_{p0} - n_{e0}\partial_x v_{e0},$$

$$B = n_{e0}(\omega_{np} + \omega_{Di0})\partial_x v_{e0} - n_{p0}\,(\omega_{ne} + \omega_{Di0})\,\partial_x v_{p0} - n_{i0}(\omega_{ne} + \omega_{np})\partial_x v_{i0},$$

$$C = n_{e0}(\nu_p + \nu_i)\partial_x v_{e0} - n_{p0}(\nu_e + \nu_i)\partial_x v_{p0} - n_{i0}(\nu_p + \nu_e)\partial_x v_{i0},$$

$$D = n_{e0}(\nu_p\nu_i - \omega_{np}\omega_{Di0})\partial_x v_{e0} - n_{p0}(\nu_e\nu_i - \omega_{ne}\omega_{Di0})\partial_x v_{p0} - n_{i0}(\nu_p\nu_e - \omega_{ne}\omega_{np})\partial_x v_{i0},$$

and

$$E = n_{e0}(\nu_p\omega_{Di0} + \nu_i\omega_{np})\partial_x v_{e0} - n_{p0}(\nu_e\omega_{Di0} + \nu_i\omega_{ne})\partial_x v_{p0} - n_{i0}(\nu_p\omega_{ne} + \nu_e\omega_{np})\partial_x v_{i0}.$$

Equation (5.23) predicts an oscillatory instability which is driven by the combined effects of shear and dissipation. The real frequency and the growth/damping rate can be written as

$$\omega_r = -\frac{P}{2} \pm \sqrt{\frac{\sqrt{R^2+S^2}+R}{8}} \tag{5.24}$$

and

$$\gamma = \frac{Q}{2} \mp \sqrt{\frac{\sqrt{R^2+S^2}-R}{8}}, \tag{5.25}$$

where $P = B/A$, $Q = C/A$, $R = \left(B^2 - C^2 + 4AD\right)/A^2$, $S = \left(4AE - 2BC\right)/A^2$. The value of γ is positive when one of the conditions is met i.e., $Q \geq 0$ or $\sqrt{\left(\sqrt{R^2+S^2}-R\right)/2} > |Q|$ provided $S^2 \neq 0$.

In the limit $\partial_x v_{k0} = D_j = 0$, Eq. (5.19) yields the following dispersion relations

$$\frac{\alpha_p(\omega-\omega_{np})}{(\omega+i\nu_p-\omega_{np})} + \frac{\alpha_e(\omega-\omega_{ne})}{(\omega+i\nu_e-\omega_{ne})} + \frac{m_e}{m_i}\frac{(\omega-\omega_{Di0})}{(\omega+i\nu_i-\omega_{Di0})} + b_{ep} = 0. \tag{5.26}$$

and

$$\omega = \omega_{Di0} + i\left(\mu_i k_\perp^2 - \nu_i\right). \tag{5.27}$$

If we assume $\omega \ll \nu_j$ and for inertialess electrons and positrons, equation (5.26) describes a mode with real frequency ω_r given by

$$\begin{aligned} \omega_r &= \varpi^{-2}\left(\alpha_e\omega_{np}+\alpha_p\omega_{ne}\right)\left[\left(\alpha_e+\alpha_p+b_{ep}\right)\omega_{np}\omega_{ne} - b_{ep}\nu_e\nu_p\right] \\ &+\varpi^{-2}\left(\alpha_e+\alpha_p+b_{ep}\right)\left[\left(\alpha_e+b_{ep}\right)\nu_p\omega_{ne} - \left(\alpha_p+b_{ep}\right)\nu_e\omega_{np0}\right] \end{aligned} \tag{5.28}$$

with a growth rate γ

$$\begin{aligned} \gamma &= \varpi^{-2}\left(\alpha_e\nu_p+\alpha_p\nu_e\right)\left[\left(\alpha_e+\alpha_p+b_{ep}\right)\omega_{np}\omega_{ne} - b_{ep}\nu_e\nu_p\right] \\ &+\varpi^{-2}\left(\alpha_e\omega_{np}+\alpha_p\omega_{ne}\right)\left[\tau\omega_{ni} - b_{ep}\left(\nu_p\omega_{ne}+\nu_e\omega_{np}\right)\right], \end{aligned} \tag{5.29}$$

where $\varpi_\nu^2 \equiv \left[\left(\alpha_e\omega_{np}+\alpha_p\omega_{ne}\right)^2 + \left(\alpha_e\nu_p+\alpha_p\nu_e\right)^2\right]$. Thus depending upon the magnitudes of drift-wave and collision frequencies, the mode can grow and become unstable.

Non-dissipative case: Consider a nondissipative plasma case for which $\nu_j = \chi_j = \mu_j = D_j = 0$ and $\omega \gg k_z v_{k0}$; $\omega_{Bk} = 0$, Eqs. (5.1), (5.4) and (5.5) yields the following result

$$\left(\omega - \omega_{Di0}\right)\Phi = \frac{1}{c}\left[k_z V_{Ai} - \frac{\omega_{LH}^2}{k_\perp^2}\left(\mathbf{S}_0 \cdot \mathbf{k}\right)\right] A_z, \tag{5.30}$$

where $\omega_{LH} = \sqrt{\omega_{ce}\omega_{ci}}$, $\mathbf{S}_0 = -\hat{\mathbf{z}}\times\left(\nabla J_0\right)/\left(n_{i0}e\omega_{ce}\right)$, $J_0 = e(n_{i0}v_{iz0} + n_{p0}v_{pz0} - n_{e0}v_{ez0})$ and $V_{Ai}^2 = B_0^2/\left(4\pi m_i n_{i0}\right)$.

From Eqs. (5.1)-(5.3), we get the following relation

$$\begin{aligned}\left(\omega - \omega_{Di0} - 5\tau^{-1}k_z^2 c_a^2/3\omega\right) V_i &= c_i k_z \left[\frac{5T_{i0}k_y\partial_x\left(n_{i0}v_{iz0}\right)}{3n_{i0}eB_0\omega} - \frac{1}{ck_z}\left(\omega - \omega_{Di0}\right)\right] A_z \\ &+ c_i k_z \left[1 - \frac{\mathbf{S}_{vo}^i \cdot \mathbf{k}}{k_z} - \frac{\omega_{ni}}{\omega}\left(\eta_i - \frac{2}{3}\right) - \frac{5}{3\omega}\left(\omega_{ni} + \tau^{-1}b_i\left(\omega - \omega_{Di0}\right)\right)\right]\Phi,\end{aligned} \tag{5.31}$$

$$\begin{aligned}\left(\omega - \omega_{ne} - k_z^2 v_{te}^2/\omega\right) V_e &= -v_{te}k_z\left(1 + \frac{\mathbf{S}_{vo}^e \cdot \mathbf{k}}{k_z} - \frac{\omega_{ne0}}{\omega}\right)\Phi \\ &+ v_{te}k_z\left(\frac{1}{ck_z}\left(\omega - \omega_{ne0}\right) + \frac{T_0 k_y \partial_x\left(n_{e0}v_{ez0}\right)}{n_{e0}eB_0\omega}\right) A_z.\end{aligned} \tag{5.32}$$

and

$$\begin{aligned}\left(\omega - \omega_{np} - k_z^2 v_{te}^2/\omega\right) V_p &= v_{te}k_z\left(1 - \frac{\mathbf{S}_{vo}^p \cdot \mathbf{k}}{k_z} - \frac{\omega_{np0}}{\omega}\right)\Phi \\ &- v_{te}k_z\left(\frac{1}{ck_z}\left(\omega - \omega_{np0}\right) - \frac{T_0 k_y \partial_x\left(n_{p0}v_{pz0}\right)}{n_{p0}eB_0\omega}\right) A_z.\end{aligned} \tag{5.33}$$

Combining Eqs. (5.30)-(5.33) and using Ampere's law i.e., $j_z = -\left(c/4\pi\right)\nabla_\perp^2 A_z$ and for flute type perturbations ($k_z = 0$), we get the following linear dispersion relation

$$\begin{aligned}1 + b_{ep} + \alpha^{-1}\frac{m_e}{m_i} &= -\frac{\omega_{LH}^2\left(\mathbf{S}_0 \cdot \mathbf{k}\right)}{\left(\omega - \omega_{Di0}\right)k_\perp^2} \\ &\times\left[\frac{m_e\alpha^{-1}\left(\mathbf{S}_{vo}^i \cdot \mathbf{k}\right)}{m_i\left(\omega - \omega_{Di0}\right)} + \frac{\alpha_p\left(\mathbf{S}_{vo}^p \cdot \mathbf{k}\right)}{\left(\omega - \omega_{np0}\right)} - \frac{\alpha_e\left(\mathbf{S}_{vo}^e \cdot \mathbf{k}\right)}{\left(\omega - \omega_{ne0}\right)}\right].\end{aligned} \tag{5.34}$$

If we consider electrons/positrons to be inertialess and assume flat density profiles, then Eq. (5.34) reduces to

$$(\omega - \omega_{Ti})\,\omega = -\frac{\omega_{LH}^2}{(1+b_e)\,k_\perp^2}\,(\mathbf{S}_0\cdot\mathbf{k})\left[\alpha_p\left(\mathbf{S}_{vo}^p\cdot\mathbf{k}\right) - \alpha_e\left(\mathbf{S}_{vo}^e\cdot\mathbf{k}\right)\right]. \tag{5.35}$$

Eq. (5.35) predicts an oscillatory instability provided that $(\mathbf{S}_0\cdot\mathbf{k})\left[(\alpha_p\mathbf{S}_{vo}^p - \alpha_e\mathbf{S}_{vo}^e)\cdot\mathbf{k}\right] < 0$ and $|(\mathbf{S}_0\cdot\mathbf{k})\left[(\alpha_p\mathbf{S}_{vo}^p - \alpha_e\mathbf{S}_{vo}^e)\cdot\mathbf{k}\right]|^2 > (1+b_e)\,\omega_{Ti}^2 k_\perp^2/4\omega_{LH}^2$.

Alfvénic modes: On the other hand, for a uniform and homogeneous plasma case, Eqs. (5.30) to (5.33) can be combined to obtain the following dispersion relation

$$\frac{\alpha^{-1}(m_e/m_i)\left[\omega^2 - \left(1 - 5\tau^{-1}b_i/3\right)k_z^2V_{Ai}^2\right]}{\left(\omega^2 - 5\tau^{-1}k_z^2c_i^2/3\right)} + \frac{\left(\omega^2 - k_z^2V_{Ai}^2\right)}{\left(\omega^2 - k_z^2v_{te}^2\right)} + b_{ep} = 0. \tag{5.36}$$

From Eq. (5.36), we can recover some fundamental dispersion relations. For example, for the waves having phase velocity much larger than the thermal velocity (v_{te}) of the inertialess electrons and positrons, the dispersion relation (5.36) reduces to the modified dispersion relation for the inertial Alfvén waves i.e.,

$$\omega = \frac{k_zV_{Ai}}{\sqrt{1+b_{ep}}}. \tag{5.37}$$

On the other hand, for the waves having phase velocity much smaller than v_{te} and of the order of $\sqrt{5/3}\tau^{-1/2}c_i$, the dispersion relation (5.36) reduces to the modified dispersion relation for the kinetic Alfvén waves

$$\omega = k_zV_{Ai}\sqrt{1 - 5\tau^{-1}b_i/3}. \tag{5.38}$$

Finally, for the waves propagating strictly parallel to external magnetic field (i.e., $k_\perp = 0$) and in the limit $\omega^2 \ll k_z^2v_{te}^2$, Eq. (5.36) yield Alfvénic and modified acoustic modes i.e.,

$$\omega^2 = k_z^2V_{Ai}^2, \quad \omega^2 = \left(1 + 5\alpha\tau^{-1}/3\right)k_z^2c_s^2. \tag{5.39}$$

where $c_s^2 = \alpha^{-1}c_i^2$ is the modified ion-acoustic speed in e-p-i plasma case.

5.2.3 Nonlinear Solutions

In the proceeding section, we have shown that how temperature, density, velocity and magnetic field gradients causes an instability of electrostatic and electromagnetic drift waves. Although it is very difficult and almost impossible to find an exact analytical solution of equations (2.21) to (2.27), we shall discuss here some approximate solutions. A possible stationary solution of a nondissipative ($\nu_j = \chi_j = \mu_j = D_j = 0$) inhomogeneous magnetoplasma can be obtained by introducing a new frame $\xi = y + \eta_0 z - u_0 t$, where η_0 is a constant and u_0 is the translational speed of the vortex, and by assuming that Φ, A_z, N_j, V_j and T are function of x and ξ only. Furthermore, assuming the vortex speed $u_0 \gg v_{Di0}$, v_{nj}, v_{Bj}, v_{j0}, c_i and $|\mathbf{v}_{EB}\cdot\nabla| \gg v_{iz}\partial_z$ in the stationary frame, Eqs. (2.21)-(2.27) may be written as

$$\mathcal{L}_\Phi\left[u_0 N_i + \tau\left(v_{ni} - v_{Bi}\right)\Phi - u_0\rho_i^2\nabla_\perp^2\Phi - v_{Bi}T\right] - \frac{T_0}{en_{i0}}\partial_x\left(\frac{J_{i0}}{eB_0}\right)\partial_\xi A_z$$
$$-\eta_0 c_i\mathcal{L}_A V_i = -\tau^{-1}\omega_{ci}\rho_i^4\nabla\cdot\left[\mathcal{J}\left[N_i + T, \nabla_\perp\Phi\right]\right], \qquad (5.40)$$

$$\mathcal{L}_\Phi\left[u_0 V_i - c_i\left\{\left(\eta_0 + \frac{\partial_x v_{i0}}{\omega_{ci}}\right)\Phi - \frac{u_0}{c}A_z\right\}\right] - \eta_0 c_i\tau^{-1}\mathcal{L}_A\left(N_i + T\right) = 0, \qquad (5.41)$$

$$\mathcal{L}_\Phi\left[u_0\left(T - \frac{2}{3}N_i\right) + \tau\left(\eta_i - \frac{2}{3}\right)v_{ni}\Phi\right] = 0, \qquad (5.42)$$

$$\mathcal{L}_\Phi\left[u_0 N_e + \left(v_{Be} - v_{ne}\right)\Phi\right] - \frac{T_0}{en_{e0}}\partial_x\left(\frac{J_{e0}}{eB_0}\right)\partial_\xi A_z - \eta_0 v_{te}\mathcal{L}_A V_e = 0, \qquad (5.43)$$

$$\mathcal{L}_\Phi\left[u_0 N_p + \left(v_{np} - v_{Bp}\right)\Phi\right] - \frac{T_0}{en_{p0}}\partial_x\left(\frac{J_{p0}}{eB_0}\right)\partial_\xi A_z - \eta_0 v_{te}\mathcal{L}_A V_p = 0, \qquad (5.44)$$

$$\mathcal{L}_\Phi\left[u_0 V_e + v_{te}\left\{\left(\eta_0 + \frac{\partial_x v_{e0}}{\omega_{ce}}\right)\Phi - \frac{u_0}{c}A_z\right\}\right] - \eta_0 v_{te}\mathcal{L}_A N_e = 0, \qquad (5.45)$$

$$\mathcal{L}_\Phi\left[u_0 V_p - v_{te}\left\{\left(\eta_0 + \frac{\partial_x v_{p0}}{\omega_{ce}}\right)\Phi - \frac{u_0}{c}A_z\right\}\right] - \eta_0 v_{te}\mathcal{L}_A N_p = 0, \qquad (5.46)$$

where $\mathcal{L}_\Phi \equiv \partial_\xi - (cT_0/u_0 eB_0)(\partial_x \Phi \partial_\xi - \partial_\xi \Phi \partial_x)$, $\mathcal{L}_A \equiv \partial_\xi - (T_0/\eta_0 eB_0)(\partial_x A_z \partial_\xi - \partial_\xi A_z \partial_x)$, $\nabla_\perp^2 = \partial^2/\partial x^2 + \partial^2/\partial \xi^2$.

Considering both electrons and positrons to be inertialess and using $\mathcal{L}_\Phi (\Phi - u_0 A_z/\eta_0 c) = \mathcal{L}_A (\Phi - u_0 A_z/\eta_0 c)$, Eq. (5.45) and (5.46) can be combined to yield a typical solution

$$N_i = \alpha \left(\Phi - \frac{u_0}{\eta_0 c} A_z\right), \tag{5.47}$$

where $\alpha = N_0/n_{i0}$. Using (5.47) in (5.42) and assuming vortex speed $u_0 \gg \alpha^{-1}\tau (1 - 3\eta_i/2) v_{ni}$, it can easily shown that Eq. (5.42) is satisfied by

$$T = \frac{2\alpha}{3} \left(\Phi - \frac{u_0}{\eta_0 c} A_z\right) \tag{5.48}$$

Substituting the values of N_i and T in Eq. (5.41), we readily obtain

$$\mathcal{L}_\Phi \left[u_0 V_i - \eta_0 c_s \left(1 + \frac{5\alpha\tau^{-1}}{3}\right)\left(\Phi - \frac{u_0}{\eta_0 c} A_z\right)\right] = 0, \tag{5.49}$$

which is satisfied by

$$V_i = \frac{\eta_0 c_i}{u_0} \left(1 + \frac{5\alpha\tau^{-1}}{3}\right)\left(\Phi - \frac{u_0}{\eta_0 c} A_z\right). \tag{5.50}$$

Under low-β approximation, the contribution of the ion current density to j_z would be negligibly small, therefore, from Eqs. (5.43), (5.44) and (5.47), we can write

$$\mathcal{L}_A \left(c u_0 \Phi - u_1^2 A_z - \eta_0 \lambda_{ep}^2 v_{te}^2 \nabla_\perp^2 A_z\right) = 0, \tag{5.51}$$

where $\eta_0 u_1^2 = [u_0^2 - (\eta_0 c T_0/\alpha e n_{i0}) \partial_x (J_{ep}/eB_0)]$. It is easy to verify that equation (5.51) is satisfied by

$$\left(1 + \lambda^2 \nabla_\perp^2\right) A_z - \beta_1 \Phi = 0, \tag{5.52}$$

where $\lambda^2 = \eta_0 \lambda_{ep}^2 v_{te}^2 / u_1^2$ and $\beta_1 = c u_0 / u_1^2$. Inserting N_i, T and V_i, respectively, from

(5.47), (5.48) and (5.50) into (5.40), we get

$$\mathcal{L}_\Phi \left[\alpha u_0 \left(\Phi - \frac{u_0}{\eta_0 c} A_z\right) - u_0 \rho_i^2 \nabla_\perp^2 \Phi\right] - \frac{T_0}{e n_{i0}} \partial_x \left(\frac{J_{i0}}{e B_0}\right) \partial_\xi A_z$$
$$= \frac{5\alpha\tau^{-1}\omega_{ci}\rho_i^4}{3} \left[\mathcal{J}\left[\Phi, \nabla_\perp^2 \Phi\right] - \nabla\cdot\mathcal{J}\left[\frac{u_0}{\eta_0 c} A_z, \nabla_\perp \Phi\right]\right]. \tag{5.53}$$

It is somewhat difficult to find the general solutions of Eqs. (5.52) and (5.53), specifically, due to the nonlinearity caused by ion-pressure-gradient force (last term on right hand side of the above equation). However, the system of nonlinear equations (5.52)-(5.53) can be solved in the limiting case, $\lambda^2\nabla_\perp^2 \ll 1$ that is the scale size of the vortex is assumed to be much smaller than the effective skin depth (λ). Therefore, Eq. (5.52) gives

$$A_z = \beta_1 \Phi \tag{5.54}$$

Inserting Eq. (5.54) into Eq. (5.53), we obtain

$$u_0\rho_i^2\partial_\xi\nabla_\perp^2\Phi + \frac{\beta_1 T_0}{n_{i0}e}\partial_x\left(\frac{J_0}{eB_0}\right)\partial_\xi\Phi - \left[1 + \frac{5T_{i0}}{3n_{i0}e}\partial_x\left(\frac{J_{ep}}{eB_0}\right)\right]\omega_{ci}\rho_i^4\mathcal{J}\left[\Phi, \nabla_\perp^2\Phi\right] = 0 \tag{5.55}$$

Equation (5.55) is satisfied by the ansätz

$$\nabla_\perp^2 \Phi = C_1 \Phi + C_2 x, \tag{5.56}$$

where the constants C_1 and C_2 are related by $u_0\rho_i^2 C_1 - (\beta_1 T_0/n_{i0}e)\partial_x(J_0/eB_0) + \sigma C_2 = 0$ and $\sigma = (1 + 5T_{i0}/3n_{i0}e)\partial_x(J_{ep}/eB_0)$.

Equation (5.56) is a second order inhomogeneous differential equation which admits spatially bounded dipolar vortex solution [90, 108, 109]. However, in the absence of equilibrium currents, Eq. (5.55) takes the form of a stationary Navier-Stokes equation, namely,

$$\partial_\xi \nabla_\perp^2 \Phi = \frac{\mu_1}{u_0} \mathcal{J}\left[\Phi, \nabla_\perp^2 \Phi\right]. \tag{5.57}$$

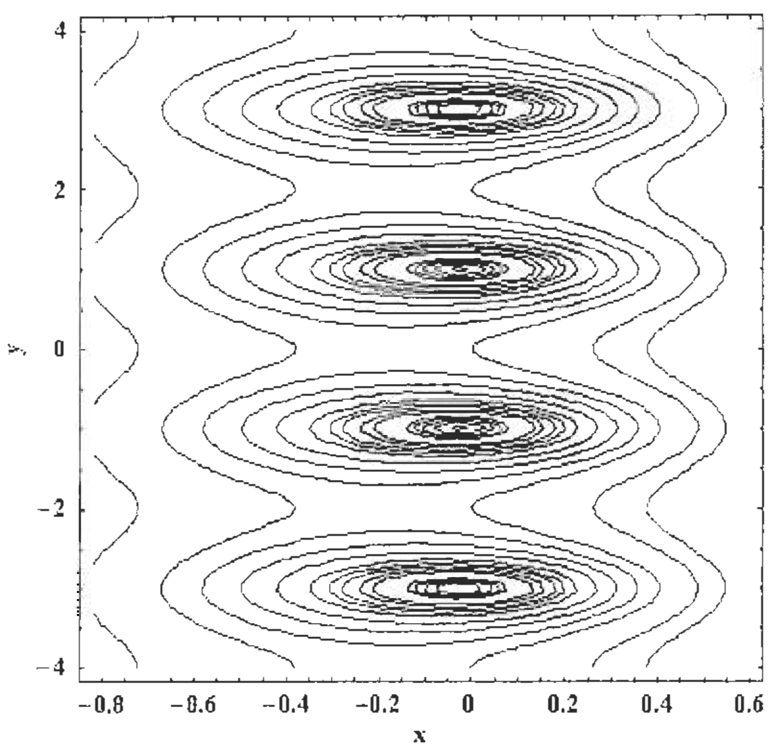

Figure 5-1: A typical vortex street profile obtained from Eq. (5.59) for $\alpha = 10$ and $u = 1.1 \times 10^7$ cm/sec.

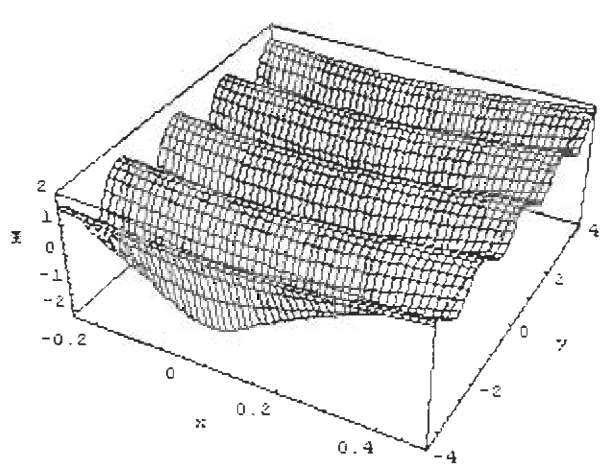

Figure 5-2: Three-dimensional view of the vortex street profile obtained from Eq. (5.59).

where $\mu_1 = cT_0/eB_0$. For $\mu_1 > 0$, Equation (5.57) is satisfied by

$$\nabla_\perp^2 \Phi = \frac{4\Phi_0 K_0^2}{a_0^2} \exp\left[-\frac{2}{\Phi_0}\left(\Phi - \frac{u_0}{\mu_1}x\right)\right], \tag{5.58}$$

where Φ_0, K_0, and a_0 are some arbitrary constants.

The solution of Eq. (5.58) is

$$\Phi = \frac{u_0}{\mu_1}x + \Phi_0 \ln\left[2\cosh(K_0 x) + 2\left(1 - \frac{1}{a_0^2}\right)\cos(K_0\xi)\right]. \tag{5.59}$$

Here we note that for $a_0 > 1$ (a_0 is the size of vortex) the vortex profile (5.59) resembles the Kelvin-Stuart "cat's eyes" that are chains of vortices [92] in an e-p-i plasma. Fig. 5-1 shows the vortex street profile Φ against x and y for some typical parameters and Fig. 5-2 presents its three-dimensional view.

5.3 Summary

In this chapter, we have described the nonlinear dynamics of electromagnetic waves in e-p-i magnetoplasma with equilibrium density, temperature, magnetic field and velocity gradients with dissipative effects. By employing the Braginskii's transport equations for the ions and continuity and momentum balance equations for electron and positron plasma, we derive seven sets of nonlinear mode coupling equations. In the linear case, we have derived local dispersion relation and obtained new class of instabilities and modes for e-p-i plasma. We found that in the presence of positrons, electromagnetic and electrostatic disturbances respond in very different way and several new types of modes and instabilities are found to exist. For instance, it has been shown that non-zero equilibrium ion-temperature and the presence of positrons modify the previously known results. It is also found that sheared equilibrium flows can cause instability of the Alfvén waves even in the absence of density inhomogeneity. On the other hand, in the nonlinear case, the mode coupling equations admit dipolar and vortex chain type of vortices.

Chapter 6

Chaotic States in Electron-Positron-Ion Magnetoplasma

6.1 Introduction

6.1.1 Basic Concepts of Nonlinear Dynamics

The state space or phase space is defined as the combined space of momentum and position. State space plays an important role in visualizing numerical solutions by turning numbers into pictures. Nonlinear system is a system whose time evolution equations are nonlinear, that is, the dynamical variables describing the properties of the system (for example; position, velocity, acceleration, pressure etc.) appears in the equations in a nonlinear form like x^2, x^3, $\cos(x)$, $\log(x)$, $\exp(x)$ etc. The study of nonlinear behavior is called *Nonlinear Dynamics.* Almost all real systems are nonlinear at least to some extent. Some sudden and dramatic changes in nonlinear systems may give rise to the complex behavior called *chaos.* The noun chaos and adjective chaotic are used to describe the time behavior of a system when that behavior is aperiodic (it never exactly repeats) and apparently random or "noisy". A system is said to be deterministic if the knowledge of the time evolution equations, the parameters that describe the system, and the initial conditions, in principle completely determine the subsequent behavior of the system. The term chaotic is assigned to that class of motion in deterministic physical and mathematical systems whose time history has a sensitive dependence on initial conditions.

As time evolves, the initial state point in state space follows a trajectory. The trajectory closes on itself if the motion is periodic. Such a closed periodic trajectory is called a *cycle*. The *attractor* is that set of points to which trajectories approach as the number of iterations goes to infinity. Sink is one of it's examples as it is just a point in phase space to which trajectories lead. The complicated systems may have more than one attractor for a given parametric value. The set of initial conditions giving rise to trajectories that approach a given attractor is called the *basins of attraction* for that attractor. The stable equilibrium (simplest attractor) is a *point attractor* for all trajectories in phase space. A second type of attractor is the *limit cycle*, namely a steady closed oscillation that attracts all adjacent motions. If the cycles of trajectory gradually move closer to the limit cycle then we call it the *stable or attracting* limit cycle. If the cycles of the trajectory which are gradually moving away from the limit cycle then we call it *unstable or repelling* limit cycle. Another possibility is that the trajectories are attracted on one side and repelled on the other known as a *saddle cycle*. A third type is the strange or *chaotic attractor* that captures the solution of a perfectly deterministic and well defined equation into a state of steady but perpetual chaos. These three types of attractors represent the most commonly observable long-term motion in dissipative systems. Thus we identify all stable final motion with attracting sets in phase space. If more than one attractor exists for a system with a given set of parameter values there will be some initial conditions form what is called a *separatrix* since they separate different basins of attraction. *Poincaré section* is the sequence of points in the phase space produced by the penetration of a continuous time evolution trajectory through a generalized surface or a planar in the space. These sequence of points shouldn't be considered as a curve. If the points or dots of the trajectories on the Poincaré surface lie at the same place then it is the indication of the periodicity of the system or trajectory but if the points are at different places then the system is aperiodic. The Poincaré section, freezes the motion of the dynamical system.

The state of zero acceleration and velocity is called *fixed point*. In dynamical system, a point in state space towards or away from which a solution may move as transient decay approaches to infinity is called "fixed point". There are different types of fixed points depending on the nature of the characteristic values. The *index* of a fixed point is defined to be the number of characteristic values of that fixed point whose real parts are positive. Fixed point turn into spiraling form if the characteristic values are of complex nature.

1. Node: All the characteristic values are real and negative. All trajectories in the neighborhood of the node are attracted toward the fixed point without looping around the fixed point. For "spiral node" two of the characteristic values have nonzero imaginary parts.

2. Repellor: All the characteristic values are real and positive. All trajectories in the neighborhood of the repellor diverge from the repellor. For "spiral repellor" two of the characteristic values have nonzero imaginary parts.

3. Saddle point: index 1: All characteristic values are real. One is positive and two are negative. Trajectories approach the saddle point on a surface and diverge along a curve. For spiral saddle point the two characteristic values with negative real parts form a complex conjugate pair.

4. Saddle point: index 2: All characteristic values are real . Two are positive and one is negative. Trajectories approach the saddle point on a curve (the in set) and diverge from the saddle point on a surface (the out set). For spiral saddle point the two characteristic values with positive real parts form a complex conjugate pair.

The set of points that form the trajectories heading directly to or directly away from a saddle point are sometimes called the invariant manifolds associated with that saddle point. More specifically, the trajectories heading directly toward the saddle point form what is called the stable manifold (because the characteristic value is negative along these trajectories), while the trajectories heading directly away from the saddle point form what is called the unstable manifold. The term *hyperbolic* is applied to any fixed point whose characteristic values are not equal to zero, and *non-hyperbolic* if the associated characteristic value is zero. *Lyapunov exponent* is the averaged rate of the exponential divergence (positive exponent) or convergence (negative exponent) of nearby orbits in phase space. It is a measure of the rate of attraction to or repulsion from the fixed point in the state space. Its value can be found by using following equation

$$\lambda = \left. \frac{df(x)}{dx} \right|_{x=x_0} \tag{6.1}$$

where λ represents Lyapunov exponent and $f(x)$ is function of x in the neighborhood of the fixed point x_0. The trajectory approaches the fixed point (a node) exponentially if λ is negative and is repelled from the fixed point (a repeller) exponentially if λ is positive. The Lyapunov exponent for a region of one-dimensional state space near a fixed point is the characteristic value λ of that fixed point. In two or higher dimensional state space, we associate a local Lyapunov exponent with the rate of expansion or contraction of trajectories for each of the directions in state space. We define a chaotic system to be a system which has at least one positive average Lyapunov exponent.

Many systems are in a slowly evolving environment, so their coefficients and parameters undergo gradual change. Then if evolving system is in steady state, periodic oscillation or chaos, the prediction of any sudden change is of crucial importance. Such *Bifurcation* of behavior will occur when one equilibrium state changes into two stable equilibrium states. Bifurcation is defined as "Splitting of the system into two regions, one above, the other below the particular parameter value at which the change occurs". Bifurcation take place due to the change in parametric values, the number of parameters that must change to produce bifurcation is called the *co-dimension* of the bifurcation. If we want to find the co-dimension of any manifold geometrically, it is mathematically written as $(n - m)$, where m is the dimension of the manifold and n is the dimension of the space around the manifold. The study of how the character of fixed points and other types of state space attractors change as parameters of the system change is called *bifurcation theory*. In the study of nonlinear dynamics, classification of understanding of bifurcation plays important role. Bifurcation is a vast field and a lot of work has been done but is still incomplete. To understand bifurcation in two dimensions, consider the following example equations

$$\dot{x}_1 = \mu - x_1^2 \Longrightarrow x_1^2 = \mu \Longrightarrow x_1 = \pm\mu \tag{6.2}$$

$$\dot{x}_2 = -x_2 \Longrightarrow x_2 = 0 \tag{6.3}$$

When $\mu > 0$, the fixed points are $(x_1, x_2) = (\mu, 0)$ and $(-\mu, 0)$. The one at $(\mu, 0)$ is a node; the one at $(-\mu, 0)$ is a saddle point. For $\mu < 0$, there is no fixed point. The $\mu = 0$ is a point of saddle-node bifurcation as system behavior splits into two states. A fixed point in two-dimensional state space may also have complex-valued characteristic values for which the trajectories have *spiral* type behavior. A bifurcation occurs when the characteristic values move from the left-hand side of the complex plane to the right-hand side; that is, the bifurcation occurs when the real part of the characteristic value goes to zero. The birth and death of a limit cycle are bifurcation events. The birth of a stable limit cycle is called a *Hopf bifurcation*. In two dimensions *Hopf bifurcation* is a good example to understand the spiral nature of node and repellor. In terms of the characteristic multipliers, the Hopf bifurcation is marked by having the two complex conjugate multipliers cross the unit circle simultaneously. Let us take the following equations to model Hopf bifurcation:

$$\dot{x}_1 = -x_2 + x_1\left[\mu - \left(x_1^2 + x_2^2\right)\right] \tag{6.4}$$

$$\dot{x}_2 = x_1 + x_2\left[\mu - \left(x_1^2 + x_2^2\right)\right] \tag{6.5}$$

If we change these equations from (x_1, x_2) cartesian coordinates into polar coordinates (r, θ), where

$$r = \sqrt{(x_1^2 + x_2^2)},\ tan\theta = \frac{x_2}{x_1}. \tag{6.6}$$

Therefore, Eqs. (6.4) and (6.5) become

$$\dot{r} = r\left(\mu - r^2\right) = f(r),\ \dot{\theta} = 1. \tag{6.7}$$

The solution of above equation is $\theta(t) = \theta_0 + t$, which shows that the angle is gradually increasing with time as the trajectory spirals around the origin. *For* $\mu < 0$, $r = 0$ is an only fixed point to find its nature. We get $df(r)/dr|_{r=0}$ which gives characteristic value $= \mu$. Thus for $\mu < 0$, we get a negative derivative value, so fixed point is stable which is a spiral node. *For* $\mu > 0$, there are two fixed points, one is an unstable, spiral repellor at the origin, trajectory spiralling away from the fixed point. Other fixed point is at $r = \sqrt{\mu}$ having a limit cycle of period 2π . This limit cycle is born at $\mu = 0$ (bifurcation point). This birth of a stable limit cycle is called a Hopf bifurcation. If some addition term is added to the dynamical equations and bifurcation remains the same then we shall call it *stable bifurcation* but on the other hand, if bifurcation changes then it will be structurally *unstable bifurcation*.

6.1.2 Chaos in Lorenz model

The sensitive dependence on initial conditions of chaotic systems is more popularly known as the *butterfly effect*. This phenomenon was first discovered by Edward Lorenz [71] during his investigation into a system of coupled ordinary differential equations used as a simplified model of 2D thermal convection, known as Rayleigh-Benard convection. These equations are now called the Lorenz equations, or *Lorenz model*. In Lorenz model, a Rayleigh-Benard convection between two horizontal plates are considered. The bottom plate is at a temperature T_b which is greater than that of the top plate, T_t. For small differences between the two temperatures, heat is conducted through the stationary fluid between the plates. However, when $T_b - T_t$ becomes large enough, buoyancy forces within the heated fluid overcome internal fluid viscosity and a pattern of counter-rotating, steady recirculating vortices is set up between the plates. Lorenz noticed that, in his simplified mathematical model of Rayleigh-Benard convection, very small variations in the initial conditions blew up and quickly led to enormous differences in the final behavior. He reasoned that if this type of behavior could occur in such a simple dynamic system, then it may also be possible in a much more complex physical system involving convection such as in the weather system. Thus a very small perturbation, caused for instance by a butterfly flapping its wings, would lead rapidly to a complete change in future weather patterns. The Lorenz equations are

$$\begin{aligned} \dot{X} &= \sigma(Y - X) \\ \dot{Y} &= (r - Z)X - Y \\ \dot{Z} &= XY - bZ \end{aligned} \tag{6.8}$$

This system has two nonlinearities, the XZ term and the XY term, and exhibits both periodic and chaotic motion depending upon the values of the control parameters σ, r and b. σ is the Prandtl number which relates the energy losses within the fluid due to viscosity to those due to thermal conduction; r corresponds to the dimensionless measure of the temperature difference between the plates known as the Rayleigh number; and b is related to the ratio of the vertical height of the fluid layer to the horizontal extent of the convective rolls within it. Note also that the variables X, Y and Z are not spatial coordinates but rather represent the convective overturning, horizontal temperature variation, and vertical temperature variation respectively.

Lorenz set $\sigma = 10$ and $b = 2.67$ and make r the adjustable control parameter. Varying the value of r reveals a critical value at $r_c = 24.74$ at which the behavior of the system changes dramatically. Below r_c the system decays to a steady, non-oscillating state. Once r increases beyond r_c continues oscillatory behavior. A value of $r = 28$ produces aperiodic behavior which Lorenz called "deterministic non-periodic flow" and which is referred to as chaos.

6.1.3 Bifurcation Characteristics in Lorenz and Lorenz-Stenflo Equations

Lorenz equations are well known in the study of deterministic chaos. Similar equations are found in many branches of Physics and Chemistry even in atmosphere and are observable easily. The stationary points of the Lorenz equations are $X_{s\pm} = \pm[-b + br]^{\frac{1}{2}}$, $Y_{s\pm} = \pm[-b + br]^{\frac{1}{2}}$ and $Z_s = -1 + r$. In original Lorenz equations there are three control parameters b, r and σ. In the traditional studies of the Lorenz system, the bifurcation behavior of the Lorenz system with the Rayleigh number r as the bifurcation parameter, the regimes of chaotic and periodic solutions with respect to the parameter r is investigated for fixed b and σ. Specially, the maxima of oscillating solutions are plotted against a given control parameter r. Thus, for each value of the controlled parameter (Rayleigh number) r, a singly periodic solution would be represented by one point, a doubly periodic one by two points etc., and chaotic one by vertical lines. By varying the control parameter in small increments, one can obtain so called the bifurcation diagram showing the location of the fixed point (or points) as a function of control parameter.

Lorenz equations always give *backward bifurcation* structure in the Rayleigh number space. The phenomenon of backward bifurcation is of special interest since the simplest (of periodic unity) periodic motion can occur at large amplitudes. This is in sharp contrast with the usual dynamical systems, where simple harmonic motion occurs only as a linear limit. Such different behavior can be related to the self-organization and stability of large-scale structures in certain physical systems. One should be careful to use large amplitude limits while applying Lorenz- like equations which depends on the validity of certain amplitude related truncations invoked in their derivation. In Lorenz equations, one can get both forward and backward bifurcations by varying σ as a control parameter.

Contrary to Lorenz equations, the bifurcation space of *Lorenz-Stenflo* equations are more complex and rich in details, it includes the phenomenon of overlapping for forward and backward bifurcation regions. Stenflo [72] showed that low frequency, short wavelength acoustic gravity waves in a rotational system can be described by a set of four simple nonlinear ordinary differential equations with four constant nondimensional parameters Prandtl number σ, geometric factor b, Rayleigh number r and rotation factor s. Lorenz-Stenflo equations are as under

$$\begin{aligned}\dot{X} &= -\sigma X + \sigma Y + sV \\ \dot{Y} &= (r - Z)X - Y \\ \dot{Z} &= XY - bZ \\ \dot{V} &= -X - \sigma V \end{aligned} \tag{6.9}$$

Lorenz equations are the subset of Lorenz-Stenflo (L-S) equations. The stationary points of the L-S system are the origin O (0, 0, 0, 0) and $X = X_{s\pm} = \pm[bZ_s/(1+s/\sigma^2)]^{\frac{1}{2}}$, $Y = Y_{s\pm} = \pm[bZ_s/(1+s/\sigma^2)]^{\frac{1}{2}}$, $Z = Z_s = r - 1 - s/\sigma^2$ and $V = V_{s\pm} = -X_{s\pm}/\sigma$ which differ considerably from the corresponding stationary points of the Lorenz equations. Lorenz equations were originally derived to describe atmospheric waves and is well known in deterministic chaos. Stenflo gave the idea that all stationary points can not exist for arbitrary values of the parameters.

6.1.4 Routh-Hurwitz Stability Criterion

Consider a given dynamical system that is moving under the action of some forces described by a set of differential equations. If any small disturbance is applied to the system, it may deviate only slightly from the previous condition of motion or it may depart from it further and further. If the deviation is slight, the system is said to be dynamically stable; otherwise, the system is dynamically unstable. The system is dynamically stable, if it is stable for all kinds of disturbances. The stability criteria are of great importance in determining the stability of many practical dynamical systems. The *Routh-Hurwitz stability criterion* [110] is one of the simple procedure to obtain the information concerning the stability of the system. Let us elaborate the use of Routh-Hurwitz stability criterion. Consider a system whose characteristic equation $D(s)$ is of the form

$$D(s) = a_0 s^n + a_1 s^{n-1} + ... + a_{n-1} s + a_n, \tag{6.10}$$

where all a_i are constants of the dynamical system. The stability and instability of the dynamical system depends on the location of roots of the polynomial $D(s)$ in the complex s plane. If real parts of all the roots of the polynomial $D(s)$ are negative numbers, the solution will be stable. If, however, one or more roots have a positive real part, the system will be unstable. An imaginary root represents a borderline between stability and instability. The Routh-Hurwitz stability criterion assures stability if

1. A necessary but not sufficient condition is that all the a_i in the Eq. (6.10) have the same sign.

2. A necessary and sufficient condition for stability is that the following test functions T_i are all positive when equation $D(s) = 0$ is put in such form that a_0 is positive:

$$T_1 = a_1, T_2 = \begin{vmatrix} a_1 & a_0 \\ a_3 & a_2 \end{vmatrix}, T_3 = \begin{vmatrix} a_1 & a_0 & 0 \\ a_3 & a_2 & a_1 \\ a_5 & a_4 & a_3 \end{vmatrix};$$

$$T_i = \begin{vmatrix} a_1 & a_0 & 0 & 0 & \cdots & \cdots \\ a_3 & a_2 & a_1 & a_0 & \cdots & \cdots \\ a_5 & a_4 & a_3 & a_2 & \cdots & \cdots \\ .... & .... & \cdots & \cdots & \cdots & \cdots \\ a_{2i-1} & a_{2i-2} & \cdots & \cdots & \cdots & a_i \end{vmatrix}. \tag{6.11}$$

where all the coefficients a_r with $r > n$ or $r < 0$ are replaced by zeros. If any of these determinants have negative values, the system is unstable. Now we present the derivation of nonlinear equations to study the temporal behavior of electrostatic/electromagnetic waves in e-p-i magnetoplasma with equilibrium flows.

6.2 Chaotic Behavior of Electrostatic Waves in Cold Ions Limit

In order to study the temporal behavior of nonlinearly interacting finite amplitude two dimensional electrostatic waves in collisional magnetoplasmas in cold ions limit [56], we assume $|\partial_t + \mathbf{v}_{EB} \cdot \nabla| \gg v_{i0}\partial_z;\, v_{iz}\partial_z$. Here we have retained the leading order terms and taken into account the small magnetic sheared effects such that $\partial_z v_{iz} \approx \partial_x f(x)\, \partial_y v_{iz}$. Consequently, Eqs. (3.1) and (3.2) take the following form,

$$(\partial_t + \mathbf{v}_{EB} \cdot \nabla + \nu_i)\, v_{iz} = -\frac{e}{m_i}\left[\partial_x f(x) - S_i\right] \partial_y \phi = -F \partial_y \phi \tag{6.12}$$

and

$$-\rho_s^2 \left[\partial_t + \mathbf{v}_{EB} \cdot \nabla + \nu_i\right] \nabla_\perp^2 \phi + \partial_t \phi - u_n \partial_y \phi + \frac{T_0 n_{i0} \partial_x f(x)}{e n_{e0}(1+\delta)} \partial_y v_{iz} = 0. \tag{6.13}$$

Here, we follow Lorenz [71] and Stenflo [72], and derive a set of equations which are appropriate for studying the temporal behavior of chaotic motion involving low-frequency electrostatic waves in a dissipative magnetoplasma with sources. Accordingly, we introduce the ansätz:

$$\phi = \phi_1(t) \sin(K_x x) \sin(K_y y), \tag{6.14}$$

$$v_{iz} = v_1(t) \sin(K_x x) \cos(K_y y) - v_2(t) \sin(2K_x x). \tag{6.15}$$

where K_x and K_y are constant parameters, and ϕ_1, v_1 and v_2 are amplitudes which are only functions of time. Substituting Eqs. (6.14) and (6.15) into Eqs.(6.12) and (6.13), we readily obtain

$$\dot{\phi}_1 = -\nu_i \frac{K_\perp^2 \rho_s^2}{(1 + K_\perp^2 \rho_s^2)} \phi_1 + \frac{K_y T_0 n_{i0} \partial_x f(x)}{e n_{e0} (1 + K_\perp^2 \rho_s^2)(1+\delta)} v_1 \tag{6.16}$$

$$\dot{v}_1 = -\nu_i v_1 + \frac{c K_x K_y}{B_0} \phi_1 v_2 - F K_y \phi_1 \tag{6.17}$$

and

$$\dot{v}_2 = -\nu_i v_2 - \frac{c K_x K_y}{2 B_0} \phi_1 v_1. \tag{6.18}$$

where $K_\perp^2 = K_x^2 + K_y^2$. The time derivative is defined by a dot on ϕ_1, v_1 and v_2. It may be noted here that we have dropped the terms proportional to $\sin(3K_x x)$ in the derivation of (6.16)–(6.18).

Equations (6.16)–(6.18) can be appropriately normalized so that they can be put in a form which is similar to that of Lorenz-Stenflo and Mirza & Shukla [71, 72, 112]. We have the following 3×3 matrix

$$\begin{pmatrix} d_\tau X \\ d_\tau Y \\ d_\tau Z \end{pmatrix} = \begin{pmatrix} -\sigma & \sigma & 0 \\ r - Z & -1 & 0 \\ Y & 0 & -1 \end{pmatrix} \begin{pmatrix} X \\ Y \\ Z \end{pmatrix} \tag{6.19}$$

which describes the nonlinear coupling between various amplitudes. Here, $\sigma = K_\perp^2 \rho_s^2 / (1 - K_\perp^2 \rho_s^2)$, $r = -(n_{e0} + n_{p0}) K_y^2 n_{i0} d_x f(x) \,/\, (\nu_i^2 K_\perp^2 \rho_s^2 e n_{e0} (1+\delta))$, $\tau = t\nu_i$.

The normalizations used here are

$$\phi_1 = a_1 X = \pm \frac{\sqrt{2} B_0 \nu_i}{c K_x K_y} X, \tag{6.20}$$

$$v_1 = a_2 Y = \pm \frac{\sqrt{2} B_0 K_\perp^2 \rho_s^2 e n_{e0} (1+\delta) \nu_i^2}{c K_x K_y^2 T_0 n_{i0} d_x f(x)} Y, \tag{6.21}$$

and

$$v_2 = a_3 Z = -\frac{B_0 K_\perp^2 \rho_s^2 e n_{e0} (1+\delta) \nu_i^2}{c K_x K_y^2 T_0 n_{i0} d_x f(x)} Z. \tag{6.22}$$

The above-mentioned equations are the generalized Lorenz-Stenflo equations with equilibrium fixed points $X_s = Y_s = \pm\sqrt{|r| - 1}$, and $Z_s = (|r| - 1)$. For $|r| > 1$, the equilibrium fixed points are unstable resulting in convective cell motions. Thus the linear instability should saturate by attracting to one of these new fixed states. The stability of the stationary states of Eq. (6.19) can be studied by letting $X = X_s + X_1$, $Y = Y_s + Y_1$, and $Z = Z_s + Z_1$, so that the system on linearization becomes

$$\begin{pmatrix} d_\tau X_1 \\ d_\tau Y_1 \\ d_\tau Z_1 \end{pmatrix} = \begin{pmatrix} -\sigma & \sigma & 0 \\ r - Z_s & -1 & -X_s \\ Y_s & X_s & -1 \end{pmatrix} \begin{pmatrix} X_1 \\ Y_1 \\ Z_1 \end{pmatrix}, \tag{6.23}$$

where $X_1 \ll X_s$, $Y_1 \ll Y_s$, and $Z_1 \ll Z_s$. (X_s, Y_s, Z_s) represents a stationary state. The corresponding characteristic equation is

$$\lambda^3 + A\lambda^2 + B\lambda + C = 0, \tag{6.24}$$

where $A = 2 + \sigma$, $B = (1 - r)\sigma + (1 + \sigma) + \sigma Z_s + X_s^2$, $C = (1 - r)\sigma + \sigma Z_s + \sigma X_s Y_s + \sigma X_s^2$. For simplicity, we choose the trivial stationary points $X_s = Y_s = Z_s = 0$ in Eq. (6.23) so that the characteristic equation becomes

$$(\lambda + 1)\left[\lambda^2 + (1 + \sigma)\lambda + (1 - r)\sigma\right] = 0. \tag{6.25}$$

For $r < 1$, the eigenvalues are $\lambda = -1, -\sigma, -1$. Thus the trivial stationary points is a hyperbolic sink and is thus stable. On the other hand, for $r = 1$, the eigen values are $\lambda = 0, -1, -(1 + \sigma)$, and thus the equilibrium becomes unstable.

Finally, for $r > 1$, the nontrivial stationary points are $X_s^{\pm} = Y_s^{\pm} = \pm\sqrt{r - 1}$ and $Z_s = r - 1$. In this case, the eigenvalues of Eq. (6.25) are $\lambda = -(\sigma + 2)$ and $\pm\, i \sqrt{2\sigma(\sigma + 1)(\sigma - 2)}$. The stability of the system can be determined by using Routh-Hurwitz criterion [96], i.e., the coefficients A, B, C of Eq. (6.24) should satisfy the inequality $AB - C > 0$. In our case, we found that the nontrivial points do not satisfy this criterion and therefore are unstable so that the stationary states ($X_s^{\pm}$, $Y_s^{\pm}$, Z_s) are sinks for $r \in (1, r_H)$, where $r_H \equiv \sigma(\sigma + 4)(\sigma - 2)$. A Hopf bifurcation occurs at r_H, the nontrivial fixed points are saddles with two dimensional unstable manifolds. Thus for $r > r_H$, all the three fixed points are unstable but the attractor set still exists. For large r values, further bifurcations may occur leading to chaotic behavior.

6.3 Chaotic Behavior of ITG-driven Electrostatic Waves

For the temporal behavior of nonlinearly interacting finite amplitude two-dimensional ($\partial z = 0$) ITG-driven electrostatic waves in collisional e-p-i magnetoplasmas, we assume $|\partial_t + \mathbf{v}_{EB} \cdot \nabla| \gg v_{i0}\partial_z;\ v_{iz}\partial_z$. Eqs. (2.31)-(2.34) can be re-written as

$$(D_t - \nu_i + \mathbf{v}_{Di0} \cdot \nabla) V_i = c_i \left(\mathbf{S}_{vo}^i \cdot \nabla\right) \Phi, \tag{6.26}$$

$$\left(D_t + \frac{5}{3}\mathbf{v}_{Bi} \cdot \nabla - \frac{2\chi_i}{3n_{i0}}\nabla_\perp^2\right) T - \frac{2}{3} D_t N_i - \tau\left(\eta_i - \frac{2}{3}\right) \mathbf{v}_{ni} \cdot \nabla\Phi = 0, \tag{6.27}$$

$$\left(D_t + \mathbf{v}_{Bi} \cdot \nabla - D_i\nabla_\perp^2\right)(\alpha\Phi) + \tau(\mathbf{v}_{Bi} - \mathbf{v}_{ni}) \cdot \nabla\Phi - \rho_i^2 \left[D_t + \nu_i + \mathbf{v}_{Di0} \cdot \nabla + \mu_i\nabla_\perp^2\right] \nabla_\perp^2\Phi$$
$$+ \mathbf{v}_{Bi} \cdot \nabla T - \rho_i^2 \nabla \cdot \left[\left(\mathbf{v}_{Di1} \cdot \nabla\right) \nabla_\perp \Phi\right] = 0, \tag{6.28}$$

where $D_t = \partial_t + \mathbf{v}_{EB} \cdot \nabla$. Here, we introduce the ansätz:

$$\Phi = \Phi_1(t) \sin(K_x x) \sin(K_y y), \tag{6.29}$$

$$T = T_1(t) \sin(K_x x) \cos(K_y y) - T_2(t) \sin(2K_x x), \tag{6.30}$$

$$V_i = V_{i1}(t) \sin(K_x x) \cos(K_y y) - V_{i2}(t) \sin(2K_x x), \tag{6.31}$$

where K_x and K_y are constant parameters, and Φ_1, A_1, A_2, V_{i1}, V_{i2}, T_1 and T_2 are some time-dependent amplitudes. The choice of $V_i(x, y, t)$ and $T(x, y, t)$ having second harmonic term $\sin(2K_x x)$ and $\cos(K_y y)$ rather than $\sin(K_y y)$ in Eqs. (4.27)-(4.29) is not purely arbitrary. Substituting Eqs. (6.29)-(6.31) into Eqs.(6.26) and (6.28), respectively, we readily obtain

$$\dot{\Phi}_1 = \varkappa_0 K_\perp^2 \Phi_1 + \varkappa_1 K_y T_1, \tag{6.32}$$

$$\dot{T}_1 = -\varkappa_2 K_\perp^2 T_1 + \varkappa_3 K_y \Phi_1 + 2\varkappa_4 K_x K_y \Phi_1 T_2, \tag{6.33}$$

$$\dot{T}_2 = -4\varkappa_2 K_x^2 T_2 - \varkappa_4 K_x K_y \Phi_1 T_1, \tag{6.34}$$

$$\dot{V}_{i1} = 2\varkappa_4 K_x K_y V_{2i} \Phi_1 - \nu_i V_{i1} + \varkappa_5 K_y \Phi_1, \tag{6.35}$$

$$\dot{V}_{i2} = -\varkappa_4 K_x K_y V_{1i} \Phi_1 - \nu_i V_{i2}, \tag{6.36}$$

where $\varkappa_0 = \left(\rho_i^2 \mu_i K_\perp^2 - \alpha D_i - \rho_i^2 \nu_i\right) / \left(\alpha + \rho_i^2 K_\perp^2\right)$, $\varkappa_1 = v_{Bi} / \left(\alpha + \rho_i^2 K_\perp^2\right)$, $\varkappa_2 = 2\chi_i / 3n_{i0}$, $\varkappa_3 = \tau\left(\eta_i - \frac{2}{3}\right) v_{ni}$, $\varkappa_4 = cT_0 / \left(2eB_0\right)$, $\varkappa_5 = c_i\left(\partial_x v_{i0} / \omega_{ci}\right)$. The terms proportional to $\sin(3K_x x)$ have been dropped in the derivation of Eqs. (6.32)–(6.36) to avoid mathematical complexity as well as the spatial dependence more rapid than allowed by the ansätz. It is clear from above set of equations that the parallel fluid velocity components (V_{i1}&V_{i2}) of ions decouple from remaining set of equations i.e., the Eqs. (6.32)–(6.34) don't depend upon V_{i1} and V_{i2}. Therefore, we are left with three independent set of equations i.e., (6.32)-(6.34) for flute-like ITG-driven electrostatic waves in a non-uniform dissipative e-p-i magnetoplasma. Eqs. (6.32)-6.34) are normalized to put in the matrix form

$$\begin{pmatrix} d_\tau X \\ d_\tau Y \\ d_\tau Z \end{pmatrix} = \begin{pmatrix} -\sigma & \sigma & 0 \\ r - Z & -1 & 0 \\ Y & 0 & -b \end{pmatrix} \begin{pmatrix} X \\ Y \\ Z \end{pmatrix}, \tag{6.37}$$

where $\sigma = \varkappa_0/\varkappa_2$, $r = \varkappa_1\varkappa_3 K_y^2 / \left(\varkappa_0\varkappa_2 K_\perp^4\right)$, is the control parameter of the system, $b = 4K_x^2/K_\perp^2$, $K_\perp^2 = K_x^2 + K_y^2$, d_τ represents $d/d\tau$ and τ is the normalized time variable and is defined as $\tau = t/t_o$; $t_o = 1/\varkappa_2 K_\perp^2$.

The normalizations used here are

$$
\begin{aligned}
\Phi_1 &\equiv a_1 X = \pm\frac{\varkappa_2 K_\perp^2}{\sqrt{2}\varkappa_4 K_x K_y} X \\
T_1 &\equiv a_2 Y = \pm\frac{\varkappa_0\varkappa_2 K_\perp^4}{\sqrt{2}\varkappa_1\varkappa_4 K_x K_y^2} Y \\
T_2 &\equiv a_3 Z = \frac{\varkappa_0\varkappa_2 K_\perp^4}{2\varkappa_1\varkappa_4 K_x K_y^2} Z
\end{aligned}
\tag{6.38}
$$

The fixed points of the flow are found by setting $d_\tau X_s = d_\tau Y_s = d_\tau Z_s = 0$ so that Eq. (6.37) reduces to

$$
\begin{pmatrix} -\sigma & \sigma & 0 \\ r - Z_s & -1 & 0 \\ Y_s & 0 & -b \end{pmatrix} \begin{pmatrix} X_s \\ Y_s \\ Z_s \end{pmatrix} = 0. \tag{6.39}
$$

or

$$
\begin{aligned}
-\sigma X_s + \sigma Y_s &= 0. \\
(r - Z_s)\, X_s - Y_s &= 0. \\
X_s Y_s - b Z_s &= 0.
\end{aligned}
\tag{6.40}
$$

Solving the above, we obtain the fixed points

$$
(X_s, Y_s, Z_s) = \left(\pm\sqrt{b(|r|-1)}, \pm\sqrt{b(|r|-1)}, |r|-1\right). \tag{6.41}
$$

It may be noted here that for $|r| > 1$, the equilibrium fixed points are unstable resulting in convective cell motions. Thus, the linear instability should saturate by attracting to one of these new fixed states. Furthermore, it is worth mentioning that a detailed behavior of chaotic motion can be studied by numerically solving the newly derived nonlinear set of equations.

The stability of the stationary state can be studied by letting $X = X_s + \tilde{X}$, $Y = Y_s + \tilde{Y}$

and $Z = Z_s + \tilde{Z}$, so that the system on linearization becomes

$$\begin{pmatrix} d_\tau \tilde{X} \\ d_\tau \tilde{Y} \\ d_\tau \tilde{Z} \end{pmatrix} = \begin{pmatrix} -\sigma & \sigma & 0 \\ r - Z_s & -1 & -X_s \\ Y_s & 0 & -b \end{pmatrix} \begin{pmatrix} \tilde{X} \\ \tilde{Y} \\ \tilde{Z} \end{pmatrix}, \tag{6.42}$$

where $\tilde{X} \ll X_s$, $\tilde{Y} \ll Y_s$ and $\tilde{Z} \ll Z_s$ and (X_s, Y_s, Z_s) represents a stationary state.

The stability of the fixed point at the origin may be found by solving the following eigenvalue problem:

$$\det \begin{bmatrix} (\lambda + \sigma) & -\sigma & 0 \\ -r & (\lambda + 1) & 0 \\ 0 & 0 & (\lambda + b) \end{bmatrix} = 0. \tag{6.43}$$

i.e.,

$$\lambda = -\frac{(\sigma + 1)}{2} \pm \frac{1}{2} \left[(\sigma + 1)^2 - 4\sigma(1 - r) \right]^{1/2}. \tag{6.44}$$

As one increases r, the following dynamical trajectories occur:

1) $0 < r < 1$. In this range, there is only one stable fixed point which is at the origin.

2) $1 < r < 1.346$. Two new stable nodes are formed and the origin becomes a saddle point with a one-dimensional, unstable manifold.

3) $1.346 < r < 13.926$. At the lower value the stable nodes become stable spirals.

4) $13.926 < r < 24.74$. Unstable limit cycles are formed near each of the spiral nodes, and the basins of attraction of each of the two fixed points become interwired. The steady-state motion is sensitive to initial conditions.

5) $24.74 < r$. All three fixed points become unstable and consequently chaos sets in.

The characteristic equation of (6.43) is

$$(\lambda + b) \left[(\lambda^2 + (1 + \sigma)\lambda + (1 - r)\sigma) \right] = 0, \tag{6.45}$$

which governs the linear stability of the stationary state. For example, if we take $r < 1$, the origin is a hyperbolic sink and is thus stable. For $r = 1$ however, the eigenvalues are

$\lambda_1 = -b$ and $\lambda_2 = -(1+\sigma)$, if λ_1 or $\lambda_2 < 0$, then the motion can flip between positive and negative eigen-directions while still moving closer to the fixed point. Finally, for $r > 1$, the nontrivial stationary points are $X_s = Y_s = \pm\sqrt{b(r-1)}$ and $Z_s = r-1$ as obtained in Eq. (6.41). The stability of the fixed points off the origin is determined by

$$\det \begin{bmatrix} -(\lambda+\sigma) & \sigma & 0 \\ r - Z_s & -(\lambda+1) & -X_s \\ Y_s & X_s & -(\lambda+b) \end{bmatrix} = 0. \tag{6.46}$$

Choosing positive values from Eq. (6.42), the above relation becomes

$$(\lambda+\sigma)\left[\lambda^2 + (1+b)\lambda + br\right] + \sigma\left[b(r-1) - (\lambda+b)\right] = 0.$$

or

$$\lambda^3 + (\sigma+b+1) + b(r+\sigma)\lambda + 2\sigma b(r-1) = 0. \tag{6.47}$$

We may re-write Eq. (6.46) as

$$\lambda^3 + a_1\lambda^2 + a_2\lambda + a_3 = 0, \tag{6.48}$$

where $a_1 = (\sigma+b+1)$, $a_2 = b(r+\sigma)$ and $a_3 = 2\sigma b(r-1)$. The corresponding eigenvalues of Eq. (6.48) are $\lambda = -(\sigma+b+1)$, $\pm i\sqrt{2\sigma(\sigma+1)/(\sigma-b-1)}$, the $\pm$ imaginary values correspond to stable or unstable spirals so that the stationary states $(X_s^{\pm}, Y_s^{\pm}, Z_s)$ act as sinks. As parameters are changed in a dynamical system, the stability of the equilibrium points can change as well as the number of equilibrium points.

The study of these changes in nonlinear problems as system parameters are varied is the subject of bifurcation theory. Values of these parameters at which the qualitative or topological nature of motion changes are known as critical or bifurcation values. As we discussed earlier that when a control parameter is varied, a pair of complex conjugate eigenvalues $\lambda = -(\sigma+b+1)$ and $\pm i\sqrt{2\sigma(\sigma+1)/(\sigma-b-1)}$ cross from the left-hand plane (a stable spiral) into the right-hand plane (an unstable spiral) and a periodic motion emerges known as a limit cycle. This type of qualitative change in the dynamics of system is known as a Hopf bifurcation. We can calculate from Eq. (6.47) a point at which Hopf bifurcation occurs $r_H \equiv \sigma(\sigma + b + 3)/(\sigma - b - 1)$. The critical condition for Hopf bifurcation [111] is

$$f = a_1 a_2 - a_3 = 0. \tag{6.49}$$

From these condition we calculate $r = r_H$, so Hopf bifurcation occurs at r_H. If the control parameter r exceeds r_H, the system undergoes two more Hopf bifurcations so that three simultaneous coupled limit cycles are present, that signals chaotic motion. According to Routh-Hurwitz criterion [110] a necessary and sufficient condition for the stationary solutions to be stable is

$$D(\lambda) = \lambda^3 + a_1\lambda^2 + a_2\lambda + a_3 = 0. \tag{6.50}$$

$$\begin{vmatrix} a_1 & 1 \\ a_3 & a_2 \end{vmatrix} = a_1 a_2 - a_3 > 0, \tag{6.51}$$

where $a_1 > 0$ and $a_3 > 0$. Using this criterion we observed that $r < r_H$ thus the system is stable below r_H. Thus, for $r > r_H$, all the three fixed points are unstable but the attractor set still exists. For larger r values, further bifurcations may occur leading to chaotic behavior.

6.4 Chaotic Behavior of ITG-driven Electromagnetic Waves

Here, we shall discuss temporal behavior of nonlinearly interacting finite amplitude two dimensional ($\partial z = 0$) ITG-driven electromagnetic waves in a collisional e-p-i magnetoplasma for the case of inertialess electrons/positrons. We assume that $|\partial_t + \mathbf{v}_{EB} \cdot \boldsymbol{\nabla}| \gg v_{iz}\partial_z; v_{i0}\partial_z$, $D_e = D_p$ and equilibrium current gradients are negligibly small. Therefore, the relevant equations i.e., Eqs. (2.21)-(2.27) can be reduced using quasineutrality condition and Ampere's law to the following set:

$$\left(D_t - \tau \mathbf{v}_{Bi} \cdot \nabla - D_e \nabla_{\perp}^2\right) N_i - \tau \mathbf{v}_{ni} \cdot \nabla \Phi + D_z \left(c_i V_i + \frac{c T_0 \nabla_{\perp}^2 A_z}{4\pi n_{i0} e^2} \right) = 0, \tag{6.52}$$

$$\begin{aligned} &\left(D_e - D_i\right) \nabla_{\perp}^2 N_i + \tau \mathbf{v}_{Bi} \cdot \nabla \Phi + \rho_i^2 \left[D_t + \nu_i + \mathbf{v}_{Di0} \cdot \nabla + \mu_i \nabla_{\perp}^2\right] \nabla_{\perp}^2 \Phi \, , \\ &- \mathbf{v}_{Bi} \cdot \nabla T + \rho_i^2 \nabla \cdot \left[\left(\mathbf{v}_{Di1} \cdot \nabla\right) \nabla_{\perp} \Phi\right] + \frac{c T_0}{4\pi n_{i0} e^2} D_z \left(\nabla_{\perp}^2 A_z\right) = 0 \, , \end{aligned} \tag{6.53}$$

$$\left(D_t + \nu_i + \mathbf{v}_{Di0} \cdot \nabla\right) V_i = -c_i \left[\frac{1}{c} \left(D_t + \mathbf{v}_{Di0} \cdot \nabla\right) A_z - \mathbf{S}_{vo}^i \cdot \nabla \Phi + \tau^{-1} D_z \left(T + N_i\right) \right] . \tag{6.54}$$

$$\left(D_t + \frac{5}{3} \mathbf{v}_{Bi} \cdot \nabla - \frac{2\chi_i}{3 n_{i0}} \nabla_{\perp}^2 \right) T - \frac{2}{3} D_t N_i - \tau \mathbf{v}_{Ti0} \cdot \nabla \Phi = 0, \tag{6.55}$$

$$\left(D_t + \alpha^{-1} \tau \left(\mathbf{v}_{ni} \cdot \nabla\right)\right) A_z - \alpha^{-1} c D_z N_i = 0, \tag{6.56}$$

where $D_t = \partial_t + \mathbf{v}_{EB} \cdot \nabla$ and $D_z = \left(T_0/B_0 e\right) \nabla_{\perp} A_z \times \hat{\mathbf{z}} \cdot \nabla$. We follow the Lorenz and Stenflo approach [72] in the derived set of coupled nonlinear equations which are necessary to study chaos. Accordingly, we introduce the ansätz:

$$\Phi = \Phi_1(t) \sin(K_x x) \sin(K_y y), \tag{6.57}$$

$$N_i = N_{i1}(t) \sin(K_x x) \sin(K_y y), \tag{6.58}$$

$$T = T_1(t) \sin(K_x x) \cos(K_y y) - T_2(t) \sin(2K_x x), \tag{6.59}$$

$$V_i = V_{i1}(t) \sin(K_x x) \cos(K_y y) - V_{i2}(t) \sin(2K_x x), \tag{6.60}$$

$$A_z = A_1(t) \sin(K_x x) \cos(K_y y) - A_2(t) \sin(2K_x x), \tag{6.61}$$

where K_x and K_y are constant parameters, and N_{i1}, A_1 and A_2 are some time-dependent amplitudes. Substituting (6.57)-(6.61) into (6.52)-(6.56), we get

$$\dot{\Phi}_1 = -\left(\nu_i - \mu_i K_\perp^2\right)\Phi_1 + \frac{v_{Bi}K_y}{\rho_i^2 K_\perp^2}T_1 + \frac{(D_e - D_i)}{\rho_i^2}N_{i1} - \frac{\omega_{ci}\lambda_i^2 K_x K_y}{K_\perp^2}(K_\perp^2 - 4K_x^2)A, \quad (6.62)$$

$$\dot{T}_1 = -\tau\left(\frac{2}{3} - \eta_i\right)v_{ni}K_y\Phi_1 + \omega_{ci}\rho_i^2 K_x K_y \Phi_1 T_2 - \frac{2\chi_i}{3n_{i0}}K_\perp^2 T_1, \quad (6.63)$$

$$\dot{T}_2 = -\frac{8\chi_i}{3n_0}K_x^2 T_2 - \frac{\omega_{ci}\rho_i^2}{2}K_x K_y \Phi_1 T_1, \quad (6.64)$$

$$\dot{N}_{i1} = -D_e K_\perp^2 N_{i1} - \omega_{ci}\rho_i^2\lambda_i^2 K_x K_y (K_\perp^2 - 4K_x^2)A, \quad (6.65)$$

$$\dot{A} = \frac{\omega_{ci}\rho_i^2}{2}K_x K_y \Phi_1 A + \frac{3\alpha^{-1}\omega_{ci}\rho_i^2}{2}K_x K_y N_{i1} A, \quad (6.66)$$

where $A = A_1 A_2$ and $\lambda_i^2 = c_i^2/\omega_{pi}^2$. Notice that the terms proportional to $\sin(3K_x x)$ have been dropped in the derivation of Eqs. (6.62)–(6.66) and low-β plasma approximation decouple the time derivative equations for V_{i1} and V_{i2} from the Eqs. (6.62)-(6.66). Thus system reduces to the following 5×5 matrix

$$\begin{pmatrix} d_\tau X \\ d_\tau Y \\ d_\tau Z \\ d_\tau U \\ d_\tau V \end{pmatrix} = \begin{pmatrix} -\sigma & \sigma & 0 & s_0 & -s_1 \\ r - Z & -1 & 0 & 0 & 0 \\ Y & 0 & -b & 0 & 0 \\ 0 & 0 & 0 & -s_2 & -1 \\ s_3 V & 0 & 0 & 0 & U \end{pmatrix} \begin{pmatrix} X \\ Y \\ Z \\ U \\ V \end{pmatrix}, \quad (6.67)$$

where $\sigma = 3n_0\left(\nu_i - \mu_i K_\perp^2\right)/\left(2\chi_i K_\perp^2\right)$, $r = 3\tau n_{i0} v_{ni}\rho_i^2\left(\nu_i - \mu_i K_\perp^2\right)\left(\eta_i - \frac{2}{3}\right)/\left(2\chi_i v_{Bi}\right)$, $b = 4K_x^2/K_\perp^2$, $s_0 = (D_e - D_i)\left(t_0 a_4/a_1\right)/\rho_i^2$, $s_1 = \omega_{ci}\lambda_i^2 K_x K_y(K_\perp^2 - 4K_x^2)\left(t_0 a_5/a_1\right)/K_\perp^2$, $s_2 = t_0 D_e K_\perp^2$, $s_3 = \omega_{ci}\rho_i^2 K_x K_y a_1 t_0/2$, with $K_\perp^2 = K_x^2 + K_y^2$, $\tau = t/t_0$, and $t_0 = 2/\omega_{ci}\rho_i^2 K_x K_y$. If we further take $K_y^2 = 4K_x^2$ and $D_e = D_i$, then Eq. (6.67) reduces to Lorenz type equations.

The normalizations used here are

$$\begin{aligned}
\Phi_1 &\equiv a_1 X = \pm\frac{2K_\perp^2}{\sqrt{3n_{i0}/\chi_i}\omega_{ci}\rho_i^2 K_x K_y} X \\
T_1 &\equiv a_2 Y = \pm\frac{2\rho_i^2 K_\perp^4\left(\nu_i-\mu_i K_\perp^2\right)}{\sqrt{3n_{i0}/\chi_i}\omega_{ci}\rho_i^2 v_{Bi} K_x K_y^2} Y \\
T_2 &\equiv a_3 Z = -\frac{\left(\nu_i-\mu_i K_\perp^2\right) K_\perp^2}{v_{Bi}\omega_{ci} K_x K_y^2} Z \\
N_{i1} &\equiv a_4 U = -\frac{4\alpha\chi_i K_\perp^2}{9n_{i0}\omega_{ci}\rho_i^2 K_x K_y} U \\
A &\equiv a_5 V = \frac{8\alpha\chi_i^2 K_\perp^4}{27n_{i0}^2\omega_{ci}^2\rho_i^4\lambda_i^2 K_x^2 K_y^2(K_-^2-4K_x^2)} V
\end{aligned} \tag{6.68}$$

The equilibrium points of Eq. (6.67) can be obtained by setting time derivative terms equal to zero and solving the nonlinear set of coupled equations. To study the stability of the stationary states, we may let $X = X_s + X_1$, $Y = Y_s + Y_1$, $Z = Z_s + Z_1$, $U = U_s + U_1$ and $V = V_s + V_1$, so that the linearized system becomes

$$\begin{pmatrix} d_\tau X_1 \\ d_\tau Y_1 \\ d_\tau Z_1 \\ d_\tau U_1 \\ d_\tau V_1 \end{pmatrix} = \begin{pmatrix} -\sigma & \sigma & 0 & s_0 & -s_1 \\ r - Z_s & -1 & 0 & 0 & 0 \\ Y_s & 0 & -b & 0 & 0 \\ 0 & 0 & 0 & -s_2 & -1 \\ s_3 V_s & 0 & 0 & 0 & U_s \end{pmatrix} \begin{pmatrix} X_1 \\ Y_1 \\ Z_1 \\ U_1 \\ V_1 \end{pmatrix}, \tag{6.69}$$

where $X_1 \ll X_s$, $Y_1 \ll Y_s$, $Z_1 \ll Z_s$, $U_1 \ll U_s$ and $V \ll V_s$ and $(X_s, Y_s, Z_s, U_s, V_s)$ represents a stationary state. Taking the fixed point at origin, the corresponding characteristic equation which governs the linear stability of the stationary state is given by

$$\lambda\,(\lambda + b)(\lambda + s_2)\left[\lambda^2 + \lambda\,(1+\sigma) + \sigma\,(1-r)\right] = 0 \tag{6.70}$$

The eigenvalues are $\lambda = 0, -b, -s_2, -\frac{(1+\sigma)}{2} \pm \frac{1}{2}\sqrt{(1+\sigma)^2 - 4\sigma\,(1-r)}$. For $0 < r < 1$, the eigenvalues become $\lambda = 0, -s_2, -b, -1, -\sigma_0$. Thus the equilibrium point is stable since all the eigenvalues are negative. At $r = 1$, we have $\lambda = 0, -s_2, -b, -(1+\sigma_0)$ i.e., the fixed point is marginally stable. It is stable for $1 < r < r_H$, where r_H is any arbitrary value known as Hopf bifurcation. Finally for $r > 1$ the nontrivial stationary points are $X_s = Y_s = \pm\sqrt{b(r-1)}$ and $Z_s = r - 1$. At $r < r_H$ two of the eigenvalues become complex i.e., two limit cycles result which are stable as long as the real part of the complex eigenvalues is smaller than zero. For $r = r_H$, where $r_H \equiv \sigma(\sigma + b + 3)/(\sigma - b - 1)$ these real parts become zero i.e. we have two eigenvalues $\lambda = -(\sigma + b + 1)$ and $\pm i\sqrt{2\sigma(\sigma+1)/(\sigma - b - 1)}$. Above r_H, the limit cycle becomes unstable (the complex eigenvalues have positive real parts) and chaos sets in.

Finally, we have numerically investigated the chaotic behavior of our nonlinear system which is represented by Eq. (6.37). For this purpose, we have used r as the arbitrary controlled parameter and fixed the parameters $\sigma = 11.4$ and $b = 1$. Figure (6-1) shows a chaotic behavior of electrostatic ITG-driven drift-dissipative mode in e-p-i magnetoplasma. Period doubling structures can easily be seen from the figure (6-1).

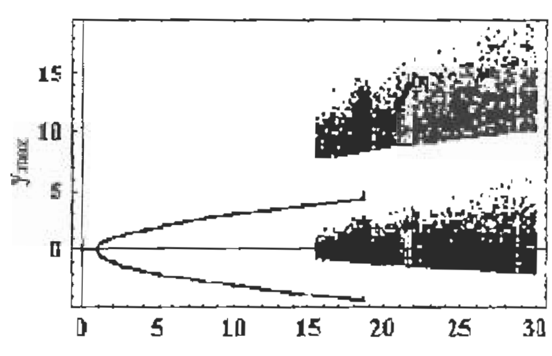

Figure 6-1: Chaotic behaviour of electrostatic ITG-driven drift-dissipative waves.

6.5 Summery

To summarize this chapter, we have studied the nonlinear dynamics of weakly interacting low-frequency flute like electrostatic and electromagnetic ITG modes in a nonuniform e-p-i magnetoplasma. Furthermore, we reduced the governing equations to those of Lorenz ones, that the temporal chaos can appear if dissipation is included. We have also numerically investigated Eq. (6.37) for some typical parameters and plotted the bifurcation diagram for some specific value of r. By varying the control parameter r, we observe the transition in the system from stable to unstable state. We calculate a critical point at which a Hopf bifurcation occurs. By using Routh-Hurwitz criterion a necessary and sufficient condition for the stability of stationary solution is also calculated.

Chapter 7

Summary and Conclusions

In this chapter, we summarize the work presented here and draw some conclusions. In this thesis, first of all, the linear and nonlinear propagation of ion acoustic and electrostatic drift waves in an e-p-i plasma have been investigated in the presence of ion sheared flow along the external magnetic field in cold ions limit [56]. It has been found that the free energy available in the form of shear flow can give rise to electrostatic instabilities of ion acoustic and drift waves in the linear limit. It is important to note that the ion acoustic wave can become unstable in both e-i and e-p-i plasmas due to ion shear flow even in the absence of density gradient. In the presence of ion collisions a drift-dissipative instability may also take place under suitable conditions. On the other hand, when the finite amplitude disturbances weakly interact among themselves, the nonlinear coupling of various modes may lead to the formation of *monopolar* vortex in a collisionless plasma.

The effect of finite ion-temperature, which was not considered in the earlier investigation [58], may drastically modify the nonlinear dynamics. Therefore, we have generalized the said work by considering a nonuniform strongly magnetized e-p plasma with ions at nonrelativistic hot temperature in the presence of sheared ion flows. In the linear case, we found that ion-acoustic and electrostatic drift-waves become unstable due to equilibrium sheared ion flow. In the nonlinear case, for some specific profiles of the equilibrium density and sheared plasma flows, the nonlinear equations admit *quadrupolar* vortices.

Physically, the ITG modes arise due to the linear coupling of the magnetic field aligned ion-sound wave and a drift wave that propagates transverse to the ambient magnetic field. Since in the presence of ion temperature gradient, the wave potential as well as the ion-temperature and density perturbations cannot keep in phase, therefore, the free energy stored in the temperature gradient can be coupled to the ITG modes, driving them at a nonthermal level. Among other instabilities, several experimental results are in favor of ITG mode as a major candidate for explaining anomalous transport. Therefore, due to the importance of ITG mode, we have extended our earlier studies [56, 58] to the ITG-driven electrostatic waves with sheared flows in an inhomogeneous e-p-i magnetoplasma. By employing the ion continuity, momentum and energy balance equations for the ion and Boltzmann distribution for the electrons and positrons, we have derived a new set of nonlinear mode coupling equations that contain scalar as well as vector nonlinearities. Neglecting the nonlinear terms, we have carried out the normal mode analysis to derive a general dispersion relation. It has been shown that non-zero equilibrium ion temperature (i.e. $\tau^{-1} \neq 0$) and the presence of positrons (i.e. $\alpha \neq 1$) modify the previously known results in the appropriate limits. For flat density profile, ITG-driven drift wave is destabilized on account of free energy stored in the inhomogeneous ion temperature and magnetic field gradients. We have also derived a cubic dispersion relation for the coupled ion-acoustic and electrostatic ion-temperature-gradient mode in the presence of sheared ion flow. One of the roots of this cubic dispersion relation predicts an instability irrespective the direction of shear and ion-temperature gradient. On the other hand, in the nonlinear case, it is shown that under certain conditions possible stationary solutions of the same set of nonlinear equations are reduced in the form of *monopolar*, *dipolar*, *tripolar*, *quadrupolar* and *chain* of vortices. We have also incorporated the self-gravitation effect of ions in this work and shown that possible stationary solutions of the nonlinear equations can also be represented in the form of *dipolar* and *tripolar* vortices of gravitational potential.

Further, in most of the laboratory and space plasmas, the plasma beta could exceed the electron to ion mass ratio, necessitating to incorporate electromagnetic effects on ITG mode. We have also studied the linear and nonlinear properties of low-frequency electromagnetic ITG-driven waves in a nonuniform collisional e-p-i magnetoplasma containing the equilibrium density gradient, ion-temperature gradient, magnetic field gradient, and parallel velocity gradient. By employing the Braginskii's transport equations for the ions and continuity and momentum balance equations for the electrons and positrons, we derive seven sets of nonlinear mode coupling equations. In the linear case, we have derived local dispersion relation and obtained new class of instabilities and modes for e-p-i plasma. We found that in the presence of positrons, electromagnetic and electrostatic disturbances respond in a very different way and several new types of modes and instabilities are found to exist. For instance, it has been shown that non-zero equilibrium ion-temperature and the presence of positrons modify the previously known results. It is also found that sheared equilibrium flow can cause instability of Alfvén waves even in the absence of density gradients. On the other hand, in the nonlinear case, the mode coupling equations admit new class of *dipolar* and *vortex chain* type solutions.

Furthermore, linearly excited finite amplitude electrostatic waves interact among themselves and lead to a chaotic state due to mode coupling in a nonuniform dissipative plasma. This has been demonstrated by looking for the time-dependent solution of the nonlinear equations that govern the dynamics of finite amplitude dissipative electrostatic waves. We find that the nonlinear dynamics of drift-dissipative waves in the presence of sheared ion-flows can be expressed as a set of three mode coupled equations, or simply the generalized Lorenz–Stenflo equations. Their linear stability analysis has been performed in various limits [56]. We have also made the study of chaotic behavior to electrostatic/electromagnetic ITG modes. With that in view, we follow the Lorenz and Stenflo approach and derive a new set of eight coupled nonlinear equations which we call the generalized Lorenz-Stenflo equations. The stability of the system is determined by the Routh-Hurwitz criterion. We found that the nontrivial stationary points do not satisfy this criterion and therefore are unstable. We have numerically investigated the periodic and chaotic solutions of the generalized Lorenz-Stenflo type of nonlinear system of equations and also plotted the bifurcation diagram.

References

[1] P. Goldreich and W. H. Julian, The Astrophysical Journal, **157**, 869 (1969).

[2] F. C. Michel, Reviews of Modern Physics, **54**, 1 (1982).

[3] M. C. Begelman, R. D. Blandford and M. D. Rees, Reviews of Modern Physics, **56**, 255 (1984).

[4] H. R. Miller and P. J. Witta, *Active Galactive Nuclei*, (Springer-Verlag, Berlin 1987), p. 202.

[5] M. A. Ruderman and P. G. Sutherland, The Astrophysical Journal, **196**, 51 (1975).

[6] M. J. Rees, Nature, **229**, 312 (1971).

[7] M. J. Rees, *The Very Early Universe*, (edited by G. W. Gibbons, S. W. Hawking and S. Siklos), (Cambridge University press, Cambridge, 1983).

[8] T. Tajima and T. Taniuti, Physical Review A, **42**, 3587 (1990).

[9] M. L. Burns, *Positron-Electron Pairs in Astrophysics*, edited by M. L. Burns, A. K. Harding, and R. Ramaty (American Institute of Physics, New York, 1983).

[10] M. E. Gedalin, J. G. Lominadze, L. Stenflo and V. N. Tsitovich, Astrophysics and Space Science, **108**, 393 (1985).

[11] E. Tandberg-Hansen and A. G. Emshie, *The Physics of Solar Flares* (Cambridge University Press, Cambridge, 1988), p. 124.

[12] T. Piran, Physics Reports, **314**, 575 (1999).

[13] T. S. Pedersen, A. H. Boozer, W. Dorland, J. P. Kremer and R. Schmitt, Journal of Physics B: Atomic, Molecular and Optical Physics, **36**, 1029 (2003).

[14] V. I. Berezhiani, L. N. Tsintsatdze and P. K. Shukla, Journal of Plasma Physics, **48**, 139 (1992).

[15] C. M. Surko, M. Leventhal, W. S. Crane, A. Passner, F. J. Wysocki, T. J. Murphy, J. Strachan and W. L. Rowan, Review of Scientific Instruments, **57**, 1862 (1986).

[16] M. D. Tinkle, R. G. Greaves, C. M. Surko, R. L. Spencer and G. W. Mason, Physical Review Letters, **72**, 352 (1994).

[17] R. G. Greaves and C. M. Surko, Physical Review Letters, **75**, 3846 (1995).

[18] P. Helander and D. J. Ward, Physical Review Letters, **90**, 135004 (2003).

[19] A. W. Trivelpiece, Comments Plasma Physics and Controlled Fusion, **1**, 57 (1972).

[20] C. M. Surko, M. Leventhal and A. Passner, Physical Review Letters, **62**, 901 (1989).

[21] R. G. Greaves, M. D. Tinkle and C. M. Surko, Physics of Plasmas, **1**, 1439 (1994).

[22] J. Zhao, J. I. Sakai and K. Nishikawa, Physics of Plasmas, **3**, 844 (1996).

[23] C. M. Ferreira, *Microwave Discharges Fundamentals and Applications* (Plenum Press, 1992).

[24] M. Hoshino and J.Arons, Physics of Fluids B, **3**, 818 (1991).

[25] S. I. Popel, S. V. Vladimirov and P. K. Shukla, Physics of Plasmas, **2**, 716 (1995).

[26] S. Jammalamadaka, P.K.Shukla and L.Stenflo, Astrophys. Space Sci., **240**, 39 (1996).

[27] H. Hasegawa , S. Irie, S. Usmani and Y. Ohsawa, Physics of Plasmas, **9**, 2549 (2002).

[28] O. A. Pokhotelov, O.G. Onishchenko, V. P. Pavlenko, L. Stenflo, P. K. Shukla, A.V. Bogdanov and F.F. Kamenets, Astrophysics and Space Science, **277**, 497 (2001).

[29] C. M. Surko and T. Murphy, Physics of Fluids B, **2**, 1372 (1990).

[30] G. S. Lakhina and B. Buti, Astrophysics and Space Science, **79**, 25 (1981).

[31] D. C. Lominadze, G. Z. Machabeli, G. I. Melikidze and A. D. Pataraya, Sov. Journal of Plasma Physics, **12**, 712 (1986).

[32] V. I. Berezhiani, D. D. Tskhakaya and P. K. Shukla, Physical Review A, **46**, 6608 (1992).

[33] E. Witten, Nuclear Physics B, **249**, 557 (1985).

[34] J. P. Ostriker, C. Thompson and E. Witten, Physics Letters B, **180**, 231 (1986).

[35] F. B. Rizzato, Journal of Plasma Physics, **40**, 289 (1988).

[36] Y. A. Gallant, J. Arons, and A. B. Langdon, Presented at the Physics of Isolated Pulsars Workshop, Taos, NM, 23-28 Feb. (1992).

[37] Y. N. Nejo, Australian Journal of Physics, **50**, 309 (1997).

[38] L. N. Tsintsatdze, Physics of Plasmas, **11**, 4107 (1998).

[39] M. Honda and Y. S. Honda, The Astrophysical Journal, **569**, 39 (2002).

[40] M. Hoshino, J. Arons, Y. Gallant and A. B. Langdon, The Astrophysical Journal, **390**, 454 (1992).

[41] M. Gail, N. Grun and W. Scheid, Atomic, Molecular and Optical Physics, **36**, 1397 (2003).

[42] H. Hasegawa, S. Usami and Y. Ohsawa, Physics of Plasmas, **10**, 3455 (2003).

[43] H. Hasegawa and Y. Ohsawa, Physics of Plasmas, **12**, 012312 (2005).

[44] S. Hasegawa, S. Irie, S. Usami and Y. Ohsawa, Physics of Plasmas, **9**, 2549 (2002).

[45] P. K. Shukla, L. Stenflo and R. Fedele, Physics of Plasmas, **10**, 310 (2003).

[46] W. Horton, B. Hu, J. Q. Dong and P. Zhu, New Journal of Physics, **5**, 14 (2003).

[47] J. G. Charney, Geophys. Public. Nors. Visenkamp. Akad. Oslo, **17**, 3 (1948).

[48] A. Hasegawa and K. Mima, Physics of Fluids, **21**, 87 (1978).

[49] V. D. Larichev and G. M. Reznik, Doklady Akademii Nauk, **231**, 1071 (1976).

[50] M. Y. Yu, P. K. Shukla and L. Stenflo, The Astrophysical Journal, **309**, L63 (1986).

[51] V. I. Berezhiani, L. N. Tsintsadze and P. K. Shukla, Journal of Plasma Physics, **48**, 139 (1992); Physica Scripta, **46**, 55 (1992).

[52] V. I. Berezhiani and S. M. Mhajan, Physical Review Letters, **73**, 1110 (1994); Physical Review E **52**, 1968 (1995).

[53] H. Kakati and K. S. Goswami, Physics of Plasmas, **7**, 808 (2000).

[54] J. Vranjes, M. Kono, E. Lazzaro and M. Lontano, Physics of Plasmas, **7**, 4872 (2000).

[55] H.Saleem, Q. Haque and J.Vranjes, Physical Review E, **67**, 057402-1 (2003).

[56] A. M. Mirza, Asma Hasan, M. Azeem and H. Saleem, Physics of Plasmas, **10**, 4675 (2003).

[57] P. K. Shukla, A. A. Mamun and L. Stenflo, Physica Scripta, **68**, 295 (2003).

[58] A. M. Mirza and M. Azeem, Physics of Plasmas, **11**, 4341 (2004).

[59] M. Azeem and A. M. Mirza, Physics of Plasmas, **11**, 4727 (2004).

[60] M. Azeem and A. M. Mirza, Physics of Plasmas, **12**, 052306 (2005).

[61] B. P. Pandey. K. Avinash and C. B. Dwivedi. Physical Review E. **49**. 5599 (1994).

[62] L. Mahanta, B. J. Saikia, B. P. Pandey and S. Bujarbarua, Journal of Plasma Physics, **55**, 401 (1996).

[63] K. Avinash and P. K. Shukla, Physics Letters A. **189**. 170 (1994).

[64] F. Verheest. P. K. Shukla,, N. N. Rao and P. Meuris. Journal of Plasma Physics. **55**. 401 (1996).

[65] J. Vranjes. Astronomy & Astrophysics. **351**, 1190 (1999).

[66] A. A. Mamun, Physics of Plasmas. **5** 3542 (1998).

[67] A. A. Mamun and P. K. Shukla. Physica Scripta, **62**, 429 (2000).

[68] M. Azeem and A. M. Mirza, Physica Scripta, (2005) accepted for publication.

[69] D. Fultz. R. R. Long, G. V. Owens, W. Bohan, R. Kaylor and J. Weil, Studies of Thermal Convection in a Rotating Cylinder with Some Implications for Large-Scale Atmospheric Motions, Meteor. Monogr., No. 4, Amer. Meteor. Soc., 1–104 (1959).

[70] R. Hide. An experimental study of thermal convection in a rotating liquid. Philos. Trans. Roy. Soc. London. **250A**. 441–478. (1958).

[71] E. N. Lorenz. Journal of the Atmospheric Sciences. **20**, 130 (1963).

[72] L. Stenflo. Physica Scripta. **53**, 83 (1996).

[73] M. Y. Yu, Physica Scripta. **54**. 321 (1996).

[74] A. M. Mirza, Physics of Plasmas. **7**. 3588 (2000).

[75] A. M. Mirza and Khalid Khan. Physica Scripta. **66**. 376 (2002).

[76] O. E. Garcia. European Journal of Physics. **24** 331 (2003).

[77] P. K. Shukla and L. Stenflo, Physics of Plasmas, **7**, 2728 (2000).

[78] N. Iwamoto, Physical Review E, **47**, 604 (1993).

[79] M. Y. Yu, P. K. Shukla and L. Stenflo, The Astrophysical Journal, **309,** L63 (1986).

[80] G. P. Zank and R. G. Greaves, Physical Review E, **51**, 6079 (1995).

[81] N. Ya. Kotsarenko, S. V. Koshevaya, G. A. Stewart and D. Maravilla, Planetary and Space Science, **46**, 429 (1998).

[82] J. Vranjes, D. Jovanovic and P. K. Shukla, Physics of Plasmas, **5**, 4300 (1998).

[83] I. L. Rudakov and R. Z. Sagdeev, Soviet Physics Doklady, **6**, 415 (1961).

[84] B. B. Kadomtsev and O. P. Pogutse, *Review of Plasma Physics* (Edited by M. A. Leontovich, Consultants Bureau, New-York **5**, 249, 1965).

[85] T. S. Hahm and W. M. Tang, Physics of Fluids B, **1**, 1185 (1989).

[86] A. Hiros and O. Ishihara, Nuclear Fusion, **24**, 1439 (1987).

[87] A. Hirose, Physics of Fluids B, **2**, 1087 (1990).

[88] F. Romanelli, Physics of Fluids B, **1**, 1018 (1989).

[89] H. Biglari, P. H. Diamond and M. N. Rosenbluth, Physics of Fluids B, **1**, 109 (1989).

[90] P. K. Shukla, Physica Scripta, **42**, 725 (1990).

[91] A. Jarmen, P. Andersson and J. Weiland, Nuclear Fusion, **27**, 941 (1987).

[92] T. Farid, A. M. Mirza and P. K. Shukla, Physics of Plasmas, **7**, 166 (2000).

[93] P. K. Shukla and J. Weiland, Physics Letters A, **136**, 59 (1989).

[94] P. K. Shukla, Physica Scripta, **42**, 725 (1990).

[95] N. Chakrabarti and J. J. Rasmussen, Physics of Plasmas, **6**, 3047 (1999).

[96] W. Horton, D. Jovanoviac and J. J. Rasmussen, Physics of Fluids, **4**, 3336 (1992).

[97] A. M. Mirza, T. Farid, P. K. Shukla and L. Stenflo, IEEE Transactions on Plasma Science, **29**, 298 (2001).

[98] T. Farid, A. M. Mirza, P. K. Shukla and A. Qamar, Physics of Plasmas, **8**, 846 (2001).

[99] A. Qamar, A. M. Mirza, G. Murtaza, J. Vranjes and P. H. Sakanaka, Physics of Plasmas, **10**, 2819 (2003).

[100] P. K. Shukla and A. A. Mamun, Physics Letters A, **271**, 402 (2000).

[101] A. B. Mikhailovskii, V. P. Lakhin, G. D. Aburdzhaniya, L. A. Mikhailovskaya, O. G. Onishenko and A. I. Smolyakov, Plasma Physics and Controlled Fusion, **29**, 1 (1984).

[102] D. L. Brower, W. A. Peebless, S. K. Kim, N. C. Luhmann, W. M. Phillips, Physical Review Letters, **59**, 48 (1987).

[103] S. Hamaguchi and W. Horton, Physics of Fluids B, **2**, 183 (1990a).

[104] S. Hamaguchi and W. Horton, Physics of Fluids B, **2**, 3040 (1990b).

[105] R. J. Hastie and K. W. Hesketh, Nuclear Fusion, **13**, 259 (1973).

[106] F. Zonca, L. Chen, J. Q. Dong and R. A. Santoro, Physics of Plasmas, **6**, 1917 (1999).

[107] M. Kotschenreuther, Physics of Fluids, **29**, 2898 (1986).

[108] L. Stenflo, Physics of Fluids, **30**, 3297 (1987).

[109] L. Stenflo, Physics Letters A, **222**, 378 (1996).

[110] L. A. Pipes and L. R. Harvill, *Applied Mathematics for Engineers and Physicists*, (McGraw-Hill, New-York, 1970).

[111] Nai-Quan Wang, Physics Letters A, **145**, 29 (1990).

[112] A. M. Mirza and P. K. Shukla, Physics Letters A, **229**, 313 (1997).

[113] T. Rafiq, A. M. Mirza, A. Qamar, G. Murtaza and P. K. Shukla, Physics of Plasmas, **6**, 3571 (1999).